Accepted Manuscript

Synthesis and biological evaluation of a novel betulinic acid derivative as inducer of apoptosis in human colon carcinoma cells (HT-29)

Biswajit Chakraborty, Debasmita Dutta, Sanjukta Mukherjee, Supriya Das, Nakul C. Maiti, Padma Das, Chinmay Chowdhury

PII: S0223-5234(15)30167-7

DOI: 10.1016/j.ejmech.2015.07.035

Reference: EJMECH 8019

To appear in: *European Journal of Medicinal Chemistry*

Received Date: 3 January 2015

Revised Date: 16 July 2015

Accepted Date: 17 July 2015

Please cite this article as: B. Chakraborty, D. Dutta, S. Mukherjee, S. Das, N.C. Maiti, P. Das, C. Chowdhury, Synthesis and biological evaluation of a novel betulinic acid derivative as inducer of apoptosis in human colon carcinoma cells (HT-29), *European Journal of Medicinal Chemistry* (2015), doi: 10.1016/j.ejmech.2015.07.035.

Graphical Abstract

Synthesis and biological evaluation of a novel betulinic acid derivative as inducer of apoptosis in human colon carcinoma cells (HT-29)

Biswajit Chakraborty[a,‡], Debasmita Dutta[a,†], Sanjukta Mukherjee[‡], Supriya Das[§], Nakul C. Maiti[§], Padma Das[*,†] and Chinmay Chowdhury[*,‡]

[‡]Organic and Medicinal Chemistry Division, [†]Cancer Biology and Inflammatory Disorder Division, [§]Structural Biology and Bioinformatics Division, CSIR-Indian Institute of Chemical Biology, 4 Raja S. C. Mullick Road, Kolkata 700032, India.

[a]Contributed equally.

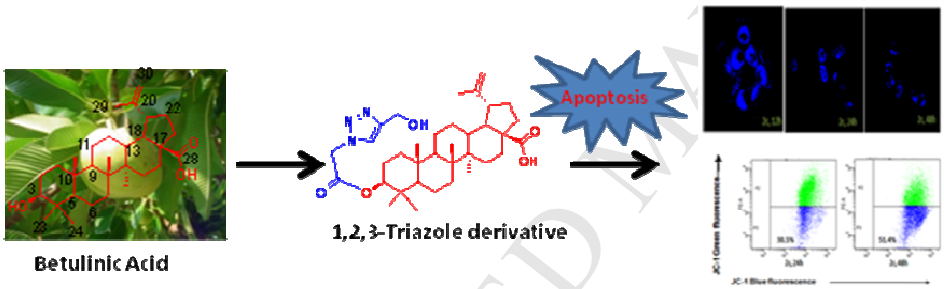

Synthesis and biological evaluation of a novel betulinic acid derivative as inducer of apoptosis in human colon carcinoma cells (HT-29)

Biswajit Chakraborty[a,‡], Debasmita Dutta[a,†], Sanjukta Mukherjee[‡], Supriya Das[§], Nakul C. Maiti[§], Padma Das[*,†] and Chinmay Chowdhury[*,‡]

[‡]Organic and Medicinal Chemistry Division, [†]Cancer Biology and Inflammatory Disorder Division, [§]Structural Biology and Bioinformatics Division, CSIR-Indian Institute of Chemical Biology, 4 Raja S. C. Mullick Road, Kolkata 700032, India.
[a]Contributed equally.

Abstract: A novel family of betulinic acid analogues, carrying a triazole unit at C-3 attached through a linker, was synthesized by the application of azide-alkyne "*Click reaction*". These were screened for their anticancer activity against different cancer cells and normal human PBMC by MTT assay. Compound **2c** [(3*S*)-3-{2-(4-(hydroxymethyl-1*H*-1,2,3-triazol-1-yl)acetyloxy}-lup-20(29)-en-28-oic acid] was found as the most potent inhibitor of cell line HT-29 with IC_{50} value 14.9 µM. Its role as an inducer of apoptosis was investigated in this cell line by Annexin-V/PI binding assay and by following its capability for ROS generation, depolarization of mitochondrial transmembrane potential, activation of caspases, PARP cleavage, nuclear degradation and expression of pro- and anti-apoptotic proteins. It exhibited much higher cytotoxicity than the standard drug 5-fluorouracil but showed negligible cytotoxicity towards normal PBMC. Elevated level of ROS generation, activation of caspase 3 and caspase 9, DNA fragmentation, higher expression of Bax and Bad, lower expression of Bcl2 and Bcl-xl, and increased level of Bax/Bcl-xl ratio identified **2c** as a promising inducer of apoptosis that follows a mitochondria dependent pathway. Bio-physical studies indicate that compound **2c** acts as a minor groove binder to the DNA.

Abbreviations: BA, Betulinic Acid; DIPEA, *N*,*N*-diisopropylethylamine; DMAP, 4-dimethylaminopyridine; MTT, 3-(4,5-dimethylthiazol-2-yl)-2,5-diphenyltetrazolium bromide; PBMC, peripheral blood mononuclear cells; ROS, Reactive oxygen species; FACS, Fluorescence-activated cell sorting; PARP, Poly(ADP-ribose)polymerase; CD, Circular dichroism.

Keywords: Betulinic acid, Triazole derivative, Cytotoxic activities, Mitochondrial dysfunction, Caspase activation, DNA binding.

Corresponding authors: E-mail: chinmay@iicb.res.in (CC), Tel: 91-33-2499 5862 (CC).
padmadas@iicb.res.in (PD), Tel: 91-33-2499 5899

1. Introduction

The synthetic anticancer drugs used along with conventional radiotherapy and chemotherapy frequently evoke adverse side effects, severe immunosuppression and alarming increase in the incidence of drug resistance. In contrast, natural products are considered to be a better option in the development of new drugs because of their potent therapeutic efficacy and minimum side effects. Indeed, some of the natural products have been used directly as a drug, while others have served as a source of structural or functional template in drug design. In recent years there has been a tremendous interest worldwide in the design and development of analogue libraries based on natural product templates. Notably, roughly around 50% of the currently used anti-cancer drugs were discovered from studies on either natural products or natural product based molecules [1].

Triterpenes represent an important class of natural products. Among these, pentacyclic lupane-type triterpenes are one of the most significant subclasses and some of them do exhibit several medicinal properties including anticancer [2]. Betulinic acid (BA) **1** (**Fig. 1**), a member of this class of pentacyclic triterpenes, has been shown to possess a range of biological activities such as anti-HIV [3a], anti-bacterial [3b], anti-malarial [3c], anti-inflammatory [3d] etc. Additionally, BA is also found to be cytotoxic towards a variety of cancer cell lines such as lung, ovarian, cervical, neuroblastoma, and gliobastoma including head and neck carcinomas [4]. Betulinic acid was also reported as a selective inhibitor of human melanoma [11a]; it induces apoptosis in human neuroblastoma [11b] as well. It has low toxicity and high safety profile in normal cell lines [5], and is safe for use even at a dose of 500 mg/Kg body weight [4a]. This feature calls for its development as anticancer drug in preference to other natural products like taxol, camptothecin, ellipticine, etoposide, vinblastin and vincristin etc. Previous reports reveal that the apoptotic properties of BA are due to modulation of Bcl-2 family and cell cycle regulatory protein [6], downregulation of NF-kB [7], inhibition of amino peptidase N [8], and growth factor induced angiogenesis [9]. Besides, BA acts as potent inhibitor of eukaryotic topoisomerase I and II [10]. The cytotoxic effects of BA have been studied in xenograft mouse models and the compound is currently undergoing clinical trials at NCI, USA [12]. From mechanistic view point, betulinic acid induces apoptosis by direct effects on mitochondria leading to cytochrome-c release, which in turn regulates the "downstream" caspase activation resulting in apoptosis ultimately [13]. This study indicates that mitochondria could be an attractive target in the development of anti-cancer therapeutics based on betulinic acid.

Despite such encouraging results, the poor solubility of BA preventing blood serum solubilizations and its low bioavailability have limited its potential to be used as a drug candidate. In order to overcome this lacuna, efforts are being made for structural modifications through judicious

manipulation of the functional groups present in the molecule [14]. In continuation of our studies [15] on structural modulations of bioactive natural products for the development of lead(s) having better efficacy and less toxicity than the parent compound, we chose betulinic acid to prepare an analogue library. We realised that a 1,2,3-triazole moiety can be attached at C3 hydroxy of BA through a linker, leading to the formation of analogues **2** (**Fig. 1**). The rationale for selecting 1,2,3-triazole was its remarkable binding affinity with biological receptors/enzymes through non-covalent interactions resulting in the discovery of various potent bioactive agents [16]. Besides, this class of compounds possess exceptional metabolic stability [17]. These favourable therapeutic indexes have led to the development of several 1,2,3-triazole containing drugs available in the market [18]. For our present study, we synthesized a number of 1,2,3-triazole derivatives **2** based on betulinic acid and assessed the potency of these compounds and the parent compound for the induction of cell death in five different cancer cell lines (derived from four different types of cancers) along with normal epithelial cell lines. 5-Fluorouracil, a well known agent in cancer chemotherapy, was used as a standard compound. The findings show that one of the developed molecules bears better anticancer potency against human colon carcinoma cells (HT-29) than the parent compound (BA) and 5-fluorouracil. The results obtained so far are described herein.

Figure 1

2. Results and discussions

2.1. *Chemistry:*

Betulinic acid used in this study was isolated in bulk quantity (~ 50 g) from methanolic extracts of the *Dillenia indica* fruits following the literature procedure [19]. Purification (>98%) was achieved by silica gel chromatography followed by fractional crystallizations. Thereafter, we initiated the study of derivatizations; we chose the C3 hydroxyl group of BA as functionalizations at this site are found to be more suited for showing anticancer activities compared to other functional groups (at C28 and C20) [4a]. Thus, (3*S*)-3-(2-chloroacetyloxy)-lup-20(29)-en-28-oic acid (**3**) was prepared (**Scheme 1**) by treating BA (**1**) with chloroacetyl chloride in the presence of *N*,*N*-diisopropylethylamine (DIPEA) and 4-dimethylaminopyridine (DMAP, catalytic amount). Azidation of **3** using sodium azide led to the isolation of the intermediate (3*S*)-(2-azidoacetyloxy)-lup-20(29)-en-28-oic acid (**4**) which served as a useful substrate for "click chemistry" employed in this work for the synthesis of targeted derivatives **2** (**Scheme 1**). On the other hand, some of the requisite acetylenic substrates **5** were prepared by the well-known "*Sonogashira coupling*"[20] between trimethylsilyl acetylene and aryl iodides followed by base

Scheme-1

mediated desilylation of the resulting products; other acetylenes were procured from commercial source. Thereafter, 1,3-dipolar cycloadditions of azide **4** with acetylenes **5** were carried out at room temperature by employing "*Click Chemistry*". The crude products **2** obtained after standard work-up of the reactions were purified (>96%) by silica gel (100-200 mesh) column chromatography; the yields (**Table 1**) and spectral data (see experimental section) usually refer to these compounds. However, for anti-cancer screening studies, these products were further purified (>99%) by HPLC using reverse phase C18 column [21]. As can be seen from **Table 1** (entries 2-10), alkyl/aryl/heteroaryl acetylenes **5b-j** underwent cycloadditions successfully with the azide **4** at room temperature within few hours affording 1,2,3-triazole derivatives **2**. Besides, even gaseous acetylene (balloon pressure) can be used as substrate in this reaction to afford the desired product **2a** with 60% yield (entry 1, Table 1). Interestingly, irrespective of the nature of the substituents (i.e., OMe, NO_2, CO_2Me, CO_2Et) in aryl/heteroaryl moiety of the acetylenic substrates **5**, all (except entry 1 of Table 1) produced their corresponding 1,2,3-triazole derivatives **2** with very good yields (80-90%). In ^{1}H-NMR, signal for the proton of 1,2,3-triazole ring of compounds **2** appeared around at δ 7.5 as singlet, while that for the methylenic protons (-$COCH_2$N-) at the C-3 side chain appeared in the region δ 4.6-5.6 as two separate doublets with coupling constant 12-17 Hz. Besides, the peaks for vinylic protons (H-29) of products **2** appeared as singlets around at δ 4.6 and 4.7, respectively, while that for H-3 was found at around δ 4.5 as multiplet (m). The remaining signals appeared at their appropriate positions.

Table 1

In a further study, we exposed the 1,4-dioxane solution of product **2d** to moist acetic acid at rt for 1h to achieve chemoselective deprotection of one of the isopropylidene moieties; this afforded the novel sugar derivative **2k** as shown in Scheme 2.

Scheme 2

In a recent study, few important betulinic acid derivatives conjugated with a well-known anti-viral agent AZT (3′-azido-3′-deoxythymidine) were synthesized and evaluated [22]. In view of the immense importance of uracil derivatives in cancer chemotherapy[23] along with our own interest[24] on these compounds, we became interested to convert the product **2e** to corresponding uracil derivative which may serve as uracil-betulinic acid conjugate via a 1,2,3-triazole linker. Indeed, treatment of compound **2e** with trimethylsilyl chloride and sodium iodide at rt led to the formation of desired uracil derivative **2l** with good yields (**Scheme 3**).

Scheme 3

2.2. *Biology:*

2.2.1. *Cytotoxic activity of Betulinic Acid analogues:*

The cytotoxic activity of betulinic acid analogues **2a-l** was studied using MTT assay on cultured cancer cells such as U937 (Human leukemic monocyte lymphoma cell line), HT-29 (Human colorectal adenocarcinoma), Jurkat (human T cell lymphoblast-like cell line), $HepG_2$ (human hepatocellular carcinoma), MCF-7 (human breast adenocarcinoma) as well as normal human PBMC (peripheral blood mononuclear cells) cells (**Table 2**). 5-Fluorouracil was used as the reference compound. We assessed the effects of different concentrations (0-50 µM) of the analogues for 48 h. Considering the IC_{50} values of **Table 2**, we conclude that compound **2c** was the most potent inhibitor of HT-29 cells (IC_{50} 14.9 µM); it also exhibited negligible cytotoxicity towards normal PBMC. All other IC_{50} values were more than 40 µM. The concentration of DMSO used to solubilize these compounds was 0.1% which had no effect on cell viability. As **2c** appeared to be the best among all the analogues tested, we compared the effects of the compound with standard drug 5-fluorouracil and the parent compound betulinic acid (see Table S1 in supplementary material); thereafter, we performed all apoptotic studies on HT-29 cell line using this compound (**2c**) as discussed below.

Table 2

2.2.2. *Compound 2c triggers ROS generation:*

Reactive oxygen species (ROS) are highly harmful elements to cells as they initiate oxidative stress and ultimately cause cellular damage. Excessive ROS generation renders cells vulnerable to apoptosis. To determine whether **2c** triggers ROS generation in HT-29 cells to induce apoptosis, the ROS level was measured with and without (control) treatment of **2c** (at IC_{50} dose) using CM-H_2DCFDA – a lipid soluble, membrane permeable non-fluorescent reduced derivative of 2,7-dichlorofluorescein. This was used based on the premise that the acetate groups of CM-H_2DCFDA are removed by esterase cleavage intracellularly to produce the hydrophilic, non-fluorescent dye dichlorodihydrofluorescein ($DCFH_2$) which is subsequently oxidized by ROS to form the highly fluorescent product dichlorofluorescein (DCF). The fluorescence generated is directly proportional to the quantum of ROS generated [25]. The ROS level was measured in terms of MFI. Interestingly, compound **2c** was capable of inducing ROS in HT-29 cells within 15 min of treatment, with MFI value 1270±14.6 which is more than two times that of control, $p<0.001$ (**Fig. 2A**). Taken together, these results indicate that **2c** causes oxidative imbalance in HT-29 cells. This induction of oxidative burst is a key factor behind the anti proliferative activity of **2c**. To confirm the elevated levels of ROS generation by **2c,** cells were pre-incubated with 2.5 mM of N-acetyl cysteine (NAC), an established anti-oxidant, for 3 h before treatment with **2c**. To determine the role

of ROS in **2c** mediated action, cells preincubated with NAC (2.5 mM; 3 h) were treated with **2c** and analyzed for cell viability assay. In the pretreated cells, there was no change in percentage of cell viability. But in cells subjected to **2c** treatment after incubation with NAC, cell viability increased two times ($IC_{50:}$ 30.4 µM, **Fig. 2B**), thereby confirming that IC_{50} concentration of **2c** was the only contributing factor responsible for excessive ROS generation and ultimately causing apoptosis.

Figure 2A and 2B

2.2.3. ***Analogue 2c induces apoptosis in HT-29 cells:***

In order to determine whether the **2c** induced reduction in cell viability was responsible for the induction of apoptosis, HT-29 cells were co-stained with PI and Annexin-V FITC, and the number of apoptotic cells was estimated by flow cytometry. Translocation of phosphatidylserine from the inner aspect to the outer leaflet of the plasma membrane occurs during apoptosis which can be detected by utilizing the high binding affinity of Annexin V, a Ca^{+2} dependent phospholipid binding protein, to phosphatidylserine [26]. In contrast, the non permeable stain propidium iodide (PI) has affinity towards nucleic acids and selectively enters necrotic or late apoptotic cells. A time-dependent increase in the percentage of apoptotic cells was noted after the cells were treated for 12, 24, and 48 h with analogue **2c** at IC_{50} concentration. As shown in **Fig. 3**, very few (0.3%) apoptotic cells were present in the control panel, whereas after treatment with **2c** the population rose to 15.6% at 12 h. Further increase to 17.6% and 23.4% occurred after treatment for 24 and 48 h, respectively. The percentage of PI positive cells is negligible. These indicate that **2c** induces significant apoptotic cell death in HT-29 cells in comparison with control, in a time-dependent manner.

Figure 3

2.2.4. ***Compound 2c triggers mitochondrial pathway dependent apoptosis:***

The loss of mitochondrial transmembrane potential ($\Delta\psi_m$) also reflects apoptosis. This was measured by using a cationic, lipophilic, fluorescent dye JC-1 capable of selectively entering mitochondria and acting as a dual emission probe [27]. With normal cells (high MMP), JC-1 displays a green fluorescence (590 nm). This is caused by spontaneous and local formation of aggregates that are associated with a large shift in the emission. In contrast, when the mitochondrial membrane is depolarized (low MMP), JC-1 forms monomers that emit blue fluorescence (at 530 nm). Here, the percentage of green fluorescence represents cells with polarized mitochondria whereas that of blue fluorescence serves as an indicator of cells with loss of mitochondrial transmembrane potential. A gradual time dependent change from green to blue fluorescence was observed in HT-29 cells after treatment with **2c**. In control cells,

percentage of cells with depolarized mitochondria was 1.75, which increased to 16.5% at 12 h, 30.5% at 24 h and 51.4 % at 48 h of treatment, suggesting the occurrence of depolarization of mitochondria by **2c** (**Fig. 4**).

Figure 4

2.2.5. ***Activation of caspases and cleavage of PARP by 2c:***

Various proteolytic enzymes (like cytochrome c which activates caspases) are released from depolarized mitochondria and are the main executors of apoptosis. Caspases are also the key regulatory proteases of apoptotic pathways. Activation of this family of proteins provides confirmatory evidence towards apoptosis. Depolarization of the mitochondrial transmembrane potential causes a change in the mitochondrial membrane permeability which helps to release apoptotic factors from mitochondria and thereby activates caspases [28]. In order to prove that **2c** induces caspase activation, cell lysates were prepared as described in materials and methods and levels of activated caspases 8, 9 and 3 were measured using quantitative detection of colorimetric tetrapeptide substrates. As shown in **Fig. 5A** and **5B**, activities of caspases 3 and 9 increased significantly after 48 h treatment with **2c** as compared to control. In contrast, the level of caspase 8 (**Fig. 5C**) did not increase significantly even after 48 h of treatment. To confirm the role of caspases in apoptosis induced by **2c**, we studied the specific cleavage of PARP (116 kDa), a well known substrate of caspase 3 [29]. When HT-29 cells were treated with analogue **2c** at IC_{50} concentration, specific cleavage of PARP yielded 85 kDa fragments (as shown in the results), which was confirmed by analysis using western blotting with anti-PARP antibodies for different time durations **(Fig. 5D)**. A well known function of PARP is its ability to repair single-strand DNA nicks. Indeed cleavage of PARP was found to be causing abatement of DNA repairing process leading to further cellular damage.

Figure 5A, 5B, 5C and 5D

2.2.6. ***Compound 2c causes DNA fragmentations and morphological changes:***

An essential hallmark of apoptosis is DNA fragmentation and morphological changes caused by the involvement of caspases. We stained the HT-29 cells with Hoechst 33258 dye. The treatment of the HT-29 cells with 14.9 µM of compound **2c** resulted in the induction of chromatin condensation, fragmentation, membrane blebbing and clear apoptotic bodies that were visualized in confocal microscopy (**Fig. 6**).

Figure 6

2.2.7. ***Compound 2c induced expression of pro- and anti-apoptotic proteins:***

Since Bax and Bcl-2 play a significant role in apoptosis [30], we studied the effect of analogue **2c** on the expression of pro-apoptotic protein Bax and Bad, and anti-apoptotic proteins Bcl-2 and Bcl-xl in HT-29 cells. The Western blot analysis demonstrated time dependent elevations in Bax and Bad (**Fig. 7A**); this was clearly reflected in the gradual reduction in Bcl-2/Bax ratio with time (**p<0.01; **Fig. 7B**). The significant reduction in the ratio suggested the involvement of Bcl-2 family proteins, a mediator of the mitochondrial apoptosis pathway, in apoptosis of HT-29 cells induced by **2c**, which is mediated by the mitochondria-dependent pathway.

Figure 7A and 7B

2.3. ***Bio-physical studies of compound 2c:***

2.3.1. ***Compound 2c decreases UV absorption of DNA binding:***

The binding efficacy and mode of binding to DNA of **2c** were measured by absorption spectroscopic analysis. DNA shows an intense absorption band at 260 nm (**Fig. 8A**). Addition of **2c** caused decrease in the absorption. The normalized absorbance vs wavelength plot clearly indicated decrease in absorbance with increase in concentration of **2c** (**Fig. 8B**).[31] This implied clearly that **2c** interacts with DNA effectively. The binding isotherm (**Fig. 9**) for DNA-**2c** interaction was obtained by plotting fraction (θ) of DNA bound to **2c** vs total compound concentration. The value of θ was calculated according to the following equation:

$$\theta = (A_0 - A_i)/(A_0 - A_\alpha)$$

where A_0 is the absorbance of DNA in the absence of the compound at 260 nm. A_i is the absorbance of DNA in the presence of the compound and A_α is the absorbance of DNA at compound concentration for which maximum binding took place. K_b was obtained from the reciprocal of the ligand concentration at the half saturation point of the binding isotherm.[32] The measured binding constant was $8.375 \times 10^4\ M^{-1}$.

Figure 8A, 8B and 9

2.3.2. ***Compound 2c caused no significant changes in the DNA conformation*****:**

Circular dichroism (CD) analysis was carried out to measure the effect of binding to conformational changes in DNA duplex structure. The CD spectra of the DNA solution (500 µg/mL) in the absence and presence of **2c** (50 µM) were recorded after 2 h incubation of the mixture at 37 °C (**Fig. 10**). DNA solution showed a positive absorbance at 275 nm due to base stacking and a negative absorbance at 245 nm due to the B-conformation of DNA [32]. The absorbance and peak position were not perturbed significantly in the presence of **2c** (red line in Figure 10). It is known from earlier reports that the

electrostatic interaction or groove binding of small molecules to DNA does not severely affect the absorbance at 275 nm, whereas, changes in absorption at 245 nm implies change in B-DNA conformation or the formation of other structures [32]. The CD spectra of the DNA in the presence of **2c** was very similar to the CD spectra of DNA itself, indicating that **2c** caused no major alteration of DNA conformation. Thus this study implied that compound **2c** may act as groove binder of DNA but not as intercalator.

Figure 10

2.3.3. ***Molecular Modeling: Compound 2c binds to a minor groove of DNA as determined by Molecular Docking:***

In order to find the type of groove binding (major or minor), we carried out molecular modeling studies on compound **2c**. Out of the 100 docking runs performed for DNA-**2c** complexes, favorable binding poses were obtained which presented most negative binding free energies. Molecular docking results showed that **2c** had the best binding energy of -10.09 kcal/mol when it bound with the DNA as a minor groove binder. A crystallographic DNA with no gap (PDB entry 1DNE, resolution 2.4 Å), which was the crystal structure of a DNA complex with the known minor groove binder [33] netropsin (obtained binding energy -7.02 kcal/mol), was chosen as the control model so that it would be capable of accommodating a minor groove binder (**Fig. 11**). Water molecules and the bound netropsin were removed from the structure. Then, the obtained DNA structure was used as receptor model for the docking studies.

Figure 11

3. Conclusion

In this endeavor, to develop promising anticancer agent(s) based on betulinic acid, a new library of compounds having 1,2,3-triazole moiety attached to C-3 of betulinic acid were synthesized and the anti-cancer activities of these compounds were evaluated (*in vitro)* against different cancer cell lines (i.e., breast, colon, liver and leukemic). Interestingly, one (**2c**) of the compounds was found to be significantly active against HT-29 (human colon adenocarcinoma) cell lines and this activity profile was better than that of the parent compound (BA). Induction of apoptosis by **2c** is characterized by ROS generation, the externalization of phosphotidylserine, loss in mitochondrial membrane potential, induced expression of pro and antiapoptotic proteins, and appreciable DNA fragmentations. The structure-activity relationship studies (SARs) indicate that the 1,2,3-triazole moiety favors the activity when substituted at C4 (of the heterocycle) with a hydroxymethyl group, but disfavors it when the substituent is an aromatic or heteroaromatic moiety. Further studies to refine it are currently under progress.

4. Experimental

4.1. *Chemistry*

4.1.1 *General methods*

Betulinic acid (**1**) was isolated from dried and powdered fruits of *Dillenia indica*. All solvents were distilled prior to use. Petroleum ether refers to fraction boiling in the range 60-80 °C. Dichloromethane (DCM) was dried over CaH_2, distilled and stored over 3Å molecular sieves. All the reactions were performed under argon atmosphere and anhydrous conditions unless otherwise noted. Reactions were monitored by thin-layer chromatography (TLC) on aluminium sheets 20 × 20 cm coated with silica gel 60 F_{254}. Visualization of the developed chromatogram was performed by UV light or iodine or Liebermann solution. Analytical (C18, 5 μm, 4.6 × 250 mm column) and semi preparative (C18, 5 μm, 10 × 250 mm column) HPLC were performed to purify the final compounds.

^1H and ^{13}C NMR spectra were recorded in 300 or 600 MHz spectrometer. Chemical shifts (δ) are reported in parts per million (ppm) downfield from tetramethylsilane (δ = 0.00) with the residual proton signal of deuterated solvents used [$CDCl_3$: ^1H NMR, δ = 7.26 ppm (s), ^{13}C NMR, δ = 77.0 ppm (t); CD_3OD : ^1H NMR, δ = 4.86 ppm, 3.32 ppm, ^{13}C NMR, δ = 49.0 ppm (m)]. Coupling constants (*J*) were expressed in Hertz (Hz) and spin multiplicities are given as s (singlet), d (doublet), dd (double doublet), t (triplet), m (multiplet) and br (broad). Mass spectra were obtained from ESI-TOF and FAB-EI MS mass spectrometer. Infrared spectra (IR) were obtained as neat or KBr plate. Specific rotations were measured on JASCO P-1020 polarimeter at 589 nm.

4.1.2. *Preparations of starting materials*

4.1.2.1. (3*S*)-3-(2-chloroacetyloxy)-lup-20(29)-en-28-oic acid (3)

The compound was prepared according to the literature procedure [34] (for details see the supplementary material).

4.1.2.2. (3*S*)-(2-azidoacetyloxy)-lup-20(29)-en-28-oic acid (4)

Compound **3** (500 mg, 0.94 mmol) was dissolved in dry DMF, mixed with NaN_3 (123 mg, 1.9 mmol) under argon atmosphere and the reaction mixture was allowed to reflux at 70 °C for 4 h. After completion of the reaction (confirmed by monitoring TLC) the solvent was evaporated to dryness under reduced pressure and the residue was extracted with ethyl acetate (3× 15 mL). The combined organic extracts were washed with water (10 mL) and brine (10 mL), dried over anhydrous Na_2SO_4, filtered and concentrated under reduced pressure. The resulting residue was purified through silica gel (100-200

mesh) column chromatography using 10% ethyl acetate in petroleum ether (v/v) as eluent to obtain the desired product **4.** Yield: 77%, white solid, m.p. = 245-246°C; IR (Neat) ν_{max} : 2944, 2107, 1738, 1695, 1196 cm^{-1}; ^1H NMR ($CDCl_3$, 300 MHz): δ 4.74 (1H, s), 4.61-4.57 (2H, m), 3.85 (2H, s), 3.04-2.97 (1H, m), 2.29-2.11 (2H, m), 2.03-1.91 (2H, m), 1.69 (3H, s), 1.65-1.39 (12H, m), 1.34-1.16 (6H, m), 0.97 (3H, s), 0.93 (3H, s), 0.87 (3H, s), 0.85 (3H, s), 0.82 (3H, s), 0.79 (3H, s); ^{13}C NMR ($CDCl_3$, 75 MHz): δ 182.7, 168.1, 150.3, 109.7, 83.2, 56.4, 55.3, 50.6, 50.3, 49.2, 46.9, 42.4, 40.6, 38.4, 38.3, 37.8, 37.1, 34.1, 32.1, 30.5, 29.6, 27.9, 25.3, 23.6, 20.8, 19.3, 18.1, 16.4, 16.1, 15.9, 14.6; MS (ESI) 562.20 $[M+Na]^+$. HRMS $[EI]^+$ m/z calculated for $C_{32}H_{49}N_3O_4$ 539.37231, found 539.37207.

4.1.3. ***General procedure for the synthesis of 1,2,3-triazole derivatives 2 (except the compound 2a) employing "Click Chemistry"*****:**

Compound **4** (1.0 eqv.) dissolved in dry DMSO (2 mL) was treated with terminal acetylenes **5** (1.1 eqv.) in the presence of sodium ascorbate (1.01 eqv.) and $CuSO_4.5H_2O$ (1.01 eqv.), and the mixture was stirred at room temperature for 2-18 h under argon atmosphere until the complete consumption of starting materials. It was then purified by silica gel (100-200 mesh) column chromatography using 70-88% ethyl acetate in petroleum ether (v/v) as eluent. The yield was calculated based on the product isolated through column chromatography; however, products screened for anti-cancer assay were further purified by HPLC.

Synthesis of compound **2a** and its spectroscopic data have been provided in supplementary material.

4.1.3.1. (3*S*)-3-[2-(4-butyl-1*H*-1,2,3-triazol-1-yl)acetyloxy]-lup-20(29)-en-28-oic acid (2b)

Yield: 98%; white solid, m.p. = 133-135 °C; $[\alpha]^{25}_D$ + 20.2 (c 0.23, $CHCl_3$); IR (Neat) ν_{max}: 3144, 3072, 2950, 2870, 1744, 1643, 1460, 1374, 1269, 1222 cm^{-1}; ^1H NMR ($CDCl_3$, 300 MHz): δ 7.40 (1H, s), 5.13 (1H, d, *J* = 17.7 Hz), 5.11 (1H, d, *J* = 17.7 Hz), 4.73 (1H, s), 4.60 (1H, s), 4.54 (1H, dd, *J* = 11.1, 4.5 Hz), 3.00-2.99 (1H, m), 2.74 (2H, t, *J* = 7.6 Hz), 2.29-2.25 (1H, m), 2.17-2.15 (1H, m), 1.99-1.95 (3H, m), 1.68 (3H, s), 1.66-1.56 (9H, m), 1.52-1.32 (12H, m), 1.27-1.15 (3H, m), 0.96 (3H, s), 0.93 (3H, s), 0.92 (3H, s), 0.82 (3H, s), 0.81 (3H, s), 0.72 (3H s); ^{13}C NMR ($CDCl_3$,150 MHz): δ 180.5, 166.2, 150.3, 148.9, 121.9, 109.7, 83.7, 56.3, 55.3, 51.1, 50.3, 49.2, 46.8, 42.4, 40.6, 38.3, 38.2, 37.8, 37.1, 37.0, 34.1, 32.1, 31.5, 30.5, 29.6, 27.9, 25.4, 25.2, 23.7, 22.2, 20.8, 19.3, 18.1, 16.3, 16.1, 16.0, 14.6, 13.8. MS (ESI) 644.39 $[M+Na]^+$. HRMS $[EI]^+$ m/z calculated for $C_{38}H_{59}N_3O_4$ 621.45056, found 621.45105.

4.1.3.2. (3*S*)-3-[2-(4-hydroxymethyl-1*H*-1,2,3-triazol-1-yl)acetyloxy]-lup-20(29)-en-28-oic acid (2c)

Yield: 84%; white solid, m.p. = 212-214 °C; $[\alpha]^{25}_D$ + 33.8 (c 0.24, $CHCl_3$); IR (Neat) ν_{max}: 3415, 3144, 3073, 2947, 2872, 1741, 1689, 1457, 1374, 1274, 1229, 1013 cm^{-1}; ^1H NMR ($CDCl_3$, 300 MHz): δ 7.62

(1H, s), 5.20 (1H, d, *J* = 17.4 Hz), 5.11 (1H, d, *J* = 17.4 Hz), 4.82 (1H, d, *J* = 13.5 Hz), 4.76 (1H, d, *J* = 13.5 Hz), 4.73 (1H, s), 4.60 (1H, s), 4.52 (1H, dd, *J* = 11.2, 4.65 Hz), 3.02-2.98 (1H, m), 2.31-2.18 (3H, m), 2.10-1.91 (4H, m), 1.68 (3H, s), 1.63-1.49 (9H, m), 1.45-1.05 (10H, m), 0.95 (3H, s), 0.89 (3H, s), 0.78 (3H, s), 0.75 (3H, s), 0.54 (3H, s); ^{13}C NMR ($CDCl_3$,75 MHz): δ 181.1, 165.5, 150.5, 148.1, 123.2, 109.6, 83.8, 56.3, 55.5, 55.1, 51.4, 50.1, 49.2, 46.8, 42.3, 40.5, 38.0, 37.7, 37.0, 33.9, 32.2, 30.5, 29.6, 27.8, 25.2, 23.5, 20.7, 19.3, 18.2, 16.1, 16.0, 14.5; MS (ESI) 618.12 $[M+Na]^+$. HRMS $(FAB)^+$ m/z calculated for $C_{35}H_{54}N_3O_5$ $[M+H]^+$ 596.40635, found 596.40790.

4.1.3.3. (3*S*)-3-[2-(4-{[5-(2,2-dimethyl-1,3-dioxolan-4-yl)-2,2-dimethyltetrahydrofuro[3,2-*d*][1,3]dioxol-6-yloxy]methyl}-1*H*-1,2,3-triazol-1-yl)acetyloxy]-lup-20(29)-en-28-oic acid (2d)

Yield: 98%; white solid, m.p. = 169-171 °C; ^{1}H NMR ($CDCl_3$, 300 MHz): δ 7.77 (1H, s), 5.87 (1H, d, *J* = 3.6 Hz), 5.17 (1H, d, *J* = 17.7 Hz), 5.14 (1H, d, *J* = 17.7 Hz), 4.86 (1H, d, *J* = 12.6 Hz), 4.81 (1H, d, *J* = 12.6 Hz), 4.73 (1H, s), 4.60 (d, J=3.3 Hz, 1H), 4.60-4.53 (2H, m), 4.34-4.28 (1H, m), 4.15-4.08 (2H, m), 4.07 (1H, brs), 4.02-3.97 (1H, m), 3.03- 2.96 (1H, m), 2.29-2.10 (3H, m), 2.04-1.91 (3H, m), 1.68 (3H, s), 1.64-1.56 (9H, m), 1.49 (3H, s), 1.42 (3H, s), 1.35 (3H, s), 1.31 (3H, s), 1.28-1.01 (10H, m), 0.96 (3H, s), 0.88 (3H, s), 0.83 (6H, brs), 0.75 (3H, s); ^{13}C NMR ($CDCl_3$, 75 MHz): 182.0, 165.9, 150.3, 145.2, 123.8, 111.8, 109.7, 109.0, 105.2, 83.8, 82.5, 81.7, 81.0, 72.3, 67.3, 63.9, 56.3, 55.2, 51.0, 50.2, 49.1, 46.8, 42.3, 40.6, 38.2, 37.8, 37.0, 34.1, 32.1, 30.5, 29.6, 27.9, 26.8, 26.1, 25.4, 23.5, 20.8, 19.2, 18.0, 16.3; MS (ESI) 860.24 $[M+Na]^+$. HRMS $(FAB)^+$ m/z calculated for $C_{47}H_{72}N_3O_{10}$ $[M+H]^+$ 838.52177, found 838.51849.

4.1.3.4. (3*S*)-3-[2-{4-(2,4-dimethoxypyrimidin-5-yl)-1*H*-1,2,3-triazol-1-yl}acetyloxy]-lup-20(29)-en-28-oic acid (2e)

Yield: 82%; white solid; $[\alpha]^{25}_D$ + 10.5 (c 0.27, MeOH); IR (Neat) ν_{max}: 3444, 2948, 2871, 1744, 1617, 1568, 1467, 1381, 1284, 1223, 1141, 1086, 1043, 1013 cm^{-1}; ^{1}H NMR ($CDCl_3$, 300 MHz): δ 9.17 (1H, s), 8.04 (1H, s), 5.23 (1H, d, *J* = 17.2 Hz), 5.21 (1H, d, *J* = 17.2 Hz), 4.73 (1H, s), 4.60-4.57 (1H, m), 4.08 (3H, s), 4.05 (3H, s), 3.00-2.99 (1H, m), 2.29-2.18 (3H, m), 2.04-1.95 (3H, m), 1.68 (3H, s), 1.64-1.56 (6H, m), 1.48-1.32 (10H, m), 1.28-1.01 (4H, m), 0.96 (3H, s), 0.92 (3H, s), 0.83 (3H, s), 0.79 (3H, s), 0.74 (3H, s); ^{13}C NMR ($CDCl_3$,75 MHz): δ 182.1, 166.8, 166.0, 164.5, 156.2, 150.4, 140.0, 123.7, 109.7, 106.2, 83.9, 56.3, 55.2, 55.0, 54.3, 51.1, 50.3, 49.2, 46.9, 42.4, 40.6, 38.3, 38.2, 37.8, 37.0, 34.1, 32.1, 30.5, 29.6, 27.9, 25.3, 23.5, 20.8, 19.3, 18.1, 16.3, 16.1; MS (ESI) 726.08 $[M+Na]^+$. HRMS $(FAB)^+$ m/z calculated for $C_{40}H_{58}N_5O_6$ $[M+H]^+$ 704.43871, found 704.43878.

4.1.3.5. (3*S*)-3-{2-[4-(1*H*-indol-5-yl)-1*H*-1,2,3-triazol-1-yl]acetyloxy}-lup-20(29)-en-28-oic acid (2f)

Yield: 70%; white solid, m.p. = 207-209 °C; $[\alpha]^{25}_{D}$ + 16.7 (c 0.16, MeOH); IR (Neat) ν_{max} : 3414, 2946, 2870, 1741, 1640, 1449, 1371, 1223, cm^{-1}; ^{1}H NMR (DMSO-d_6, 300 MHz): δ 11.1 (1H, s), 8.44 (1H, s), 8.01 (1H, s), 7.58 (1H, dd, *J* = 8.4, 1.2 Hz), 7.44 (1H, d, *J* = 8.4 Hz), 7.36 (1H, t, *J* = 2.5 Hz), 6.47 (1H, s), 5.49 (1H, d, *J* = 17.4 Hz), 5.36 (1H, d, *J* = 17.7 Hz), 4.68 (1H, s), 4.55 (1H, s), 4.47 (1H, t, *J* = 7.8 Hz), 4.05 (1H, brs), 2.99-2.91 (3H, m), 2.25-2.08 (3H, m), 1.90-1.72 (3H, m), 1.63 (3H, s), 1.50 (6H, m), 1.47-1.10 (10H, m), 0.93 (3H, s), 0.85 (3H, s), 0.80 (3H, s), 0.78 (3H, s), 0.68 (3H, s); ^{13}C NMR (DMSO-d_6, 75 MHz): δ 166.9, 150.3, 147.9, 135.7, 127.9, 126.1, 121.6, 121.5, 119.0, 116.8, 111.8, 101.4, 82.0, 55.4, 54.4, 50.6, 49.5, 48.5, 46.6, 42.0, 37.5, 36.5, 33.6, 31.7, 30.1, 29.2, 27.5, 25.0, 23.2, 20.4, 18.9, 17.6, 16.1, 15.8, 15.7, 14.3; MS (ESI) 703.36 $[M+Na]^+$. HRMS $(FAB)^+$ m/z calculated for $C_{42}H_{57}N_4O_4$ $[M+H]^+$681.43798, found 681.43800.

4.1.3.6. (3*S*)-3-[2-(4-phenyl-*1H*-1,2,3-triazol-1-yl)acetyloxy]-lup-20(29)-en-28-oic acid (2g)

Yield: 98%; white solid, m.p. = 148-151 °C; $[\alpha]^{25}_{D}$ -119.8 (c 0.21, $CHCl_3$); IR (Neat) ν_{max} : 3442, 3138, 3074, 2946, 1746, 1718, 1643, 1465, 1376, 1266 cm^{-1}; ^{1}H NMR ($CDCl_3$, 300 MHz): δ 7.90 (1H, s), 7.84 (2H, d, *J* = 7.2 Hz), 7.46-7.32 (3H, m), 5.21 (2H, s), 4.73 (1H, s), 4.60 (1H, s), 4.57-4.55 (1H, m), 3.00-2.98 (1H, m), 2..28- 2.14 (3H, m), 2.04-1.95 (3H, m), 1.68 (3H, s), 1.64-1.56 (3H, m), 1.45-1.37 (10H, m), 1.28-1.06 (6H, m), 0.96 (3H, s), 0.92 (3H, s), 0.84-0.83 (6H, m), 0.74 (3H, s); ^{13}C NMR ($CDCl_3$, 75 MHz): δ 181.4, 165.9, 150.3, 148.2, 130.3, 128.8, 128.2, 125.8, 120.9, 83.9, 56.3, 55.3, 51.2, 50.3, 49.2, 46.9, 42.4, 40.6, 38.3, 37.9, 37.1, 34.1, 32.1, 30.5, 29.6, 28.0, 25.4, 23.6, 20.8, 19.3, 18.1, 16.3, 16.1, 15.9, 14.6; MS (ESI) 664.36 $[M+Na]^+$. HRMS $(FAB)^+$ m/z calculated for $C_{40}H_{56}N_3O_4$ $[M+H]^+$ 642.42708, found 642.42600.

4.1.3.7. (3*S*)-3-{2-[4-(4'-nitrophenyl)-1*H*-1,2,3-triazol-1-yl]acetyloxy}-lup-20(29)-en-28-oic acid (2h)

Yield: 80%; white solid, m.p. = 233-235 °C; $[\alpha]^{25}_{D}$ + 18.1 (c 0.15, $CHCl_3$);IR (Neat) ν_{max}: 3442, 3139, 3074, 2948, 2871, 1743, 1688, 1606, 1517, 1459, 1341, 1231, 1108, 1044 cm^{-1}; ^{1}H NMR ($CDCl_3$, 300 MHz): δ 8.31 (1H, d, *J* = 8.7 Hz), 8.07 (1H, s), 8.02 (1H, d, *J* = 8.7 Hz), 5.25 (2H, s), 4.73 (1H, s), 4.60-4.57 (2H, m), 2.99-2.96 (1H, m), 2.28-2.15 (3H, m), 1.97-1.95 (3H, m), 1.68 (3H, s), 1.64-1.56 (8H, m), 1.45-1.37 (8H, m), 1.28-1.15 (5H, m), 0.96 (3H, s), 0.92 (3H, s), 0.85 (3H, s), 0.84 (3H, s), 0.76 (3H, s); ^{13}C NMR (DMSO-d_6, 75 MHz): δ 177.2, 166.6, 150.3, 146.7, 144.4, 136.9, 125.9, 124.9, 124.6, 115.6, 109.6, 82.2, 55.8, 55.4, 54.3, 50.8, 49.5, 48.5, 46.6, 42.0, 37.5, 37.4, 36.5, 36.3, 33.6, 32.1, 31.6, 30.1, 29.1, 29.0, 27.5, 25.0, 23.2, 20.4, 18.9, 17.6, 16.1, 15.8, 15.6, 14.3; MS (ESI) 709.57 $[M+Na]^+$. HRMS $(FAB)^+$ m/z calculated for $C_{40}H_{55}N_4O_6$ $[M+H]^+$ 687.41216, found 687.41205.

4.1.3.8. (3*S*)-3-{2-[4-(4'-methoxycarbonyl-phenyl)-1*H*-1,2,3-triazol-1-yl]acetyloxy}-lup-20(29)-en-28-oic acid (2i)

Yield: 91%; white solid, m.p. = 181-182 °C; $[\alpha]^{25}_{D}$ + 11.0 (c 0.13, MeOH); IR (Neat) ν_{max} : 3427, 3143, 3072, 2948, 2871, 1722, 1616, 1458, 1375, 1281, 1226, 1109, 1017 cm^{-1}; ^{1}H NMR ($CDCl_3$, 600 MHz): δ 8.10 (2H, d, *J* = 8.4 Hz), 8.00 (1H, s), 7.91 (2H, d, *J* = 8.4 Hz), 5.24 (1H, d, *J* = 17.4 Hz), 5.21 (1H, d, *J* = 17.4 Hz), 4.72 (1H, s), 4.60 (1H, s), 4.57 (1H, d, *J* = 4.8 Hz), 3.93 (3H, s), 3.01-2.97 (1H, m), 2.26 (1H, d, *J* = 12.6 Hz), 2.17 (1H, t, *J* = 5.4 Hz), 2.02-1.94 (2H, m), 1.78-1.70 (2H, m), 1.68 (3H, s), 1.65-1.58 (3H, m), 1.53-1.42 (4H, m), 1.41-1.34 (7H, m), 1.32-1.23 (4H, m), 1.85-1.62 (1H, m), 1.06-0.99 (2H, m), 0.96 (3H, s), 0.91 (3H, m), 0.83 (3H, s), 0.82 (3H, s), 0.78-0.76 (1H, m), 0.74 (3H, s); ^{13}C NMR ($CDCl_3$, 150MHz): δ 166.7, 165.8, 150.3, 147.2, 134.6, 130.2, 129.7, 125.6, 121.8, 109.7, 84.0, 56.2, 55.3, 52.1, 51.2, 50.3, 49.2, 46.9, 42.4, 40.6, 38.3, 38.2, 37.8, 37.06, 37.01, 36.5, 34.1, 32.1, 31.4, 30.5, 29. 7, 29.6, 28.0, 25.3, 23.6, 20.8, 19.3, 18.0, 16.3, 16.1, 16.0, 14.6. MS (ESI) 722.49 $[M+Na]^+$. HRMS $(FAB)^+$ m/z calculated for $C_{42}H_{58}N_3O_6$ $[M+H]^+$ 700.43256, found 700.43353.

4.1.3.9. (3*S*)-3-{2-[4-(4'-ethoxycarbonyl-phenyl)-1*H*-1,2,3-triazol-1-yl]acetyloxy}-lup-20(29)-en-28-oic acid (2j)

Yield: 90%; white solid, m.p. = 144-146 °C; $[\alpha]^{25}_{D}$ + 16.9 (c 0.23, $CHCl_3$); IR (Neat) ν_{max} : 3443, 3144, 3072, 2947, 2871, 1714, 1617, 1460, 1372, 1277, 1228, 1107, 1018 cm^{-1}; ^{1}H NMR ($CDCl_3$, 600 MHz): δ 8.10 (2H, d, *J* = 8.4 Hz), 8.00 (1H, s), 7.91 (2H, d, *J* = 7.8 Hz), 5.24 (1H, d, *J* = 18 Hz), 5.21 (1H, d, *J* = 18 Hz), 4.72 (1H, s), 4.60 (1H, s), 4.59-4.57 (1H, m), 4.40 (1H, d, *J* = 7.2 Hz), 4.37 (1H, d, *J* = 7.2 Hz), 3.01-2.97 (1H, m), 2.26 (1H, d, *J* = 12.6 Hz), 2.19-2.15 (1H, m), 2.05-2.00 (2H, m), 1.73-1.70 (1H, m), 1.68 (3H, s), 1.65-1.56 (3H, m), 1.54-1.46 (4H, m), 1.49-1.39 (7H, m), 1.36-1.32 (3H, m), 1.30-1.21 (4H, m), 1.20-1.59 (1H, m), 1.07-0.99 (2H, m), 0.96 (3H, s), 0.91 (3H, s), 0.83 (3H, s), 0.82 (3H, s), 0.78-0.76 (1H, s), 0.74 (3H, s); ^{13}C NMR ($CDCl_3$, 150MHz): δ 166.2, 165.8, 150.3, 147.2, 134.5, 130.1, 125.5, 121.8, 109.7, 84.0, 61.0, 55.2, 51.2, 50.3, 49.2, 46.9, 42.4, 40.6, 38.3, 38.2, 37.8, 37.0, 34.1, 32.1, 30.5, 29.6, 27.9, 25.3, 23.6, 20.8, 19.3, 18.0, 16.3, 16.1, 16.0, 14.6, 14.3. MS (ESI) 736.50 $[M+Na]^+$. HRMS $(FAB)^+$ m/z calculated for $C_{43}H_{60}N_3O_6$ $[M+H]^+$ 714.44821, found 714.44507.

4.2. *Biology*

4.2.1. *Ethics Statement*

Ethical approvals of blood samples used in this study and consent procedure were obtained from Internal Review Board (Ethical Committee on Human Subjects) of CSIR-Indian Institute of Chemical Biology.

All clinical investigations have been conducted according to the principles expressed in the Declaration of Helsinki.

4.2.2. *Materials*

3-(4,5-Dimethylthiazol-2-yl)-2,5-diphenyl-tetrazolium bromide (MTT) was purchased from USB Corporation (USA). Pen strep, RPMI 1640, High Glucose DMEM, and Heat inactivated Fetal Bovine Serum (FBS), 5,5',6,6'-tetrachloro-1,1',3,3'- tetraethyl benzimidazolyl carbocyanine iodide (JC-1), and 5-(and-6)-chloromethyl-2',7'-dichloro dihydrofluorescein diacetate (CM-H_2DCFDA) were obtained from Invitrogen (Carlsbad, CA, USA). Caspase-3, Caspase-8, Caspase-9 colorimetric assay kits were procured from Biovision (Milpitas, CA, USA). The antibodies against Bcl2, Bax, Bcl-xl, Bad, β-Actin, and PARP, Alkaline phosphatase/Horseradish peroxidase conjugated secondary antibodies, and enhanced chemiluminescence kit were purchased from Santa Cruz Biotechnology (Santa Cruz, CA, USA).

4.2.3. *Apoptosis Assay*

In brief, HT-29 cells (2.5 x 10^5/ml) were incubated with or without compound **2c**, the most potent betulinic acid derivative (IC_{50}: 14.9 μM), for 12, 24 and 48 h at 37 °C, 5% CO_2. Cells were then washed twice in PBS and resuspended in Annexin V binding buffer (10 mM HEPES, 140 mM NaCl, 2.5 mM $CaCl_2$; pH 7.4). Annexin V-FITC was then added according to the manufacturer's instructions and the mixture was incubated for 15 min under dark conditions at 25 °C. PI (0.1 mg/ml) was added just prior to acquisition. Data was acquired using a FACS Aria flow cytometer (Becton Dickinson, USA) at an excitation wavelength of 488 nm and an emission wavelength of 530 nm, and analyzed with BD FACS Diva software (Becton Dickinson, USA).

4.2.4. *Measurement of Intracellular Reactive Oxygen Species (ROS)*

The effect of IC_{50} concentration of compound **2c** on generation of ROS was measured in HT-29 cells (2.5 × 10^5/ml). After treatment for 0-2 h, cells were washed with PBS (2000 × g, 5 min), resuspended in PBS and then incubated with CM-H_2DCFDA (5 μM in1X PBS) for 30 min at 37 °C in dark condition. Subsequently, cells were again washed and resuspended in 500 μl of PBS. DCF fluorescence was determined by flow cytometry at an excitation wavelength of 488 nm and an emission wavelength of 530 nm in FACS Calibur (Becton Dickinson, USA) using forward vs. side scatter to gate the cell population and a FL1 histogram to quantify fluorescence of viable cells. The subsequent analyses were done using BD CellQuest Pro software. To confirm the elevated levels of ROS induced by **2c** for the inhibition of ROS generation, cells were pre-incubated with 2.5 mM of N-Acetyl cysteine (NAC), an established anti-

oxidant, for 3 h before treatment with **2c** and analyzed for cell viability assay. Mean fluorescence intensities (MFI) were obtained using the FACS Diva software.

4.2.5. *Detection of Mitochondrial Membrane Potential*

Briefly, HT 29 cells (2.5×10^5/ml) were incubated with compound **2c** (14.9 µM) for 12, 24, and 48 h at 37 °C, 5% CO_2. The cells were then washed with PBS and incubated with JC-1 (7.5 mM in PBS) under dark conditions for 15 min at 20–25 °C. Cells were acquired using FACS and analyzed using FACS Diva software. HT-29 cells treated with H_2O_2 (30 mM; 37°C; 15 min), illustrative of cells with depolarized mitochondrial membrane potential, served to set the quadrants.

4.2.6. *Western Blotting Analysis*

Control and **2c** treated (14.9 µM; 0–48 h) HT-29 cells were lysed in lysis buffer (50 mM Tris–HCl pH 7.4, 150 mM NaCl, 1 mM EDTA, 1 mM EGTA, 1 mg/ml protease inhibitor cocktail, 5 mM PMSF and 1 mM DTT containing 1% Triton X-100), sonicated and centrifuged for 10 min at 4 °C at 10,000×g, and the protein concentration was estimated. Electrophoretic separations (50 mg protein/lane) were carried out on 10% SDS-polyacrylamide gel, and electrotransferred onto a PVDF membrane. Blots were blocked for 1 h at 37 °C in 20 mM Tris-HCl, pH 7.4, 150 mM NaCl, 0.02% Tween 20 (TBST) containing 5% skimmed milk, and probed using 1:2000 dilution of appropriate antibodies (Bax, Bad, Bcl-2, Bcl-xl, PARP, and β-Actin) by incubating overnight at 4 °C. The membranes were washed thrice with TBST, incubated with alkaline phosphatase/Horseradish peroxidase conjugated secondary antibody, and the bands were visualized using a 5-bromo-4-chloro-3-indolyl phosphate/nitro blue tetrazolium substrate or enhanced chemiluminescence kit.

4.2.7. *Caspase activity analysis*

The enzymatic activities of caspase -8, -9, -3 were assayed in cell lysates (100 µg protein in 50 µl lysis buffer) using colorimetric assay kits as per the manufacturer's instructions. Briefly, control and compound **2c** treated (14.9 µM; 0–48 h) HT-29 cells (2.5×10^5/ml) were washed with ice cold PBS, cell lysates were prepared and subsequently protein concentration was estimated. Lysates were combined with reaction buffer and incubated with specific colorimetric peptide substrates (Ac-IETD-pNA for Caspase-8, Ac-LEHD-pNA for Caspase-9, Ac-DEVD-pNA for Caspase-3; 4 mM, 5 µl) at 37 °C for 6 h. The emission of paranitroanilide (pNA) was measured at 405 nm in an ELISA reader every 30 min for 6 h.

4.2.8. *Cellular and Nuclear Morphology Analysis*

HT 29 cells were seeded (2.5×10^5 cells/ml) in a 6-well tissue culture plate and the drug (**2c**) was added. Plates were incubated for 48 h at 37 °C in a humidified 5% CO_2 incubator. Hoechst 33258 solution was prepared in MilliQ water at a concentration of 5 µg/ml. Cells were washed twice in PBS, fixed in 4% paraformaldehyde, and incubated at 4 °C for 30 min. Cells were again washed twice in PBS. Hoechst 33258 was added to a final concentration of 5 µg/ml and incubated at 37 °C for 30 min under dark conditions. Cells were again washed twice in PBS [35], and spotted on to poly-L-lysine coated slides and mounted using 50% glycerol. Slides were then analyzed in a laser scanning confocal microscope (Leica TCS SP2 System Leica Microsystem, Heidelberg, Germany, 100×). At least 20 randomly selected microscopic fields were observed per sample.

4.3. *Bio-physical studies*

4.3.1. *UV-vis absorption spectroscopic study*

Unless otherwise stated, all chemicals were of analytical grade and were purchased from Sigma-Aldrich Chemicals. The CT-DNA was purchased from Bangalore Genie.

The UV-vis absorption spectrophotometric studies were carried out with 1 cm path length quartz cuvette using UV-vis spectrophotometer; (UV-2401PC, Shimadzu). The spectra were scanned in the wavelength range 200-400 nm. Stock solution of each of the compounds having different concentration was prepared in 60% ethanol in 50 mM Tris-HCl/NaCl buffer (pH 7.5) and then diluted to varied concentrations with the buffer. Then the absorption spectra for different concentrations were taken to obtain the molar extinction coefficient which was used to determine the actual concentration of the compound throughout the experiment. CT DNA concentration was kept fixed at 50 µg/ml and the concentration of the compound was varied from 0 to a higher concentration as required for individual compounds. The DNA-compound complex was incubated at 37 °C for 2 h and the absorption spectra were taken with proper dilution in the range 200-400 nm.

4.3.2. *Circular dichroism (CD) spectroscopic study*

CD spectroscopic measurements were performed at 25 °C with cuvettes having path length 1 mm using CD spectrometer (Jasco J- 815) with the sensitivity of 100 millidegree and in continuous scanning mode with a speed of 100 nm/min; band-width was 1 nm and the number of accumulations was three. Scans

were taken from 190 to 250 nm. CT-DNA (1000 mg/ml) was used for recording spectra in the presence and absence of compound **2c** (100 µM).

4.3.3. *Molecular Docking Study*

A crystallographic DNA with no gap (PDB entry 1DNE, resolution 2.4 Å), which was a crystal structure of a minor groove binder netropsin-DNA complex, was chosen as the receptor capable of accommodating a minor groove binder. Water molecules and the bound netropsin were removed from the structure. The obtained DNA structure was used as receptor.

The compound structure was optimized using Gaussian 09W with DFT method and basis set 3-21G. The obtained structure was used as ligand model. Netropsin was used as control with DNA as receptor. AutoDock Tools was used for docking. Polar and aromatic hydrogens were added with computing the Gasteiger charges on ligand atoms. Torsional degree of freedom for the ligand was defined automatically using the software. The grid box was centered on the receptor and the dimension of the grid was adjusted to include the entire DNA fragment with the spacing between the grid points 0.403 Å. Grid potential maps were calculated using the module AutoGrid 4.0. The Lamarckian genetic algorithm was used to perform docking simulation, with an initial population of 150 randomly placed individuals with a maximum number of 250000 energy evaluations, 150000 generations, mutation rate of 0.02, a crossover rate of 0.8 and an elitism value of 1. The number of docking runs was chosen to be 100. Then least energetical docking conformation was chosen from the output file.

Acknowledgements

This work is financially supported by CSIR network projects ORIGIN (CSC0108), miND (BSC-0115) and TREAT (BSC 0116). Partial financial supports from Department of Biotechnology (DBT), Govt. of West Bengal and Department of Biotechnology (DBT), New Delhi are also gratefully acknowledged. The authors are thankful to Dr. B. Achari, Emeritus Scientist for checking the manuscript and to Dr. Sib Sankar Roy, Cell Biology and Physiology Division of this institute for extending his laboratory facilities. S.D. thanks UGC, Government of India for a fellowship during this study.

Appendix A. Supplementary material

Supplementary material related to this article can be found at http://dx.doi.orgXXX

References and notes:

1. (a) F. E. Koehn, G. T. Carter, The evolving role of natural products in drug discovery, Nat. Rev. Drug Disc. 4 (2005) 206-220. (b) J.W.-H. Li, J.C. Vederas, Drug Discovery and Natural Products: End of an Era or an Endless Frontier?, Science. 325 (2009) 161-165.

2. F. Sandberg, H. Dutschewska, V. Christov, S. Spassov, Spondianthus preussii var. glaber Engler. Pharmacological screening and occurrence of triterpens, Acta Pharm. Suec. 24 (1987) 253-256.

3. (a) F. Li, R. Goila-Gaur, K. Salzwedel, N. R. Kilgore. M. Reddick, C. Matallana, A. Castillo, D. Zoumplis, D. E. Martin, J. M. Orenstein, G. P. Allaway, E. O. Freed, C. T. Wild, PA-457: A potent HIV inhibitor that disrupts core condensation by targeting a late step in Gag processing, Proc. Natl. Acad. Sci. U.S.A. 100 (2003) 13555-13560; (b) C. Chandramu, R. D. Manohar, D. G. Krupadanam, R. V. Dashavantha, Isolation, Characterization and Biological Activity of Betulinic Acid and Ursolic Acid from *Vitex negundo L*, Phytother. Res. 27 (2003) 129-134; (c) G. Bringmann, W. Saeb, L. A. Assi, G. Francois, A. S. S. Narayanan, K. Peters, E. M. Petera, Betulinic Acid: Isolation from *Triphyophyllum peltatum* and *Ancistrocladus heyneanus*, Antimalarial activity, and crystal structure of the benzyl ester, Planta Med. 63 (1997), 255-257; (d) P. K. Mukherjee, K. Saha, J. Das, M. Pal, B. P. Saha, Studies on the anti-inflammatory activity of rhizomes of *Nelumbo nucifera*, Planta Med. 63 (1997) 367–369.

4. (a) R. H. Cichewicz, S. A. Kouzi, Chemistry, biological activity, and chemotherapeutic potential of betulinic acid for the prevention and treatment of cancer and HIV infection, Med. Res. Rev. 24 (2004) 90-114. (b) D. A. Eiznhamer, Z.-Q. Xu, Betulinic acid: a promising anticancer candidate, IDrugs. 7 (2004) 359-373. (c) E. Pisha, H. Chai, I. S. Lee, T. E. Chagwedera, N. R. Farnsworth, G. A. Cordell, C. W. W. Beecher, H. H. S. Fong, A. D. Kinghorn, D. M. Brown, M. C. Wani, M. E. Wall, T. J. Hieken, T. K. Dasgupta, J. M. Pezzuto, Discovery of betulinic acid as a selective inhibitor of human melanoma that functions by induction of apoptosis, Nat. Med. 1 (1995) 1046-1051. (d) D. Thurnher, D. Turhani, M. Elzmann, B. Wannemacher, B. Knerer, M. Formanek, V. Wacheck, E. Selzer, Betulinic acid: a new cytotoxic compound against malignant head and neck cancer cells, Head Neck. 25 (2003) 732-740. (e) J. H. Kessler, F. B. Mullauer, D. M. de Roo, J. P. Medema, Broad in vitro efficacy of plant-derived betulinic acid against cell lines derived from the most prevalent human cancer types, Cancer Lett. 251 (2007) 132-145. (f) S. Fulda, C. Friesen, M. Los, C. Scaffidi, W. Mier, M. Benedict, G. Nunes, P. H. Krammer, M. E. Peter, K. M. Debatin, Betulinic acid triggers CD95 (APO-lIFas)- and p53-independent apoptosis via activation of caspases in neuroectodermal tumors, Cancer Res. 57 (1997) 4956-4964.

5. V. Zuco, R. Supino, S. C. Righetti, L. Cleris, E. Marchesi, C. G. Passerini, F. Formelli, Selective cytotoxicity of betulinic acid on tumor cell lines, but not on normal cells, Cancer Lett. 175 (2002) 17-25.

6. (a) W. Rzeski, A. Stepulak, M. Szymanski, M. Sifringer, J. Kaczor, K. Wejksza, B. Zdzisinska, M. N.-S. Kandefer-Szerszen, Betulinic acid decreases expression of bcl-2 and cyclin D1, inhibits proliferation, migration and induces apoptosis in cancer cells, Arch. Pharmacol. 374 (2006) 11-20; (b) E. Selzer, C. Thallinger, C. Hoeller, P. Oberkleiner, V. Wacheck, H. Pehamberger, B. Jansen, Betulinic acid-induced Mcl-1 expression in human melanoma: mode of action and functional significance, Mol. Med. 8 (2002) 877-884.

7. (a) Y. Takada, B. B. Aggarwal, Betulinic acid suppresses carcinogen-induced NF-κB activation through inhibition of IκBα Kinase and p65 phosphorylation: Abrogation of cyclooxygenase-2 and matrix metalloprotease-9, J. Immunol. 171 (2003) 3278-3286; (b) H. Kasperczyk, K. La Ferla-Bruhl, M. A. Westhoff, L. Behrend, R. M. Zwacka, K. M. Debatin, S. Fulda, Betulinic acid as new activator of NF-κB: molecular mechanisms and implications for cancer therapy, Oncogene. 24 (2005) 6945-6956.

8. M. F. Melzig, H. Bormann, Betulinic acid inhibits aminopeptidase N activity, Planta Med. 64 (1998) 655-657.

9. H. J. Kwon, J. S. Shim, J. H. Kim, H. Y. Cho, Y. N. Yum, S. H. Kim, J. Yu, Betulinic acid inhibits growth factor-induced *in vitro* angiogenesis via the modulation of mitochondrial function in endothelial cells, Jpn. J. Cancer Res. 93 (2002) 417-425.

10. A. Ganguly, B. Das, A. Roy, N. Sen, S. B. Dasgupta, S. Mukhopadhayay, H. K. Majumder, Betulinic acid, a catalytic inhibitor of Topoisomerase I, inhibits reactive oxygen species–mediated apoptotic Topoisomerase I–DNA cleavable complex formation in prostate cancer cells but does not affect the process of cell death, Cancer Res. 67 (2007) 11848-11858.

11(a) Y. Tan, R. Yu, J.M. Pezzuto, Betulinic acid-induced programmed cell death in human melanoma cells involve mitogen-activated protein kinase activation, Clin. Cancer Res. 9 (2003) 2866-2875; (b) M. L. Schmidt, K. L. Kuzmanoff, L. Ling-Indeck, J. M. Pezzuto, Betulinic acid induces apoptosis in human neuroblastoma cell lines, Eur. J. Cancer. 33 (1997) 2007-2010.

12. http://clinicaltrials.gov/show/NCT00346502.

13. S. Fulda, K.-M. Debatin, Betulinic acid induces apoptosis through direct effect on mitochondria in neuroectodermal tumors, Med. Pediatr. Oncol. 35 (2000) 616-618.

14. (a) Y. Kashiwada, F. Hashimota, L.M. Cosentina, C.H. Chen, P.E. Garren, K.H. Lee, Betulinic Acid and Dihydrobetulinic Acid Derivatives as Potent Anti-HIV Agents, J. Med. Chem. 39 (1996) 1016-1017; (b) Y. Kashiwada, J. Chiyo, Y. Ikeshino, T. Nagao, H. Okabe, L.M. Cosentino, K. Fowke, K.H. Lee, 3,28-Di-*O*-(dimethylsuccinyl)-betulin isomers as anti-HIV agents, Bioorg. Med. Chem. Lett. 11 (2001) 183-185; (c) I. D. Bori, H. Y. Hung, K. Qian, C. H. Chen, S.L. M. Natschke, K. H. Lee, Anti-AIDS agents 88. Anti-HIV conjugates of betulin and betulinic acid with AZT prepared via click chemistry, Tetrahedron Letters. 53 (2012) 1987-1989; (d) K. Nakagawa-Goto, K. Yamada, M. Taniguchi, H. Tokuda, K.-H. Lee, Cancer preventive agents 9. Betulinic acid derivatives as potent cancer chemopreventive agents, Bioorg. Med. Chem. Lett. 19 (2009) 3378-3381; (e) R. Majeed, P. L. Sangwan, P. K. Chinthakindi, I. Khan, N. A. Dangroo, N. Thota, A. Hamid, P. R. Sharma, A. K. Saxena, S. Koul, Synthesis of 3-*O*-propargylated betulinic acid and its 1,2,3-triazoles as potential apoptotic agents, Eur. J. Med. Chem. 63 (2013) 782-792; (f) W. Zhang, X. Men, P. Lei, Review on anti-tumor effect of triterpene acid compounds, J. Can. Res. Ther. 10 (2014) 14-19; (g) R.Csuk, Betulinic acid and its derivatives: a patent review (2008-2013) Expert Opin. Ther. Patents. 24 (2014) 913-923; (h) D. Emmerich, K. Vanchanagiri, L. C. Baratto, H, Schmidt, R. Paschke, Synthesis and studies of anticancer properties of lupane-type triterpenoid derivatives containing a cisplatin fragment, Eur. J. Med. Chem. 75 (2014) 460-466; (i) S. Schwarz, B. Siewert, N. M. Xavier, A. R. Jesus, A. P. Rauter, R. Csuk, A “natural” approach: Synthesis and cytoxicity of monodesmosidic glycyrrhetinic acid glycosides, Eur. J. Med. Chem. 72 (2014) 78-83; (j) H. Zhang, P. Zhu, J. Liu, X. Yang, S. Xu, H. Yao, J. Jiang, W. Ye, X. Wu, J. Xu, Synthesis and antitumor activity of novel 3-oxo-23-hydroxybetulinic acid derivatives, Eur. J. Med. Chem. 87 (2014) 159-167.

15. (a) R. Preet, B. Chakraborty, S. Siddharth, P. Mohapatra, D. Das, S. R. Satapathy, S. Das, N. C. Maiti, P.R. Maulik. C. N. Kundu, C. Chowdhury, Synthesis and biological evaluation of andrographolide analogues as anti-cancer agents, Eur. J. Med. Chem. 85 (2014) 95-106; (b) B. Das, C. Chowdhury, D. Kumar, R. Sen, R. Roy, P. Das, M. Chatterjee, Synthesis, cytotoxicity, and structure–activity relationship (SAR) studies of andrographolide analogues as anti-cancer agent, Bioorg. Med. Chem. Lett. 20 (2010) 6947-6950; (c) V. Srivastava, M. P. Darokar, A. Fatima, J.K. Kumar, C. Chowdhury, H.O. Saxsena, G.R. Dwivedi, K. Shrivastava, V. Gupta, S.K. Chattopadhya, S. Luqman, M.M. Gupta, A.S. Negi, P.S. Khanuja, Synthesis of diverse analogues of Oenostacin and their antibacterial activities, Bioorg. Med. Chem. 15 (2007) 518-525.

16. See a recent review article: S. G. Agalave, S.R. Maujan, V. S. Pore, Click Chemistry: 1,2,3-Triazoles as Pharmacophores, Chem. Asian J. 6 (2011) 2696-2718.

17. J. M. Holub, K. Kirshenbaum, Tricks with clicks: modification of peptidomimetic oligomers via copper-catalyzed azide-alkyne [3 + 2] cycloaddition, Chem. Soc. Rev. 39 (2010) 1325−1337

18. (a) M. J. Soltis, H. J. Yeh, K. A. Cole, N. Whittaker, R. P. Wersto, E. C. Kohn, Identification and characterization of human metabolites of CAI [5-amino-1-1(4'-chlorobenzoyl-3,5-dichlorobenzyl)-1,2,3-triazole- 4-carboxamide), Drug Metab. Dispos. 24 (1996) 799-806; (b) C. Sheng, W. Zhang, New Lead Structures in Antifungal Drug Discovery, Curr. Med. Chem. 18 (2011) 733-766 and see also reference 16.

19. D. Kumar, S. Mallick, J. R. Vedasiromoni, B. C. Pal, Anti-leukemic activity of *Dillenia indica* L. fruit extract and quantification of betulinic acid by HPLC, Phytomedicine. 17 (2010) 431.

20. (a) K. Sonogashira, Y. Tohda, N. A. Haghihara, Convenient synthesis of acetylenes: catalytic substitutions of acetylenic hydrogen with bromoalkenes, iodoarenes and bromopyridines, Tetrahedron Lett. 16 (1975) 4467-4470; (b) K. Sonogashira, in Comprehensive Organic Synthesis, ed. B. M. Trost,; I. Fleming; Pergamon, Oxford, 1991, vol 3, pp. 521; (c) K. Sonogashira, In Metal Catalysed Cross Coupling Reactions; F. Diederich, A. de Meijera, , Eds; Wiley-VCH:Weinheim, 2004, vol 1, pp 319.

21. Products **2a**, **2b**-**d**, **2k** and **2l** were separated in HPLC using acetonitrile/water/acetic acid (65:35:1) as mobile phase with flow rate 2.5 mL/min. The retention time (t_R) of these compounds were found to be 30.2, 22.5, 15.0, 18.8, 19.2 and 26.4 min, respectively. The other products (**2f**, **2g-i** and **2j**) were separated in HPLC using acetonitrile/water/acetic acid (90:10:1) as mobile phase with the same flow rate. The retention times (t_R) were 18.2, 17.3, 14.3, 15.6 and 17 min, respectively.

22. I. D. Bori, H.-Y. Hung, K. Qian, C.-H. Chen, S. L. Morris-Natschke, K.-H. Lee, Tetrahedron Lett. 53 (2012) 1987-1989.

23.(a) C. Heidelberger, J. F. Holand , E. Frei (Eds.), Pyrimidine and Pyrimidine Antimetabolites in Cancer Medicine, Lea and Febiger, Philadelphia, PA, 1984, pp. 801–824; (b) D. Pizzirani, C. Pagliuca, N. Realini, D. Branduardi, G. Bottegoni, M. Mor, F. Bertozzi, R. Scarpelli, D. Piomelli, T. Bandiera, Discovery of a New Class of Highly Potent Inhibitors of Acid Ceramidase: Synthesis and Structure−Activity Relationship (SAR), J. Med. Chem. 56 (2013) 3518−3530; (c) F. Focher, D. Ubiali, M. Pregnolato, C. Zhi, J. Gambino, G. E. Wright, S. Spadari, Novel Nonsubstrate Inhibitors of Human Thymidine Phosphorylase, a Potential Target for Tumor-Dependent Angiogenesis, J. Med. Chem. 43 (2000) 2601-2607.

24. N. G. Kundu, J. S. Mahanty, C. Chowdhury, S. K. Dasgupta, B. Das, C. P. Spears, J. Balzarini, E. De Clercq, 5-(Acylethynyl)uracils, 5-(Acylethynyl)-2'-deoxyuridines and 5-(Acylethynyl)-1-(2-

hydroxyethoxy)methyluracils. Their synthesis, antiviral and cytotoxic activities, Eur. J. Med. Chem. 34 (1999) 389-398.

25. L. Gibellini, M. Pinti, M. Nasi, S. D. Biasi, E. Roat, Interfering with ROS Metabolism in Cancer Cells: The Potential Role of Quercetin, Cancers. 2 (2010) 1288–1311.

26. R. C. Widaua, A. D. Parekha, M. C. Rancka, D. W. Goldena, K. A. Kumara, R. F. Sooda, S. P. Pitrodaa, Z. Liaoa, X. Huanga, T. E. Dargaa, D. Xua, L. Huangb, J. Andradeb, B. Roizmanc, R. R. Weichselbauma, N. N. Khodareva, RIG-I–like receptor LGP2 protects tumor cells from ionizing radiation, PNAS. (2014) E484-E491; see also reference 15b.

27. D. Deeb, X. Gao, H. Jiang, B. Janic, A. S. Arbab, Y. Rojanasakul, S. A. Dulchavsky, S. C. Gautam, Oleanane triterpenoid CDDO-Me inhibits growth and induces apoptosis in prostate cancer cells through a ROS-dependent mechanism, Biochem Pharmacol. 79 (2010) 350–360.

28. M. Leist, M. Jäättelä, Four deaths and a funeral: From caspases to alternative mechanisms, Nat. Rev. Mol. Cell. Biol. 2 (2001) 589–598.

29. C. Mandal, A. Dutta, A. Mallick, S. Chandra, L. Misra, R. S. Sangwan, C. Mandal, Withaferin A induces apoptosis by activating p38 mitogen-activated protein kinase signaling cascade in leukemic cells of lymphoid and myeloid origin through mitochondrial death cascade, Apoptosis. 13 (2008) 1450–1464.

30. M.H. Harris, C.B. Thompson, The role of the Bcl-2 family in the regulation of outer mitochondrial membrane permeability, Cell Death Differ. 7 (2000) 1182–1191.

31. S.K. Samanta, D. Dutta, S. Roy, K. Bhattacharya, S. Sarkar, A.K. Dasgupta, B.C. Pal, C. Mandal, C. Mandal, Mahanine a DNA minor groove binding agent exerts cellular cytotoxicity with involvement of C-7-OH and -NH functional groups, J. Med. Chem. 56 (2013) 5709-5721.

32. S. Panja, B. Jana, P. Aich, T. Basu, In vitro interaction between calf thymus DNA and *Escherichia coli* LPS in the presence of divalent cation Ca^{2+}, Biopolymers. 89 (2008) 606-613; see also reference 15a.

33. M. Coll , J. Aymami, G.A. Van der Marel, J.H. Van Boom, A. Rich, A.H. J. Wang, Molecular structure of the netropsin-d(CGCGATATCGCG) complex: DNA conformation in an alternating AT segment, Biochemistry. 28 (1989) 310-320.

34. R. D. Goff, J. S. Thorson, Enhancing the Divergent Activities of Betulinic Acid via Neoglycosylation, Org. Lett. 11(2) (2009) 461-464.

35. R. Roy, D. Kumar, B. Chakraborty, C. Chowdhury, P. Das, Apoptotic and Autophagic Effects of Sesbania grandiflora Flowers in Human Leukemic Cells, Plos One (2013) 8(8): e71672.

****

Captions for Figures, Schemes and Tables

Figure 1. Betulinic acid (**1**) and its designed analogs (**2**)

Scheme 1: Preparation of 1,2,3-triazole derivatives of betulinic acid **2**. *Reagents and conditions*: (a) chloro acetyl chloride, *N*,*N*-diisopropylethylamine (DIPEA), 4-dimethylaminopyridine (DMAP, cat.), THF, r.t., 2 h, 86%; (b) sodium azide, DMF, 70 °C, 4 h, 77%; (c) alkyl/aryl acetylene **5**, sodium ascorbate, copper sulphate ($CuSO_4.5H_2O$), DMSO, 2-18 h, 70-98%.

Table 1. Synthesis of 1,2,3-triazole derivatives **2** using "*Click chemistry*"

Table 2. Cytotoxic activity of betulinic acid derivatives **2** on different cancer cell lines

Figure 2: Analogue 2c triggers redox imbalance in HT-29 cells. (A) Increase in ROS levels. HT29 cells (2.5×10^5/mL) were treated with IC_{50} concentration of **2c** for 0–2 h (time-dependence). After treatment, cells were washed and resuspended in PBS, incubated with CM-H_2DCFDA (5 µM) for 30 min, and the fluorescence was measured using flow cytometry as described in materials and methods. (**B**) For the inhibition of ROS generation, cells were pre-treated with NAC (2.5 mM) for 3 h before treatment with

2c (14.9 µM; 48 h) and ROS was similarly quantified. Values are expressed as Mean Fluorescence Intensity ± SEM of three independent experiments (***p<0.001).

Figure 3: Induction of apoptosis by 2c. Control and **2c** (at IC_{50} concentration) treated (for 12, 24, and 48 h) HT-29 cells (2.5×10^5/mL). HT-29 cells were co-stained with PI and Annexin-V FITC and analysed using flow cytometry as described in materials and methods. The figure is a representative profile of at least three experiments.

Figure 4: Analogue 2c causes depolarization of mitochondrial transmembrane potential. Estimation of involvement of mitochondrial pathway in apoptosis induced by compound **2c** and loss of mitochondrial membrane potential. Cells were incubated with **2c** (14.9 µM, 0-48 h) and loaded with JC-1 for flow cytometric analysis of mitochondria transmembrane potential. Data is a representative of three different experiments.

Figure 5: Caspase activation by 2c. Activities of caspase 3 **(A)**, 9 **(B)**, 8 **(C)** were measured in control and **2c** treated (14.9 µM, 0-48 h) HT-29 cells using colorimetric tetrapeptide substrates. Results are expressed as mean±SEM from three independent experiments. **(D)** PARP cleavage was evaluated by Western blotting analysis in extracts of control and **2c** (14.9 µM, 0-48 h) treated cells. The compound enhances PARP cleavage. Data was confirmed with three different sets of experiments.

.

Figure 6: Nuclear degradation induced by 2c. Control and **2c** treated (14.9 µM; 0–48 h) HT-29 cells (2.5×10^5/mL) were stained with Hoechst 33258 and observed under a Leica confocal microscope (100×). The figure is a representative profile of at least three experiments.

Figure 7: Expression of pro- and anti-apoptotic proteins in control and 2c treated HT-29 cells. (A) Expression levels of pro- and anti-apoptotic proteins. Whole cell lysates were prepared from control and HT-29 cells (2.5×10^5/mL) treated with IC_{50} concentration of betulinic acid analogue **2c**. Then equal amounts of cell lysates were loaded in each lane for SDS-PAGE and probed with specific antibodies against Bax, Bad, Bcl-2, Bcl-xl and β-actine. Analysis was confirmed with three different sets of extracts.

β-Actin served as a loading control. **(B)** Histogram shows time dependent decrease in Bcl-2/Bax ratio (**p<0.01, as compared with control).

Figure 8: UV-VIS absorption spectra of DNA (100 μg/mL) in 50 mM Tris-HCl/NaCl, pH 7.5, after incubation with different concentrations of **2c**, at 37 °C for 2 h. **(A)** original plot, **(B)** normalized plot.

Figure 9: Binding isotherm of DNA in presence of compound **2c**.

Figure 10: CD spectra of DNA in the presence of **2c** in 50 mM Tris-HCl, NaCl buffer: Blue and red lines represent the spectra of DNA itself (500 µg/mL) and DNA in the presence of compound **2c** (50 mM) respectively.

Figure 11: **(A)** Energy minimized docked structure of compound **2c** and DNA (PDB ID: 1DNE); DNA is shown in surface representation (with colour code green for C, blue for N, red for O, white for H, orange for P), whereas **2c** is represented as sticks (whole compound was coloured in white) model. **(B)** Energy minimized docked structure of netropsin and DNA (PDB ID: 1DNE); DNA is shown in surface representation (with colour code green for C, blue for N, red for O, white for H, orange for P), whereas netropsin is represented as sticks (whole compound was coloured in white) model.

Table 1

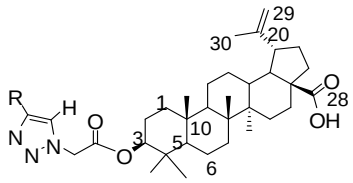

2

Entry	R≡CH, (**5**) R=	Time in hours	Products 2	% Yield[b]
1[c]	—H **(5a)**	18	**2a**	60
2	**(5b)**	10	**2b**	98
3	**(5c)** OH	4	**2c**	84
4	**(5d)**	2	**2d**	98
5	OMe **(5e)** MeO	3	**2e**	82
6	**(5f)**	5	**2f**	70
7	**(5g)**	1.5	**2g**	98
8	NO_2 **(5h)**	2	**2h**	80
9	COOMe **(5i)**	2	**2i**	91
10	COOEt **(5j)**	2	**2j**	90

[a]Reagents and conditions: Acetylene **5** (1.1 eqv.), azide **4** (1.0 eqv.), sodium ascorbate (1.01 eqv.) and $CuSO_4.5H_2O$ (1.01 eqv.) in dry DMSO (2 mL) were stirred at r.t. for 2-18 h. [b]Yield was calculated based on the pure product obtained through silica gel (100-200 mesh) column chromatography. [c]For product **2a**, acetylene gas (balloon pressure) was used in lieu of any acetylenic reagent.

Table 2

Compounds	Cell growth inhibition in terms of IC_{50} (µM)					
	U937	**HT29**	**Jurkat**	**HepG2**	**MCF-7**	**PBMC**
2a	>50	>50	>50	>50	>50	>50
2b	>50	>50	>50	49.8±0.9	>50	N.D
2c	>50	**14.9±1.3**	41.41±1.9	>50	>50	>50
2d	>50	>50	>50	>50	>50	N.D
2e	41.93±2.1	39.80±2.4	>50	>50	44.69±2.9	>50
2f	>50	>50	>50	>50	>50	N.D
2g	>50	>50	>50	>50	>50	>50
2h	>50	>50	44.8±1.6	42.7±2.2	45.7±1.7	>50
2i	>50	>50	>50	>50	>50	N.D
2j	40.1±2.8	>50	>50	>50	>50	N.D
2k	>50	>50	>50	>50	>50	N.D
2l	>50	>50	>50	>50	>50	N.D

Log phase cells (1.25-2.5×10^4/100 µL of RPMI 1640 medium/well) were treated with betulinic acid analogs (0–50 µM) for 48 h, and cell viability was measured by MTT assay as described in materials and methods. Each IC_{50} (Mean ± SEM) has been derived from at least three experiments in duplicate.

Schemes and Figures

Scheme 1

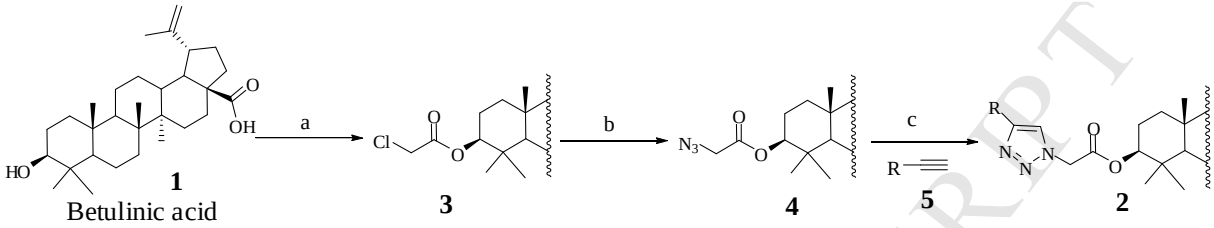

Scheme 2

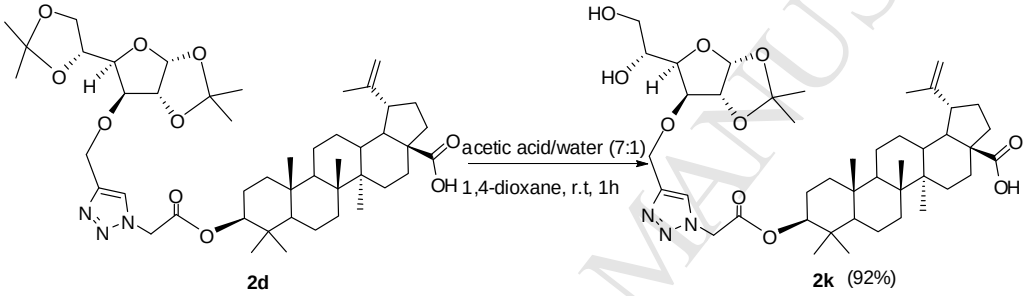

Scheme 3

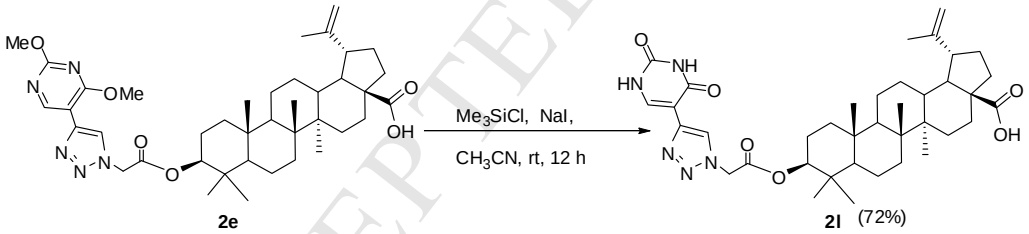

Figure 1.

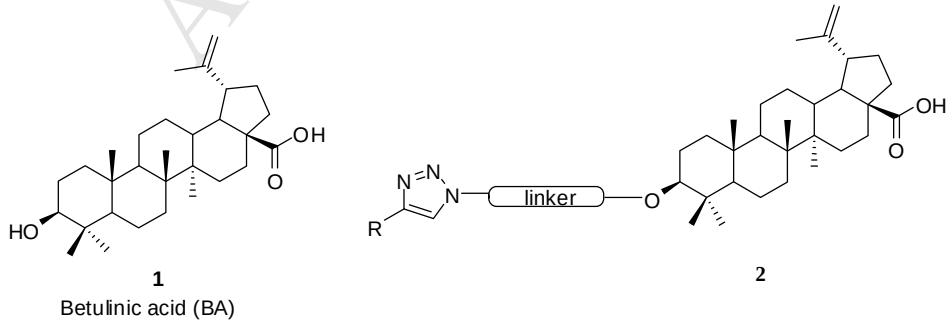

Figure 2

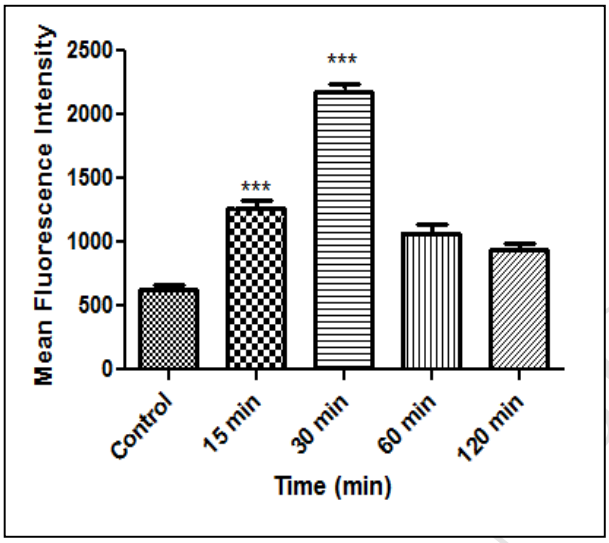
Mean Fluorescence Intensity
2500
2000
1500
1000
500
0
***
***
Control
15 min
30 min
60 min
120 min
Time (min)

(A)

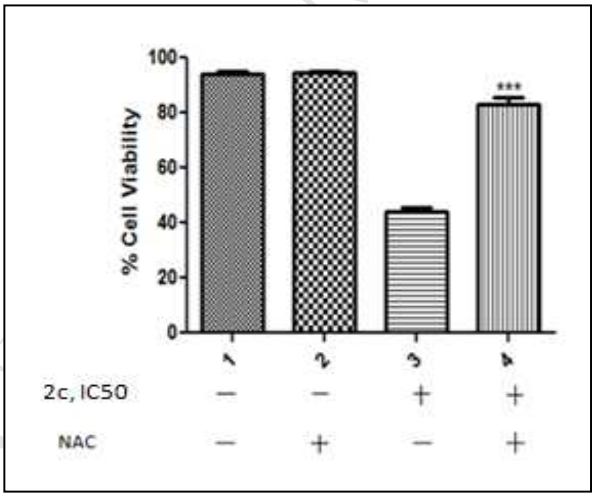
% Cell Viability
100
80
60
40
20
0
***
1
2
3
4
2c, IC50
NAC

(B)

Figure 3

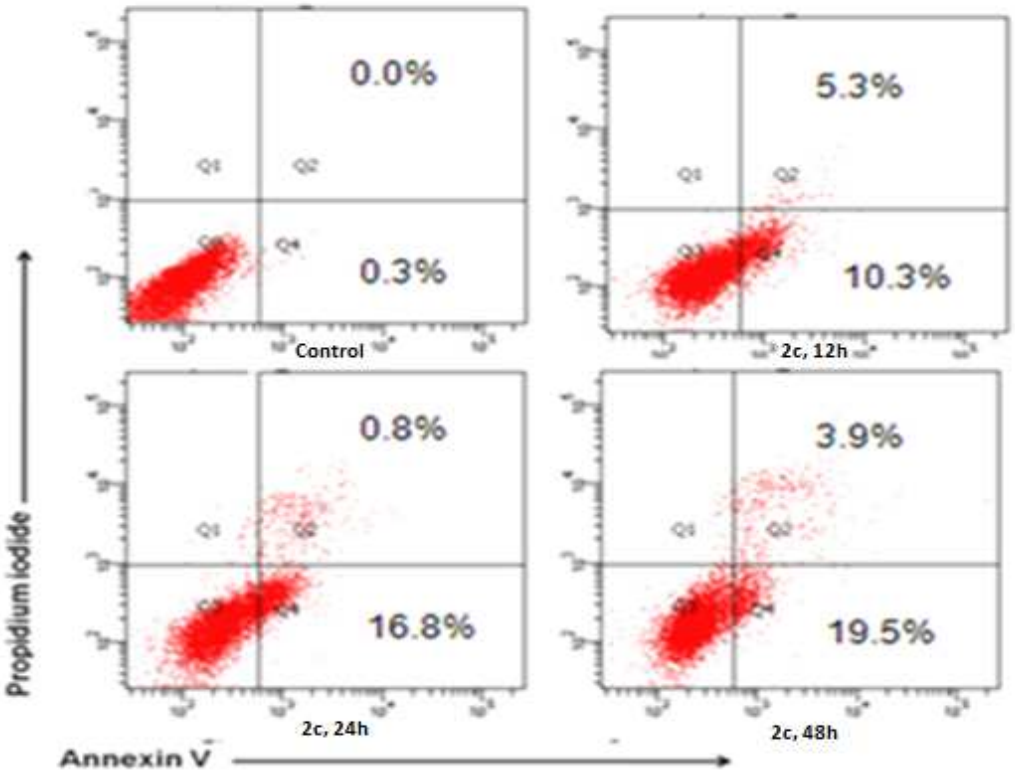

Figure 4

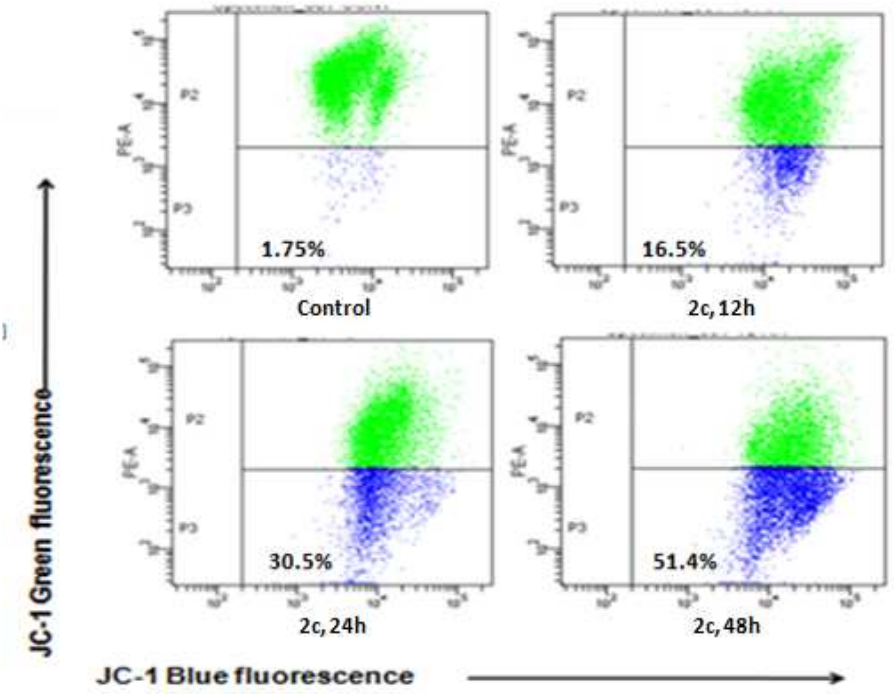

Figure 5

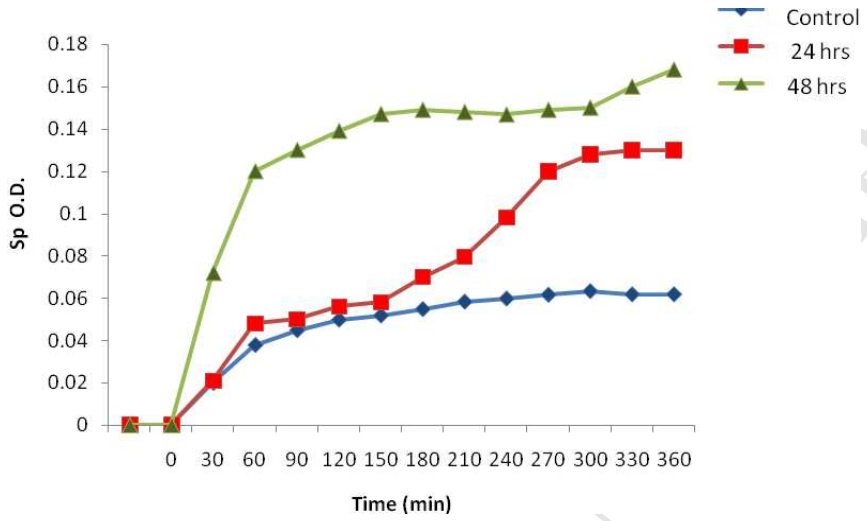
Control
24 hrs
48 hrs
Sp O.D.
0.18
0.16
0.14
0.12
0.1
0.08
0.06
0.04
0.02
0
0 30 60 90 120 150 180 210 240 270 300 330 360
Time (min)

(A)

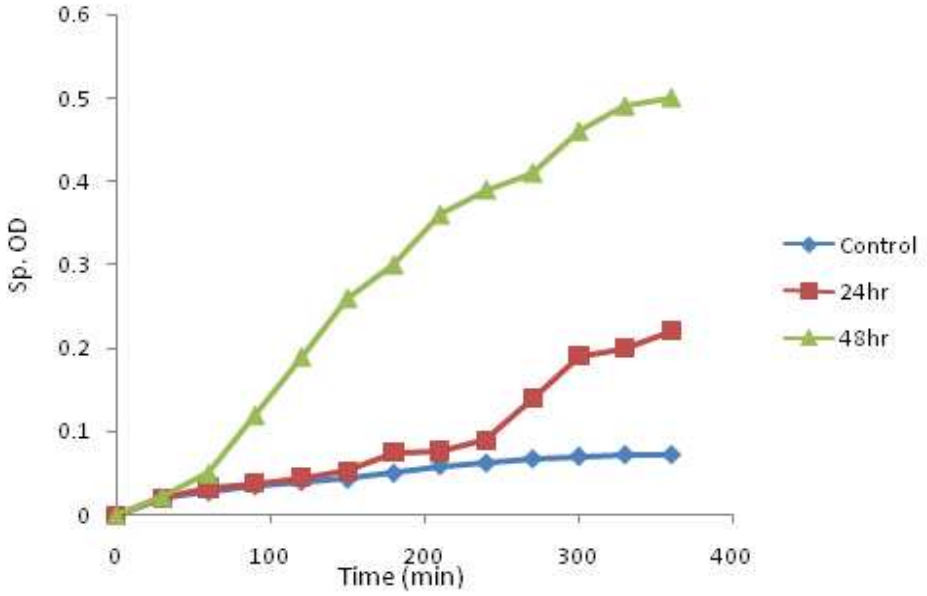
Sp. OD
0.6
0.5
0.4
0.3
0.2
0.1
0
0 100 200 300 400
Time (min)
Control
24hr
48hr

(B)

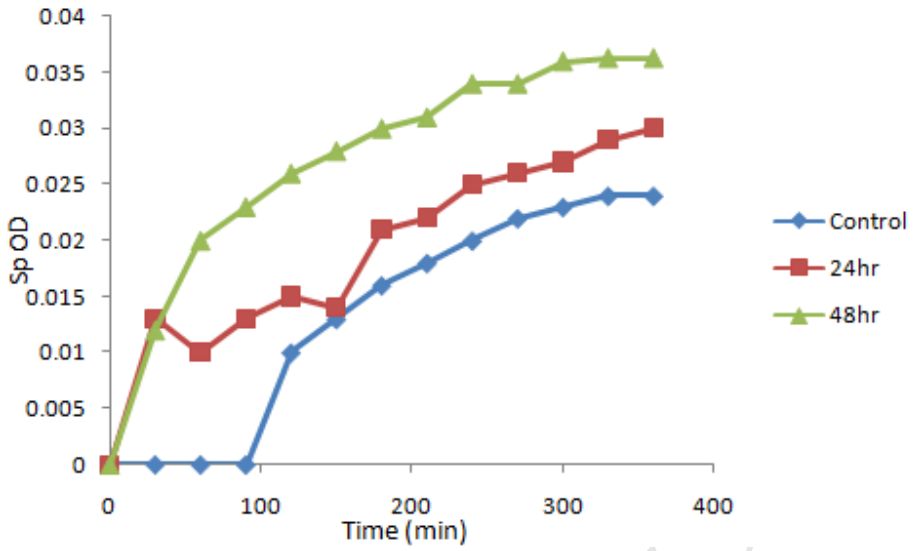
0.04
0.035
0.03
0.025
0.02
0.015
0.01
0.005
0
Sp OD
0
100
200
300
400
Time (min)
Control
24hr
48hr

(C)


PARP
β-Actine

(D)

Figure 6

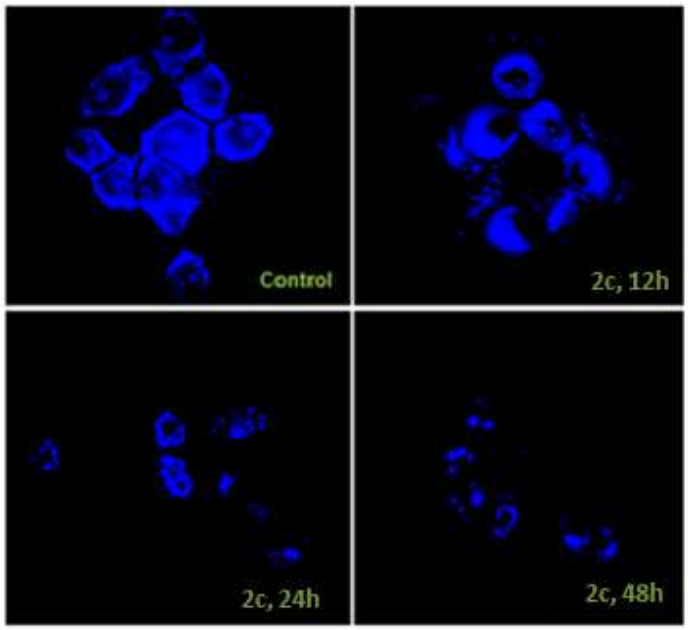

Figure 7

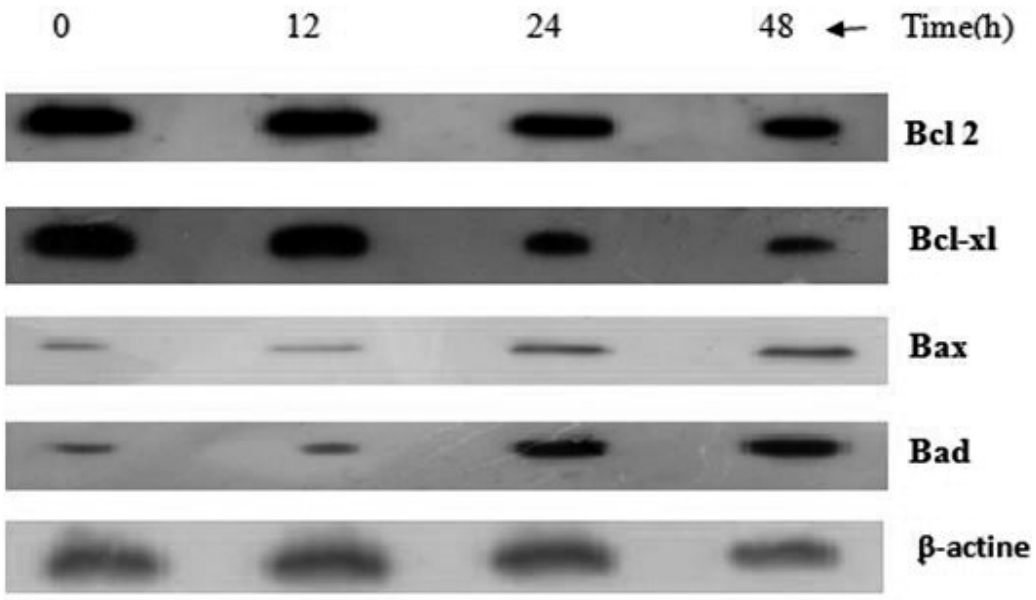
0
12
24
48
Time(h)
Bcl 2
Bcl-xl
Bax
Bad
β-actine

(A)

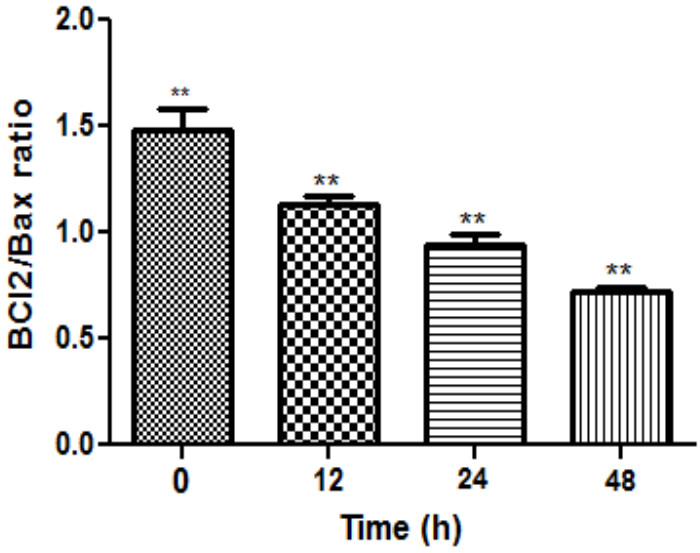
BCl2/Bax ratio
2.0
1.5
1.0
0.5
0.0
**
**
**
**
0
12
24
48
Time (h)

(B)

Figure 8

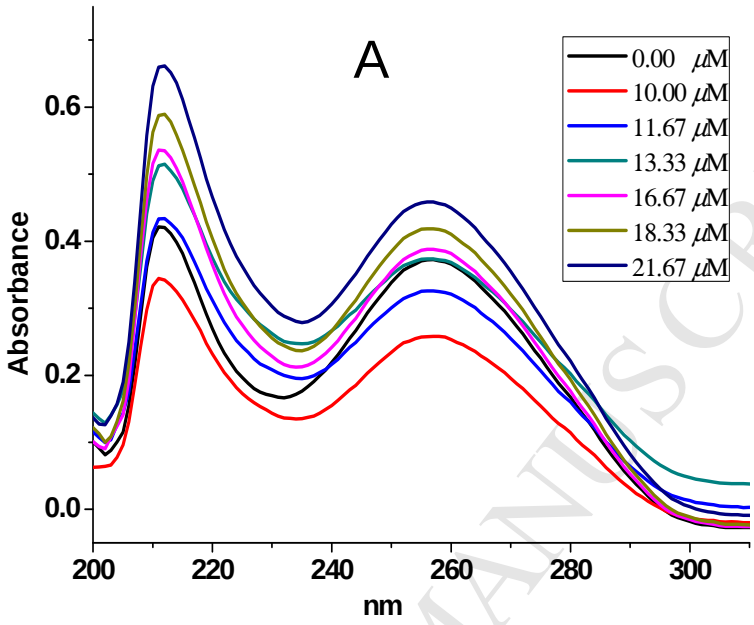

(A)

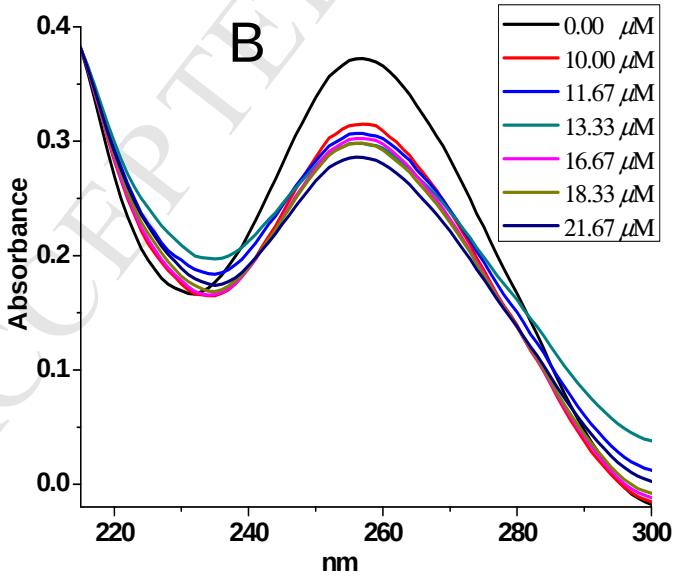

(B)

Figure 9

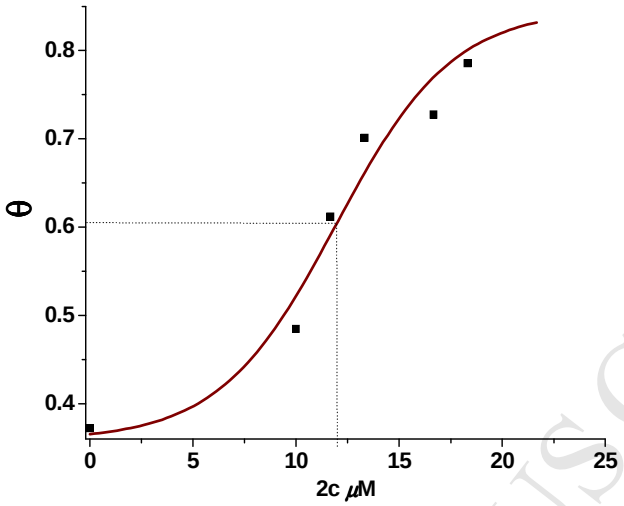

Figure 10

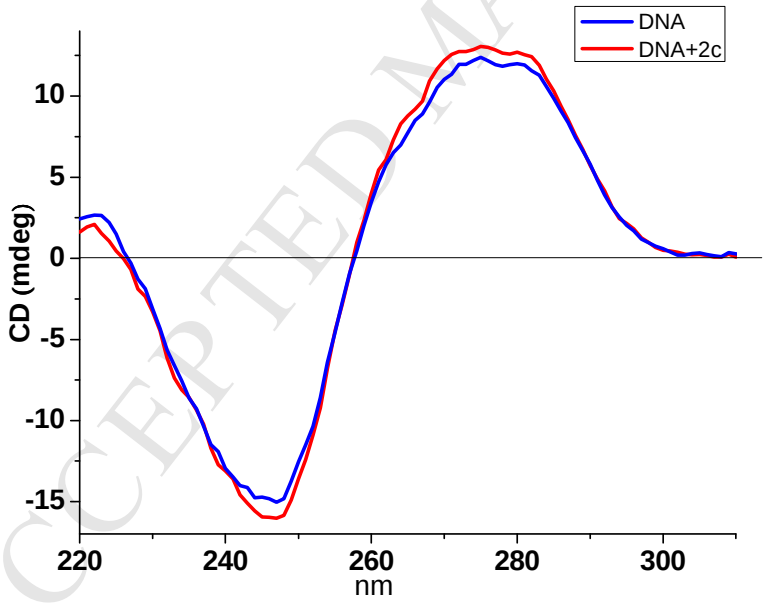

Figure 11

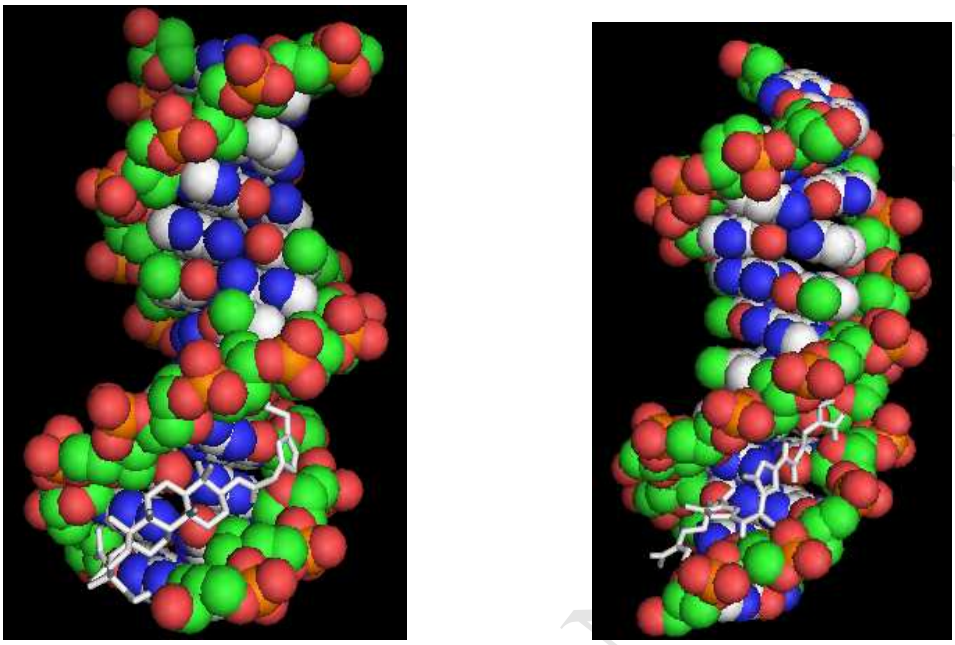

(A) **(B)**

Highlights

- Several betulinic acid analogues belonging to a novel family have been synthesized.
- The products were screened against different cancer cell lines and normal human PBMC by MTT assay.
- Compound **2c** was the most potent inducer of apoptosis in HT-29 cells but was negligibly cytotoxic to normal PBMC.
- Studies showed that **2c** causes apoptosis via mitochondrial dependent pathway.
- Molecular Modeling and CD experiments suggested that **2c** binds to a minor groove of DNA.

Supplementary Material

Synthesis and biological evaluation of a novel betulinic acid derivative as inducer of apoptosis in human colon carcinoma cells (HT-29)

Biswajit Chakraborty[a,‡], Debasmita Dutta[a,†], Sanjukta Mukherjee[‡], Supriya Das[§], Nakul C. Maiti[§], Padma Das[*,†] and Chinmay Chowdhury[*,‡]

[‡]Organic and Medicinal Chemistry Division, [†]Cancer Biology and Inflammatory Disorder Division, [§]Structural Biology and Bioinformatics Division, CSIR-Indian Institute of Chemical Biology, 4 Raja S. C. Mullick Road, Kolkata 700032, India.

[a]Contributed equally.

Table of Contents

1. Preparation of (3*S*)-3-(2-chloroacetyloxy)-lup-20(29)-en-28-oic acid (3)

To a well-stirred solution of betulinic acid (500 mg, 1.0 eqv.) in dry THF (2 mL) were added successively chloroacetyl chloride (0.08 mL, 1.2 eqv.), diisopropylethyl amine (0.2 mL, 1.5 eqv.) and a catalytic amount of 4-dimethylaminopyridine (7 mg, 0.1 eqv.). The mixture was allowed to stir at room temperature (for 2 h) until the completion of the reaction (monitored by TLC). Solvent was removed *in vacuo*; the residue was mixed with H_2O (10 mL) and then extracted with EtOAc (3×15 mL). The combined organic extracts were dried over anhydrous Na_2SO_4, filtered and concentrated under reduced pressure. The resulting residue was purified through silica gel (100-200 mesh) chromatography to afford the desired product **3** (565 mg, 96% yield).

2. (3*S*)-3-(2-chloroacetyloxy)-lup-20(29)-en-28-oic acid (3)

Yield: 96%, white solid yield, m.p. = 284-286 °C. IR (KBr) ν_{max}: 3071, 2946, 2872, 1733, 1693, 1457, 1372, 1287, 1189 cm^{-1}; ^1H NMR ($CDCl_3$, 300 MHz): δ 4.74 (1H, s), 4.61 (1H, s), 4.59-4.53 (1H, m), 4.05 (2H, s), 3.00-2.97 (1H, m), 2.29-2.14 (2H, m), 1.98-1.91 (2H, m), 1.69 (3H, s), 1.66-1.57 (8H, m), 1.52-1.33 (9H, m), 1.29-1.16 (5H, m), 0.97 (3H, s), 0.93 (3H, s), 0.86 (3H, s), 0.85 (6H, s); ^{13}C NMR ($CDCl_3$, 75 MHz): δ 182.4, 167.1, 150.3, 109.7, 83.3, 56.4, 55.3, 50.3, 49.2, 46.9, 42.4, 41.2, 40.6, 38.3, 38.2, 38.0, 37.1, 34.1, 32.1, 30.5, 29.6, 27.9, 25.3, 23.5, 20.8, 19.3, 18.1, 16.3, 16.1, 16.0, 14.6; MS (ESI) 555.20 $[M+Na]^+$. HRMS $[EI]^+$ m/z calculated for $C_{32}H_{49}ClO_4$ 532.33194, found 532.33203.

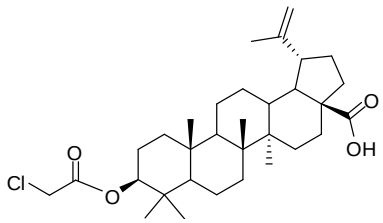

3. Preparation of aryl/alkyl substituted terminal acetylenes 5

Some of the requisite aryl substituted terminal acetylenes (**5**) used as substrate in the preparation of the 1,2,3-triazole library of betulinic acid were prepared employing "*Sonogashira reaction*"[1] followed by base induced desilylation (**Scheme 1**), while rest of the acetylenes (**5a**, **5b**, **5c** and **5g**) were purchased from commercial sources. Thus, iodide **6** (500 mg) was allowed to react with trimethyl silyl acetylene (1.5 eqv.) at room temperature in the presence of $Pd(PPh_3)_2Cl_2$ (2 mol%), CuI (4 mol%) and triethylamine (0.5 mL) in dry DMF under argon atmosphere to yield the intermediate product **7**, which was desilylated by treating with a solution of K_2CO_3 (1 eqv.) dissolved in dry methanol (4.0 mL) to yield the terminal acetylene **5**.

Scheme 1

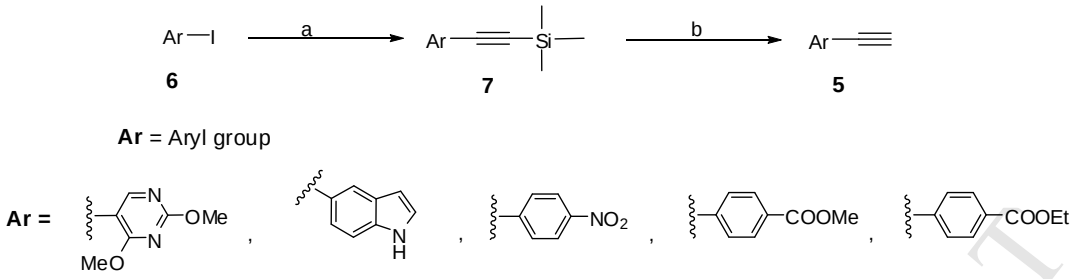

Scheme 1. Reagents and conditions: (a) TMS-Acetylene, $Pd(PPh_3)_2Cl_2$ (2 mol%), CuI (4 mol%), NEt_3 (2 eqv.), dry DMF, r. t., 2h, 98%; (b) K_2CO_3 (1.1 eqv.), dry methanol, r. t., 2 h, 95%.

On the other hand, acetylenic substrate **5d** (see **Table 1** in text) was synthesized from commercially available diacetone-*D*-glucose as shown in **Scheme 2**. To a well stirred solution of diacetone-*D*-glucose (500 mg, 1.9 mmol) in dry dichloromethane (25 mL) were successively added propargyl bromide (343 mg, 1.5 eqv.), 25 mL of 50% sodium hydroxide solution (aqueous) and a catalytic amount (10 mg) of tetrabutyl ammonoum bromide (TBAB). The reaction mixture was allowed to stir at room temperature for overnight. The crude product was isolated using standard work-up and separated through silica gel (100-200 mesh) column chromatography using 15% ethyl acetate in petroleum ether as eluent to obtain the the desired propargylated diacetone-*D*-glucose (**5d**) with 82% yield (448 mg).

Scheme 2

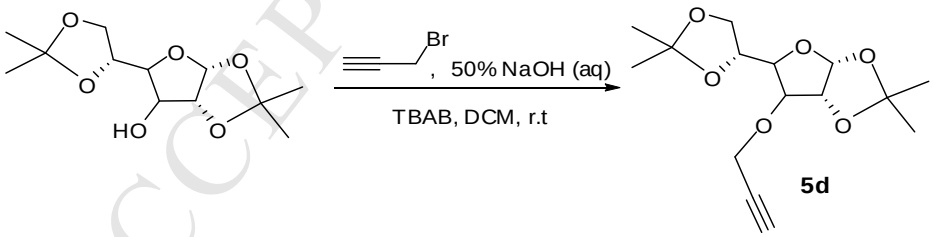

4. Procedure for the synthesis of compound (3*S*)-3-[2-(1*H*-1,2,3-triazol-1-yl)acetyloxy]-lup-20(29)-en-28-oic acid (2a)

To a well stirred solution of azide **4** (40 mg, 1.0 eqv.) in dry DMSO (2 mL) were added sodium ascorbate (1.01 eqv.) and $CuSO_4.5H_2O$ (1.01 eqv.) successively. The reaction mixture was then stirred under acetylene gas atmosphere (balloon pressure). The reaction mixture was stirred another 18 h at room temperature. After completion of the reaction (monitored by TLC), the reaction mixture was extracted with ethyl acetate (2×10 mL); the extract was dried over Na_2SO_4 and

evaporated under reduced pressure. The crude residue obtained was separated through column chromatography using 70% ethyl acetate in petroleum ether (v/v). Finally, this crude product was further purified (>99%) by HPLC where acetonitrile/water/acetic acid (65:35:1) was used as mobile phase and the flow rate was kept at 2.5 mL/min.

5. (3*S*)-3-[2-(1*H*-1,2,3-triazol-1-yl)acetyloxy]-lup-20(29)-en-28-oic acid (2a)

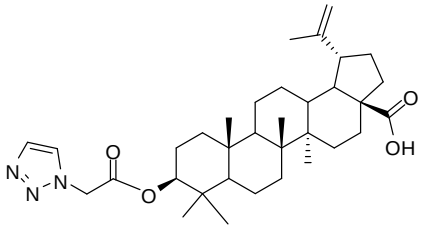

Yield: 60%; white solid, m.p. = 259-262 °C; $[\alpha]^{25}_{D}$ +23.5 (c 0.28, $CHCl_3$); IR (Neat) ν_{max}: 3443, 2942, 2870, 1747, 1695, 1459, 1375, 1224, 1110, 1078, 1028 cm^{-1}; ^1H NMR ($CDCl_3$ 300 MHz): δ 7.78 (1H, s), 7.70 (1H, s), 5.20 (2H, s), 4.73 (1H, s), 4.60-4.53 (2H, m), 3.03-2.97 (1H, m), 2.29-2.11 (2H, m), 1.99-1.95 (2H, m), 1.68 (3H, s), 1.64-1.57 (6H, m), 1.52-1.31 (10H, m), 1.27-1.10 (5H, m), 0.96 (3H, s), 0.92 (3H, s), 0.82 (3H, s), 0.81 (3H, s), 0.71 (3H, s); ^{13}C NMR ($CDCl_3$, 75MHz): δ 181.5, 165.8, 150.3, 134.0, 124.7, 109.6, 83.7, 56.2, 55.2, 50.9, 50.2, 49.1, 46.8, 42.3, 40.5, 38.2, 38.1, 37.7, 36.9, 34.0, 32.0, 30.4, 29.5, 27.8, 25.2, 23.4, 20.7, 19.2, 17.9, 16.2, 16.0, 15.9, 14.5, 0.91; MS (ESI) 566.13 $[M+H]^+$. HRMS [EI] $^+$ m/z calculated for $C_{34}H_{51}N_3O_4$ 565.38796, found 565.38806

6. Transformations of compounds 2 to other derivatives:

A. Deprotection of isopropylidene group of 2d

To a well-stirred solution of compound **2d** (30 mg, 0.03 mmol) in 1,4-dioxane (1mL) was added 2 mL aqueous acetic acid (7:1, v/v) and the whole reaction mixture was then allowed to stir at room temperature for 1h (**Scheme 3**). After completion of the reaction (monitored by TLC), the solvent was evaporated under reduced pressure. The crude residue obtained was separated through column chromatography using 88% ethyl acetate in petroleum ether (v/v) as eluent. Finally, this product was further purified (>99%) by HPLC where acetonitrile/water/acetic acid (65:35:1) was used as mobile phase and the flow rate was kept at 2.5 mL/min. The retention times t_R (for compound **2k)** was found to be 18.8 min.Yield: 92% (after purification on silica-gel column);

Scheme 3

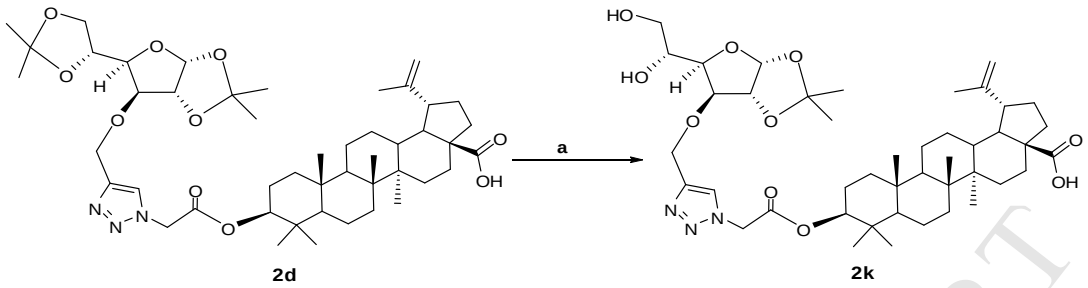

Scheme 3. Reagents and conditions: (a) acetic acid/water (7:1) in 1,4-dioxane, r.t, 1h, 92%.

6.1. (3*S*)-3-[2-(4-{[5-(1,2-dihydroxyethyl)-2,2-dimethyltetrahydrofuro[2,3-*d*][1,3]dioxol-6-yloxy]methyl}-1*H*-1,2,3-triazol-1-yl)acetyloxy]-lup-20(29)-en-28-oic acid (2k).

Yield: 92%; white solid, m.p. = 162-165 °C; $[\alpha]^{25}_{D}$ + 5.44 (c 0.15, MeOH); IR (Neat) ν_{max}: 3435, 2946, 2872, 1742, 1642, 1459, 1377, 1221, 1082, 1019 cm^{-1}; ^{1}H NMR (CD_3OD, 300 MHz): δ 8.04 (1H, s), 5.83 (1H, d, *J* = 3.6 Hz), 5.36 (1H, d, *J* = 17.4 Hz), 5.29 (1H, d, *J* = 17.4 Hz), 4.80 (1H, s), 4.75 (1H, s), 4.71-4.69 (2H, m), 4.66 (1H, d, *J* = 3.6 Hz), 4.58-4.50 (4H, m), 4.09-4.06 (2H, m), 3.90-3.86 (1H, m), 3.74 (1H, dd, *J* = 11.4, 2.7 Hz), 3.56 (1H, dd, *J* = 11.5, 5.8 Hz), 3.34 (1H, s), 3.05-2.99 (1H, m), 2.34-2.17 (3H, m), 1.97-1.85 (3H, m), 1.68 (3H, s), 1.61-1.48 (2H, m), 1.44 (3H, s), 1.40-1.34 (9H, m), 1.29 (3H, s), 1.28-1.23 (3H, m), 1.18-1.04 (3H, m), 1.00 (3H, s), 0.96 (3H, s), 0.87 (3H, s), 0.84 (3H, s), 0.74 (3H, s); ^{13}C NMR (CD_3OD, 75 MHz): δ 180.1, 168.3, 152.1, 146.0, 126.7, 113.0, 110.3, 106.8, 84.8, 83.4, 83.2, 81.3, 69.9, 65.4, 64.1, 57.6, 56.8, 52.2, 51.9, 50.5, 43.7, 42.1, 39.7, 39.6, 39.1, 38.4, 38.2, 35.5, 33.4, 31.8, 30.9, 28.5, 27.1, 26.9, 26.6, 24.6, 22.2, 19.7, 19.3, 17.0, 16.9, 16.7, 15.3; MS (ESI) 820.59 $[M+Na]^+$. HRMS $(FAB)^+$ m/z calculated for $C_{44}H_{67}N_3O_{10}$ $[M+H]^+$ 797.48265, found 797.48278.

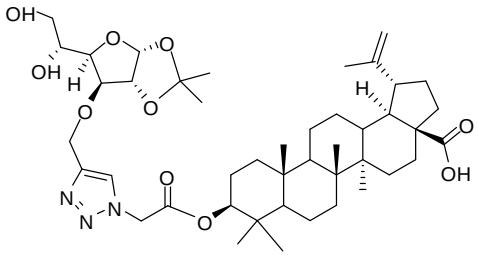

B. Synthesis of uracil derivative 2l

To a well-stirred solution of compound **2e** (32 mg, 0.045 mmol) in anhydrous acetonitrile were added trimethylsilyl chloride (0.02 mL, 0.13 mmol) and sodium iodide (21 mg, 0.13 mmol) successively and the reaction mixture was allowed to stir at room temperature overnight under argon atmosphere (**Scheme 4**). After completion of the reaction (TLC), the solvent was evaporated under reduced pressure; the residue was triturated with saturated aqueous solution of sodium metabisufite (5 mL)

and filtered. The solid residue was washed with water (5 mL) and dried to get the expected uracil derivative **2l** (15 mg, 72%).

Scheme 4

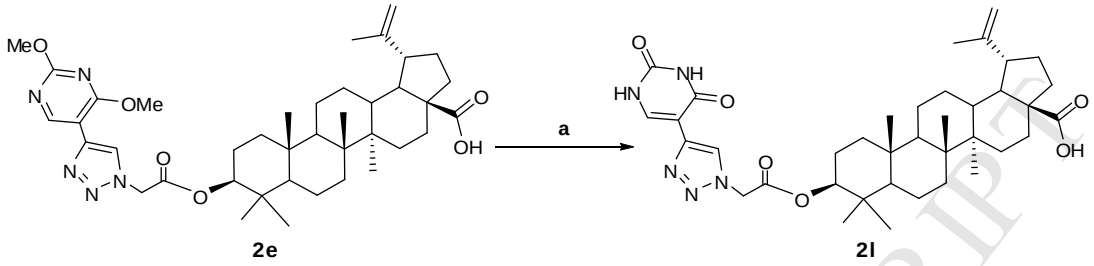

Scheme 4. Reagents and conditions: (a) Trimethylsilyl chloride (3 eqv.), sodium iodide (3 eqv.), dry CH_3CN, rt, overnight, 72%.

6.2. (3*S*)-3-{2-[4-(2,4-dioxo-1,2,3,4-tetrahydropyrimidin-5-yl)-1*H*-1,2,3-triazol-1yl]acetyloxy}-lup-20(29)-en-28-oic acid (2l)

Yield: 72%; white solid, m.p. = 298-300 °C; $[\alpha]^{25}_{D}$ + 9.9 (c 0.34, $CHCl_3$); IR (Neat) ν_{max} : 3448, 2945, 1714, 1692, 1551, 1455, 1386, 1199, 1113 cm^{-1}; ^1H NMR (DMSO-d_6, 300 MHz): δ 11.4 (1H, brd), 8.40 (1H, s), 8.31 (1H, s), 8.05 (1H, s), 5.48 (1H, d, *J* = 17.4 Hz), 5.37 (1H, d, *J* = 17.7 Hz), 4.68 (1H, s), 4.55 (1H, s), 4.45-4.42 (1H, m), 3.00-2.80 (3H, m), 2.29-1.77 (8H, m), 1.64 (3H, s), 1.58-1.51 (7H, m), 1.37-1.29 (8H, m), 1.23 (3H, s), 0.93 (3H, s), 0.86 (3H, s), 0.79 (3H, s), 0.69 (3H, s); ^{13}C NMR (DMSO-d6, 75 MHz): δ 177.3, 167.0, 162.2, 150.6, 150.3, 138.9, 137.6, 123.5, 109.7, 103.7, 82.0, 55.5, 54.4, 50.4, 49.6, 48.5, 46.6, 42.0, 37.5, 36.6, 36.3, 33.7, 31.7, 30.1, 29.2, 29.0, 27.5, 25.0, 23.2, 20.5, 18.9, 17.6, 16.1, 15.8, 15.7, 14.3; MS (ESI) 698.21 $[M+Na]^+$, 676.25 $[M+H]^+$ HRMS $(FAB)^+$ m/z calculated for $C_{38}H_{54}N_5O_6$ $[M+H]^+$ 676.40741, found 676.40801.

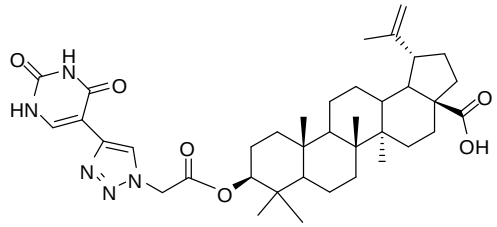

7. HPLC separations:

The crude 1,2,3-triazole derivates **2** obtained through silica gel chromatography were further purified by HPLC using reverse phase C18 column (5 μm, 250 mm × 10 mm) in isocratic mode using detector at wavelength of 220 nm. Compounds **2a-d**, **2k** and **2l** were separated using acetonitrile/water/acetic acid (65:35:1) as mobile phase with flow rate 2.5 mL/min. The retention times (t_R) of these

compounds were found to be 30.2, 22.5, 15.0, 18.8, 19.2 and 26.4 min, respectively. On the other hand, compounds **2f-j** were separated using acetonitrile/water/acetic acid (90:10:1) as mobile phase with the same flow rate as maintained above; the retention times were 18.2, 17.3, 14.3, 15.6 and 17.0 min, respectively.

8. Cytotoxic activity of betulinic acid and standard drug 5-fluorouracil

Compound	HT29 cells(IC_{50} µM)48h	PBMC(IC_{50}µM)48h
Betulinic acid	42.9±1.2	>50
5-Fluorouracil	31.2±0.9	>50
2c	14.9±1.3	>50

Table S1: Log phase cells (1.25-2.5×10^4/100 µL of RPMI 1640 medium/well) were treated with betulinic acid, its analogue **2c** as well as standard drug 5-fluorouracil (0–50 µM) for 48 h, and cell viability was measured by MTT assay as described in materials and methods. Each IC_{50} (Mean ± SEM) has been derived from at least three experiments in duplicate.

9. Cell Lines

Five human cancer cell lines, viz. U937-leukemic monocytic lymphoma (a suspension cancer cell line), HT-29-colon carcinoma (an adherent cancer cell line), MCF-7-breast adenocarcinoma (an adherent cancer cell line), HepG2-Hepato carcinoma (an adherent cancer cell line), and Jurkat-immortalized T lymphocytes (a suspension cell line) were obtained from National Centre for Cell Sciences, Pune, India. All of them were maintained in RPMI-1640 medium except HepG2 which was maintained in high glucose DMEM. Both the media were supplemented with 10% FBS and antibiotics (50 IU/mL penicillin G and 50 µg/mL streptomycin). The cells were incubated at 37 °C in a humidified incubator containing 5% CO_2, and subcultured every 72 h using an inoculum of 5 × 10^5 cells/mL. Cell viability (>95%) was confirmed by trypan blue exclusion test.

10. Isolation of Human Peripheral Blood Mononuclear Cells (PBMC)

PBMCs were isolated from anticoagulated blood of six healthy donors by density gradient centrifugation on an equal volume of Ficoll-Hypaque (Histopaque-1077) at 400 × g for 30 min. Cells were harvested from the interface, washed twice in phosphate buffered saline (PBS, 0.01 M, pH 7.4), and resuspended in RPMI-1640 medium supplemented with penicillin (50 IU/mL), streptomycin (50 µg/mL) and 10% FBS [3]. Cell viability was confirmed by trypan blue exclusion test (>95%).

11. Cell Viability Assay

The cytotoxic activities of betulinic acid and its derivatives dissolved in DMSO (final DMSO concentration <0.1%) were evaluated in U937, HT-29, Jurkat, HepG2, MCF-7 and PBMC using MTT assay. In brief cells (1.25–2.5 × 10^4 cells/100 µl of RPMI 1640 or high glucose DMEM medium/well) were seeded in 96-well tissue culture plates and incubated with a solution of betulinic acid or its derivatives in DMSO (using 0-50 µM concentration) for 48 h at 37 °C, 5% CO_2. Following treatment, cell viability was measured by adding 20 µL MTT (5 mg/mL in PBS) and cells incubated for 4 h at 37 °C. Subsequently, 100 µL DMSO was added to each well and the resultant optical densities were measured at 540 nm in an ELISA Reader (BIO RAD, CA, USA). The specific absorbance that represented formazan production was calculated by subtraction of background absorbance from total absorbance. The mean percentage viability was calculated as follows:

$$\frac{\text{Mean specific absorbance of treated cells}}{\text{Mean specific absorbance of untreated cells}} \times 100$$

The results were expressed as IC_{50} values which were enumerated by graphical extrapolation using Graph Pad Prism software (version 5, Graph Pad Prism software Inc, San Diego, CA, USA). Each experiment was performed at least three times and in duplicate.

12. References

[1]. (a) K. Sonogashira, Y. Tohda, N. Hagihara, Convenient synthesis of acetylenes: catalytic substitutions of acetylenic hydrogen with bromoalkenes, iodoarenes and bromopyridines, Tetrahedron Lett. 16 (1975) 4467-4470; (b) K. Sonogashira, in Comprehensive Organic Synthesis, ed. Trost, B. M.; Fleming, I.; Pergamon, Oxford, 1991, vol 3, pp. 521; (c) K. Sonogashira, In Metal Catalysed Cross Coupling Reactions; Diederich, F.; de Meijera, A., Eds; Wiley-VCH: Weinheim, 2004, vol 1, pp 319.

[2]. C. Heidelberger, *Pyrimidine and Pyridine Antimetabolites in Cancer medicines*; J. F. Holland, E. Frei, Eds, Lea and Febiger: Philadelphia, 1984; pp 801-824. (b) T. Onishi, C. Mukai, R. Nakagawa, T. Sekiyama, M. Aoki, K. Suzuki, H. Nakazawa, N. Ono, Y. Ohmura, S. Iwayama, M. Okunishi, T. Tsuji, Synthesis and Antiviral Activity of Novel Anti-VZV 5-Substituted Uracil Nucleosides with a Cyclopropane Sugar Moiety, J. Med. Chem. 43 (2000) 278 and references cited therein.

[3]. S.Y. Al Omar, E. Marshall, D. Middleton, S.E. Christmas, Increased numbers but functional defects of CD56+CD3+ cells in lung cancer, Int. Immunol. 24 (2012) 409–415.

13. Spectra of the synthesized compounds

^{1}H NMR Spectrum of compound 2a

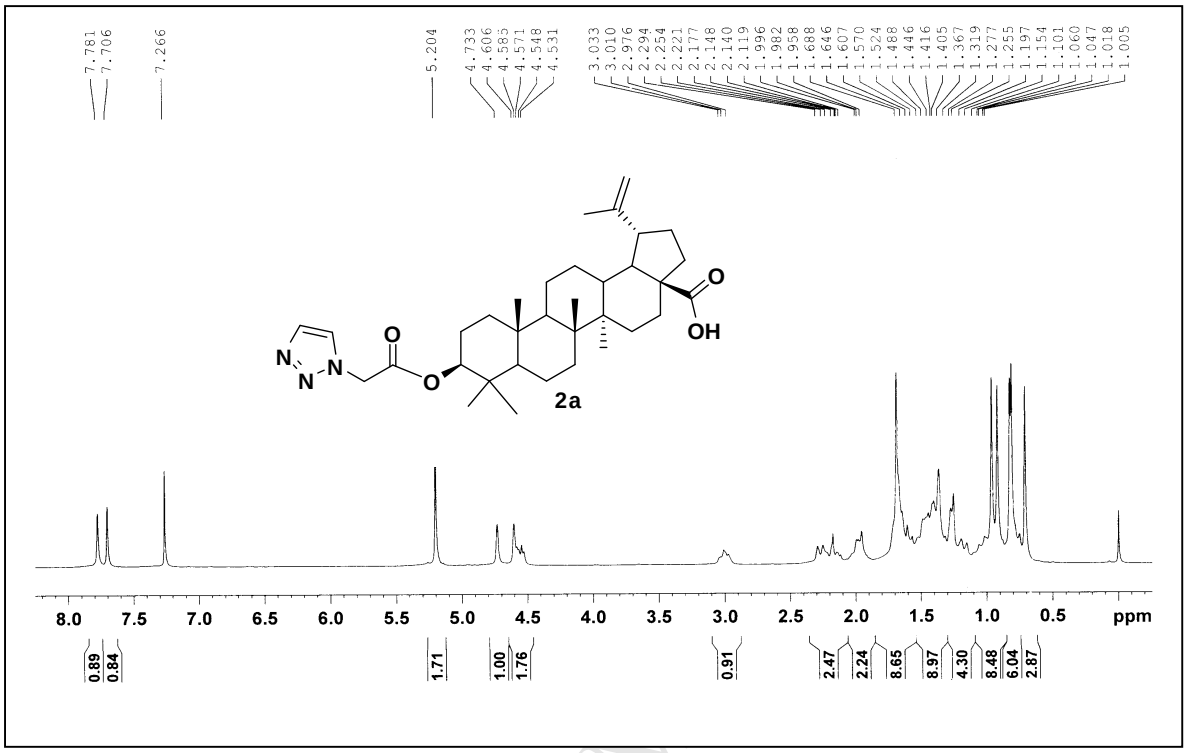

^{13}C NMR Spectrum of compound 2a

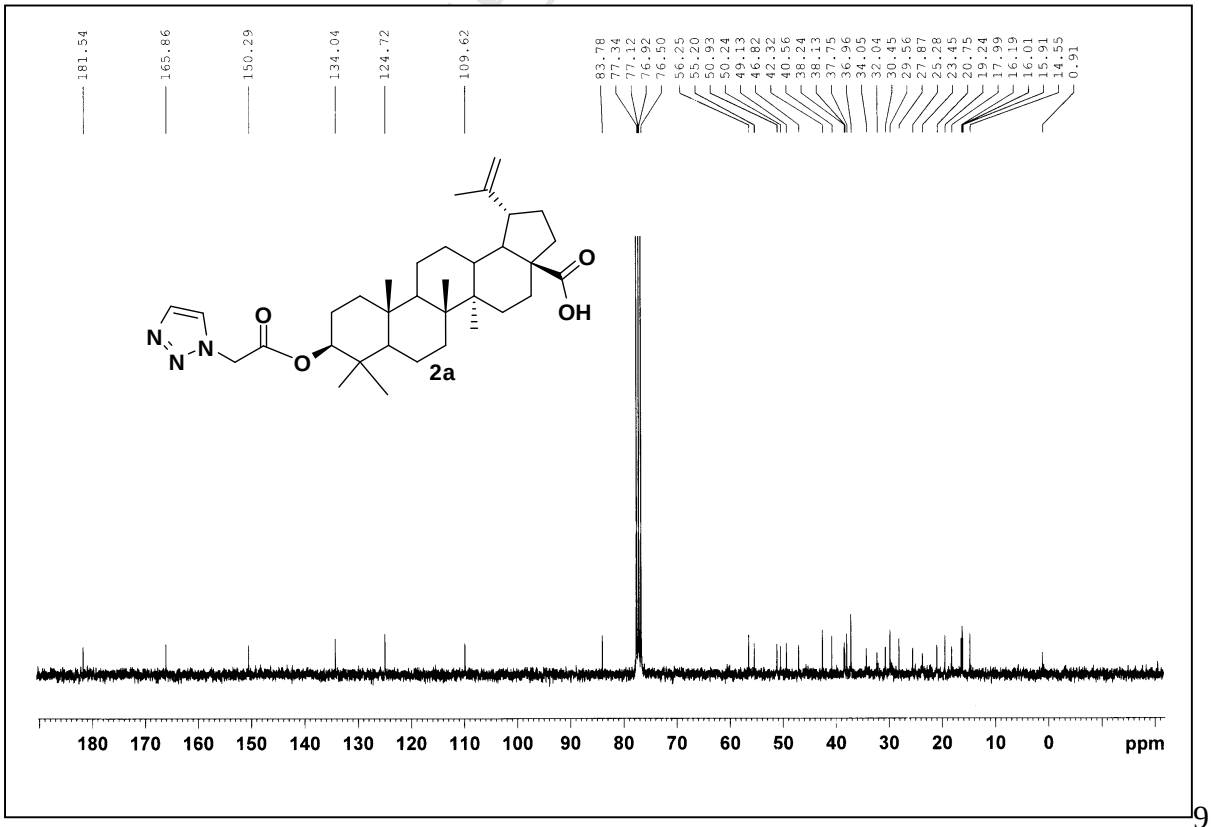

[1]H NMR Spectrum of compound 2b

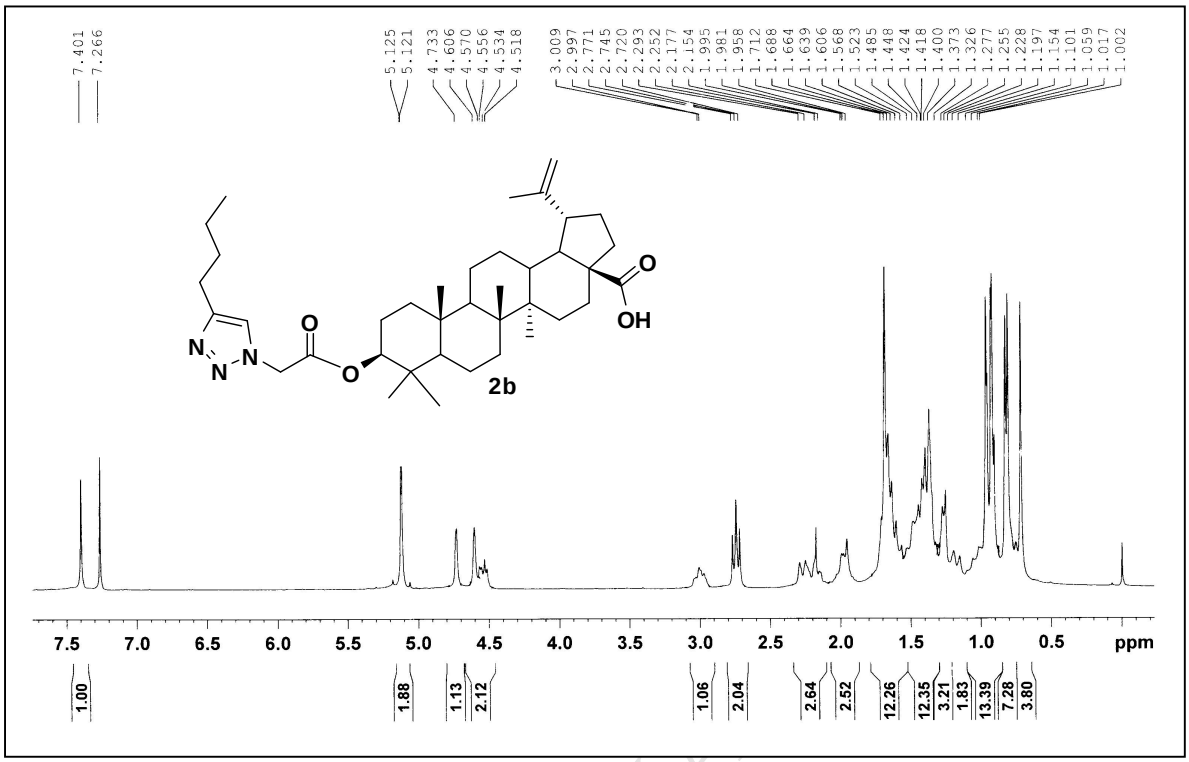

[13]C NMR Spectrum of compound 2b

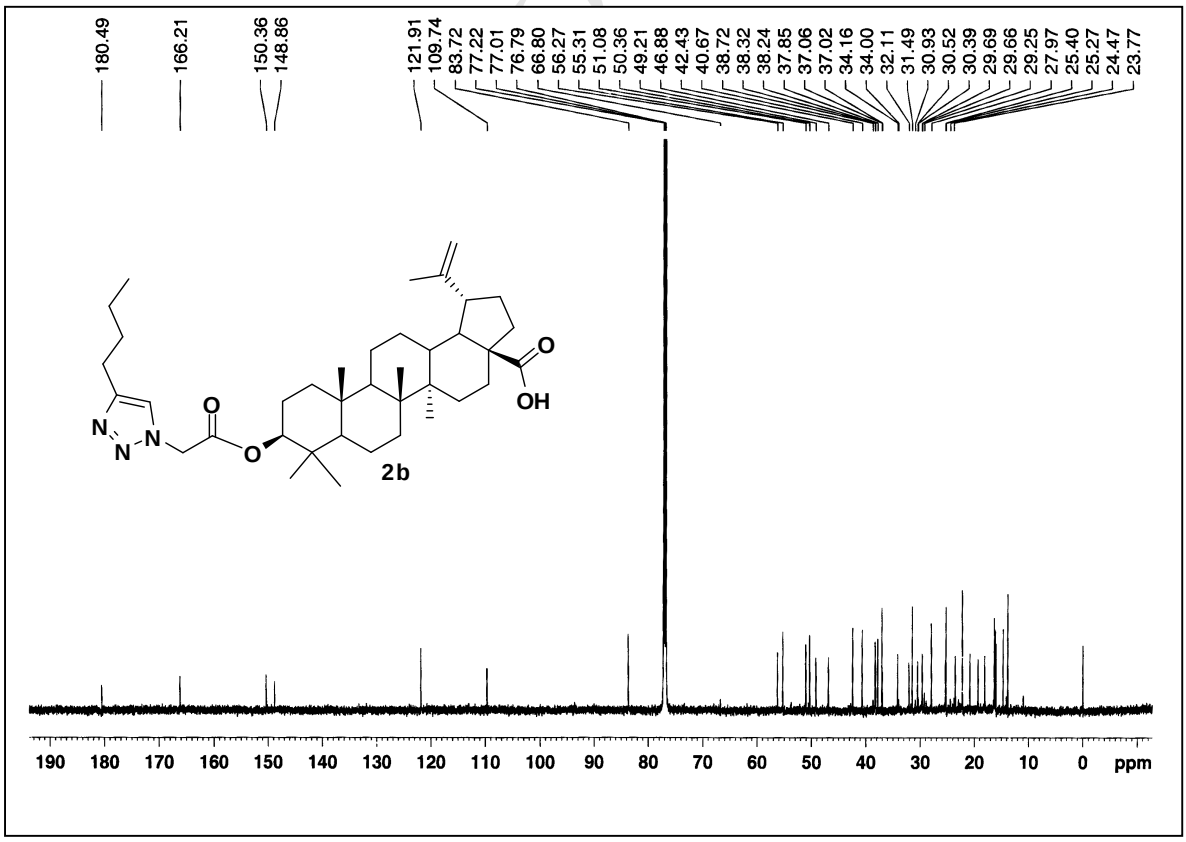

^{1}H NMR Spectrum of compound 2c

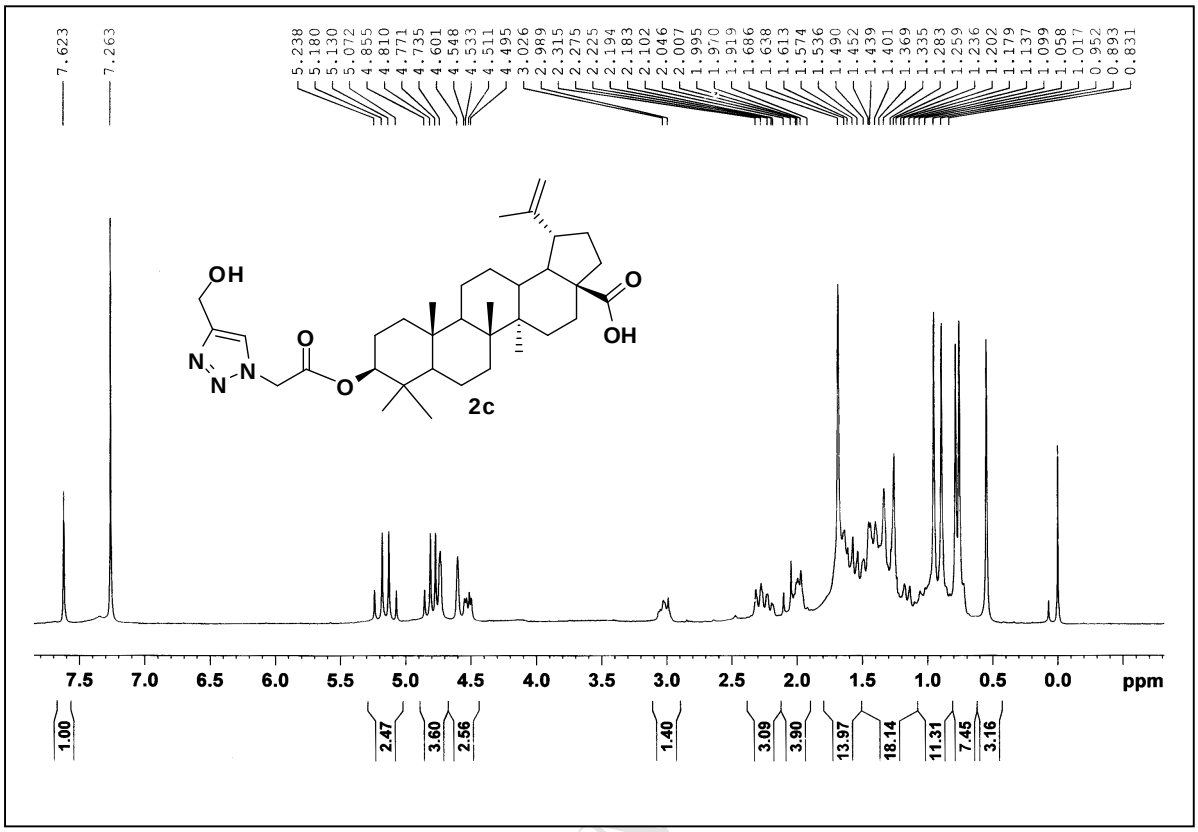

^{13}C NMR Spectrum of compound 2c

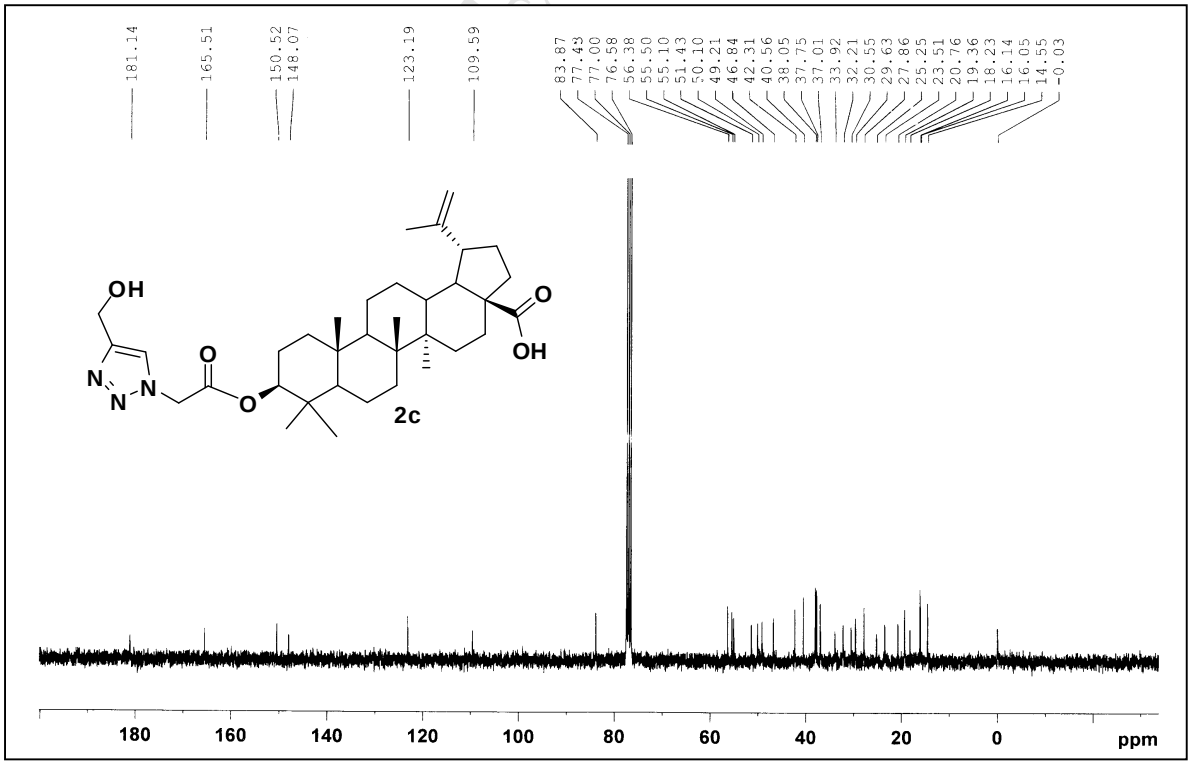

^{1}H NMR Spectrum of compound 2d

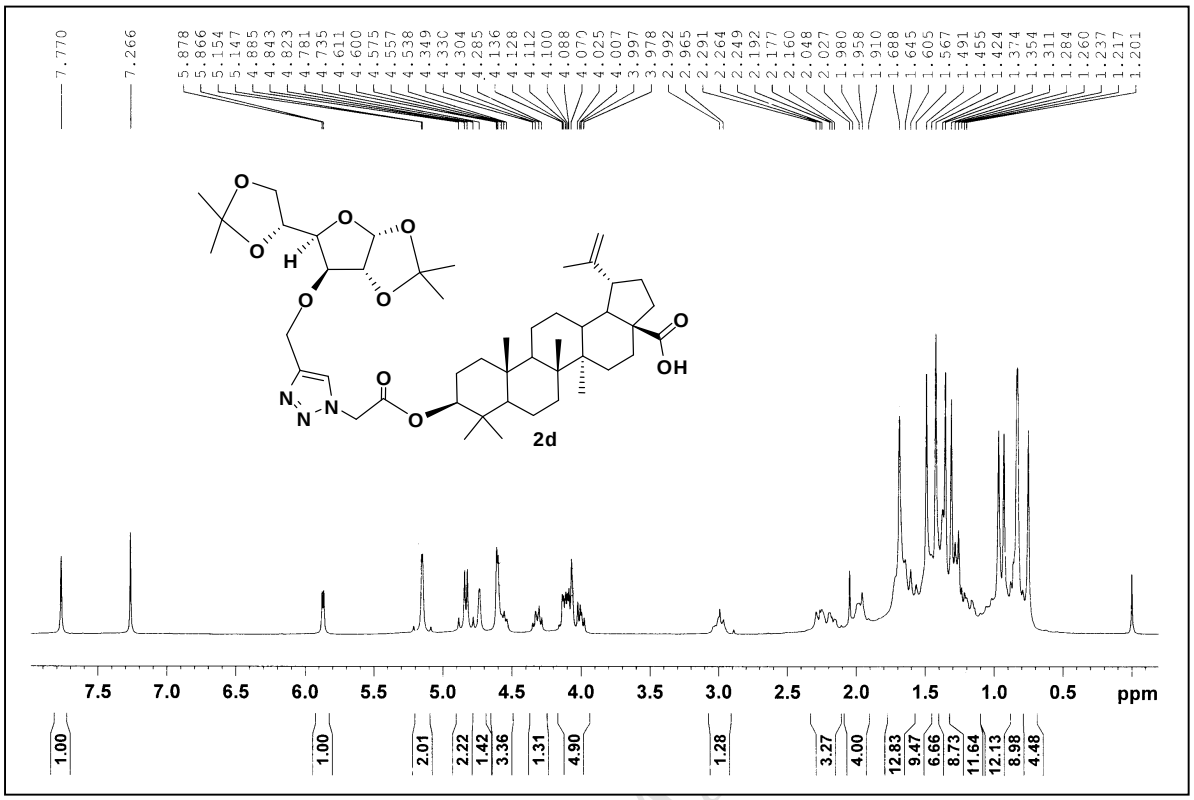

^{13}C NMR Spectrum of compound 2d

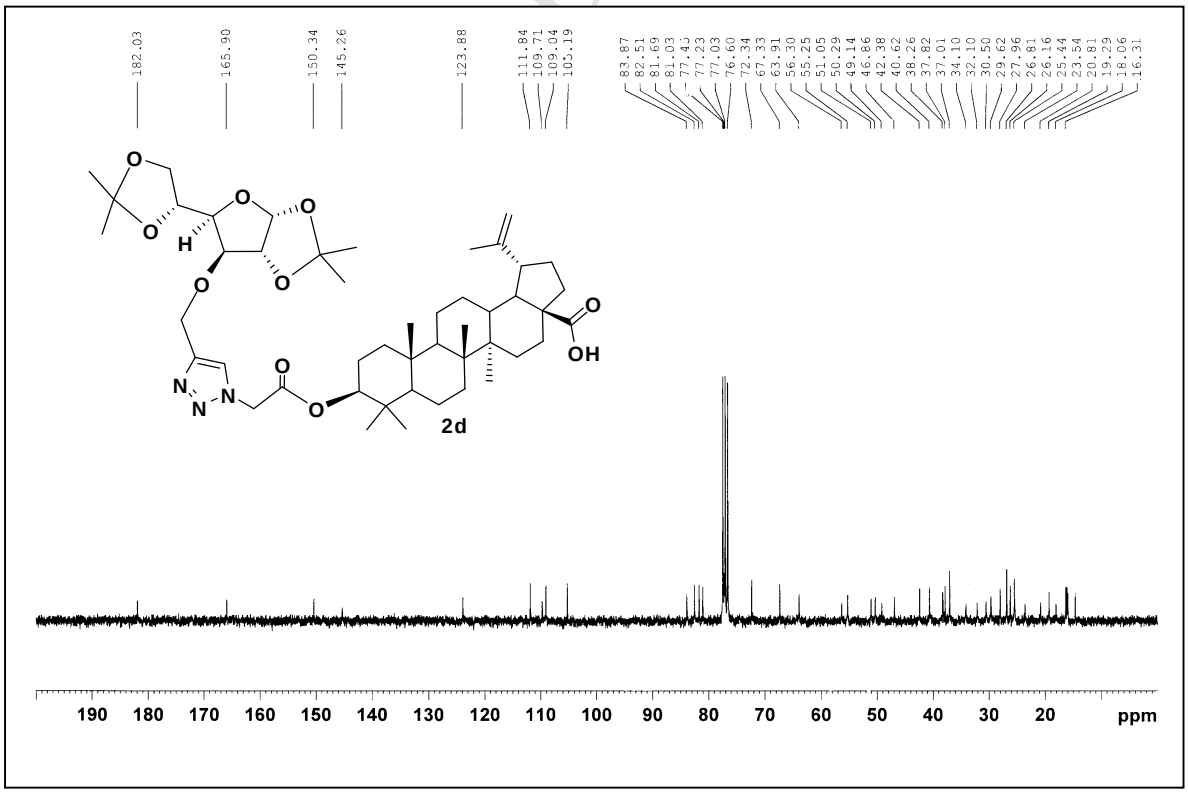

^{1}H NMR Spectrum of compound 2e

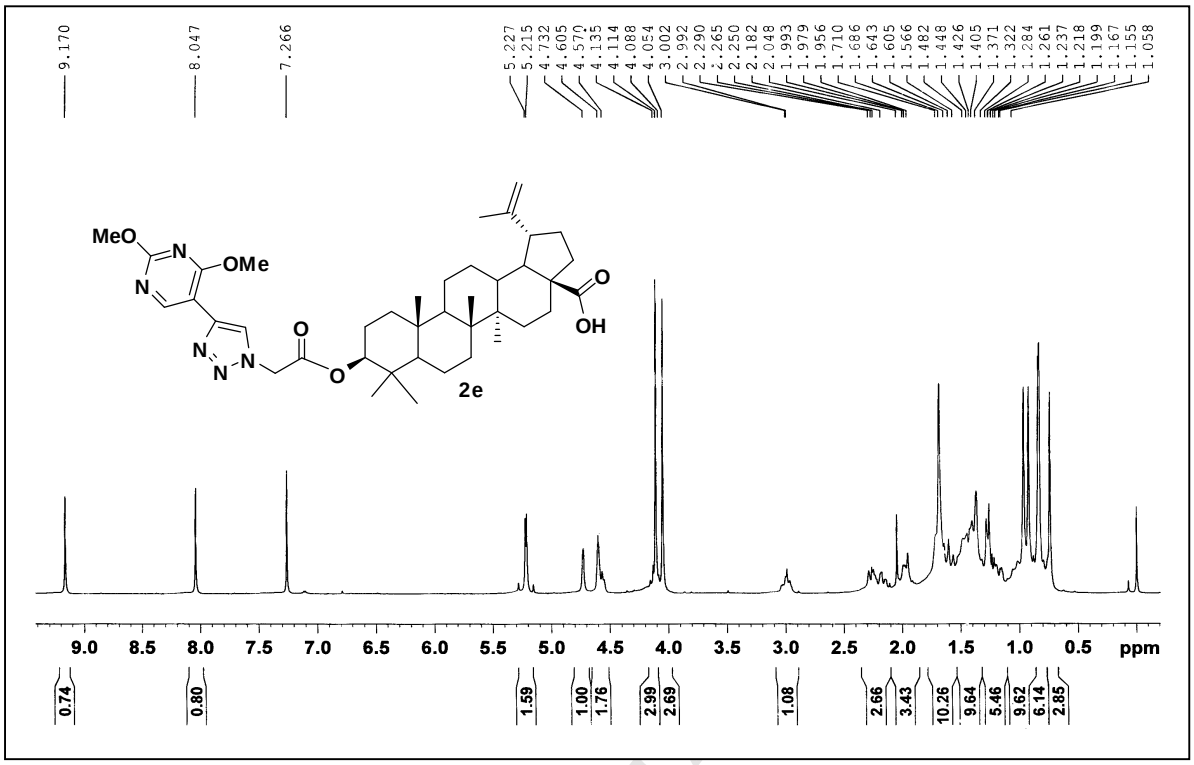

^{13}C NMR Spectrum of compound 2e

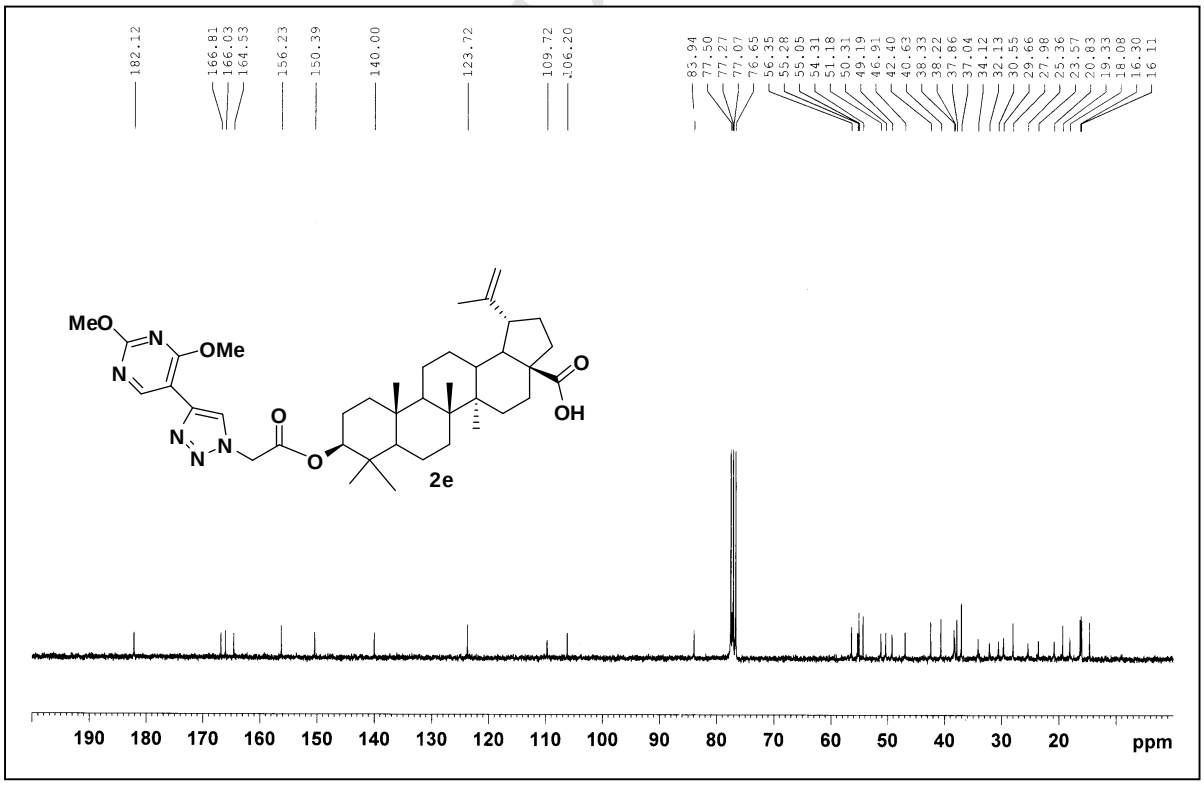

^{1}H NMR Spectrum of compound 2f

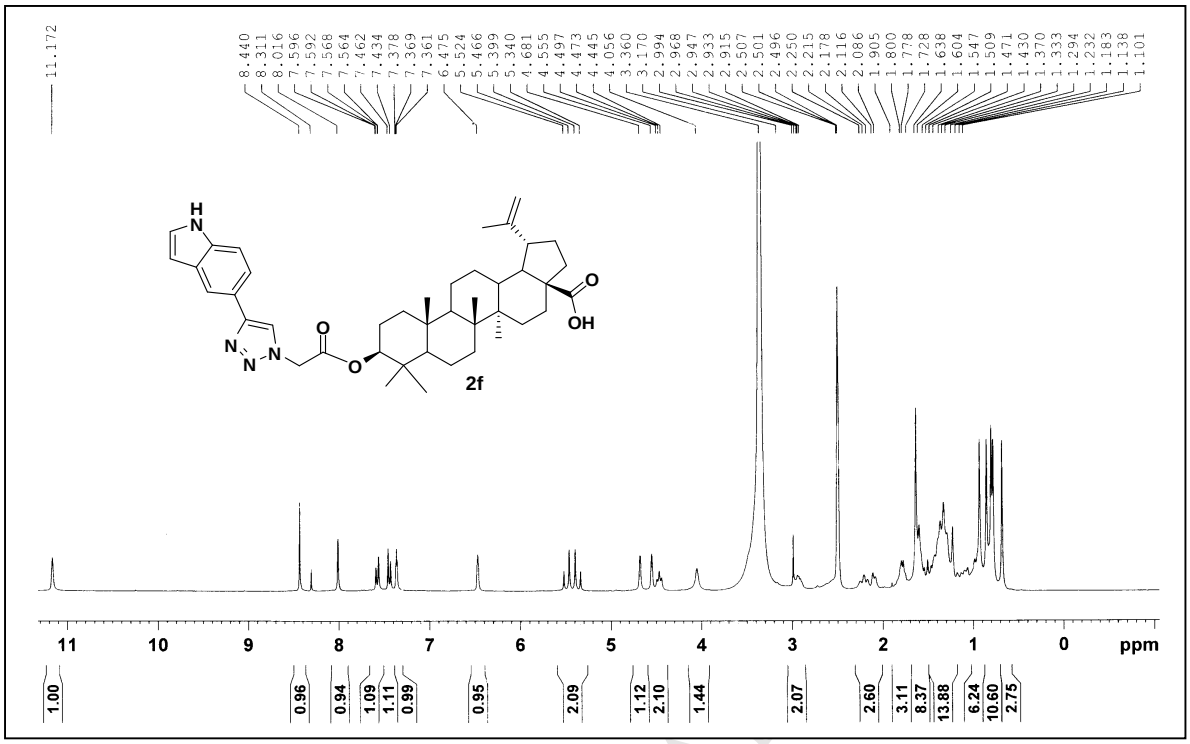

^{13}C NMR Spectrum of compound 2f

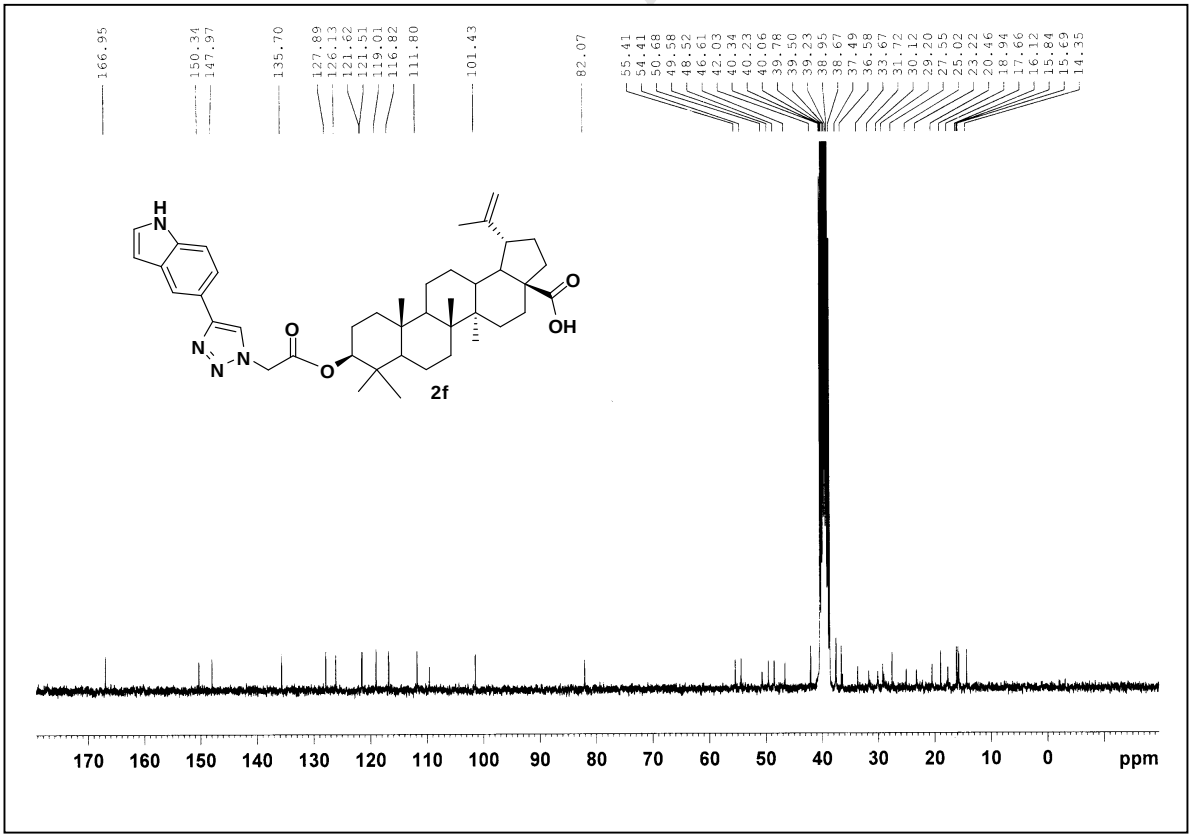

^{1}H NMR Spectrum of compound 2g

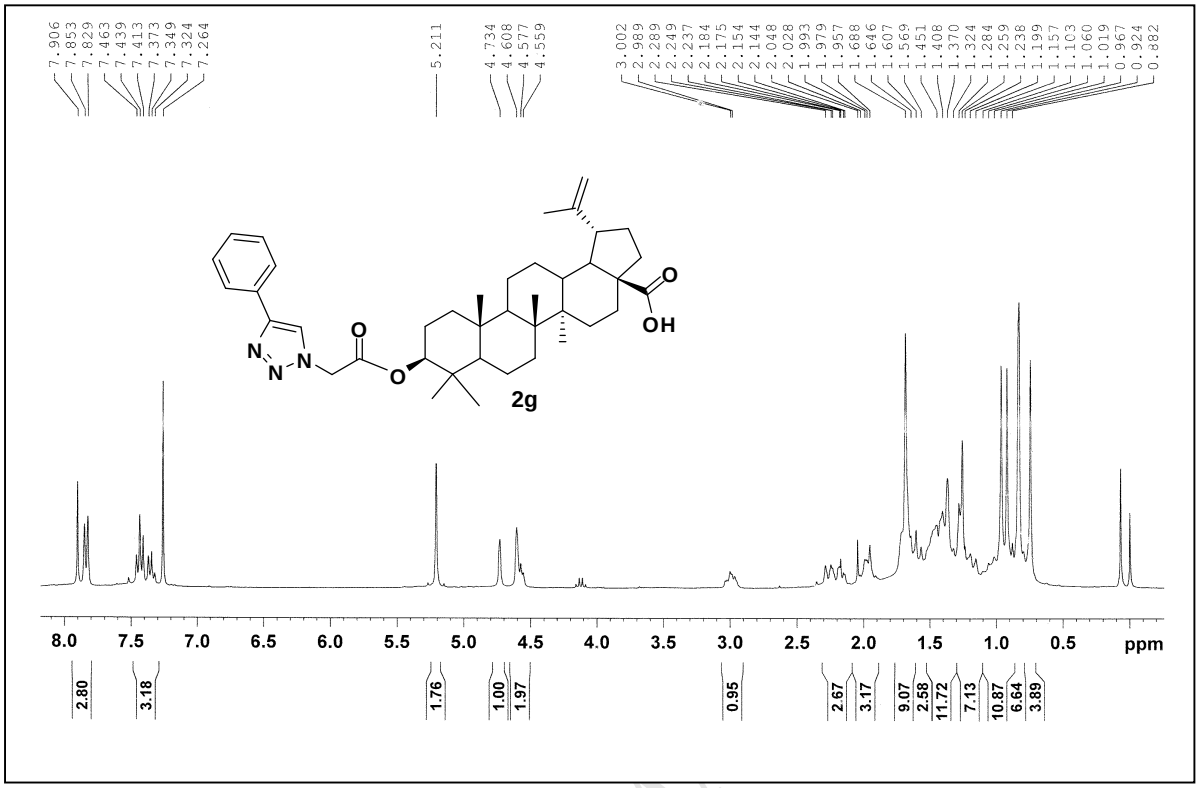

^{13}C NMR Spectrum of compound 2g

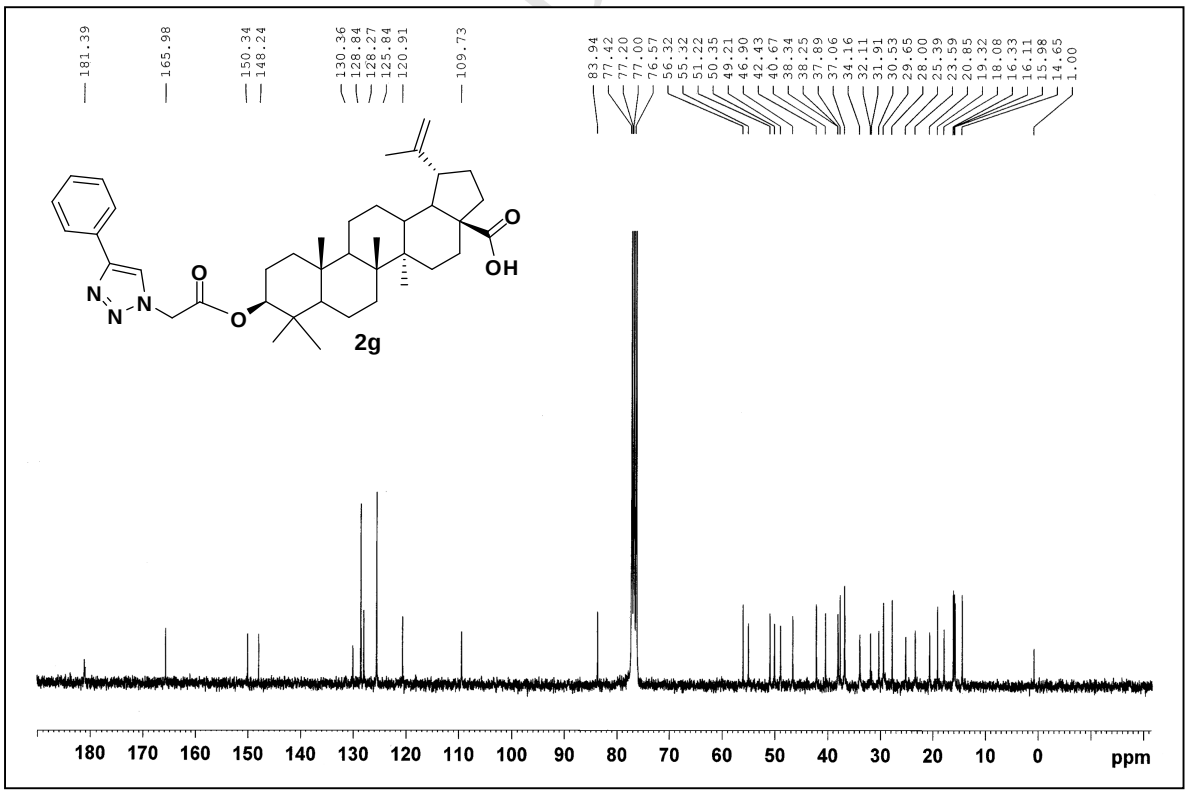

^{1}H NMR Spectrum of compound 2h

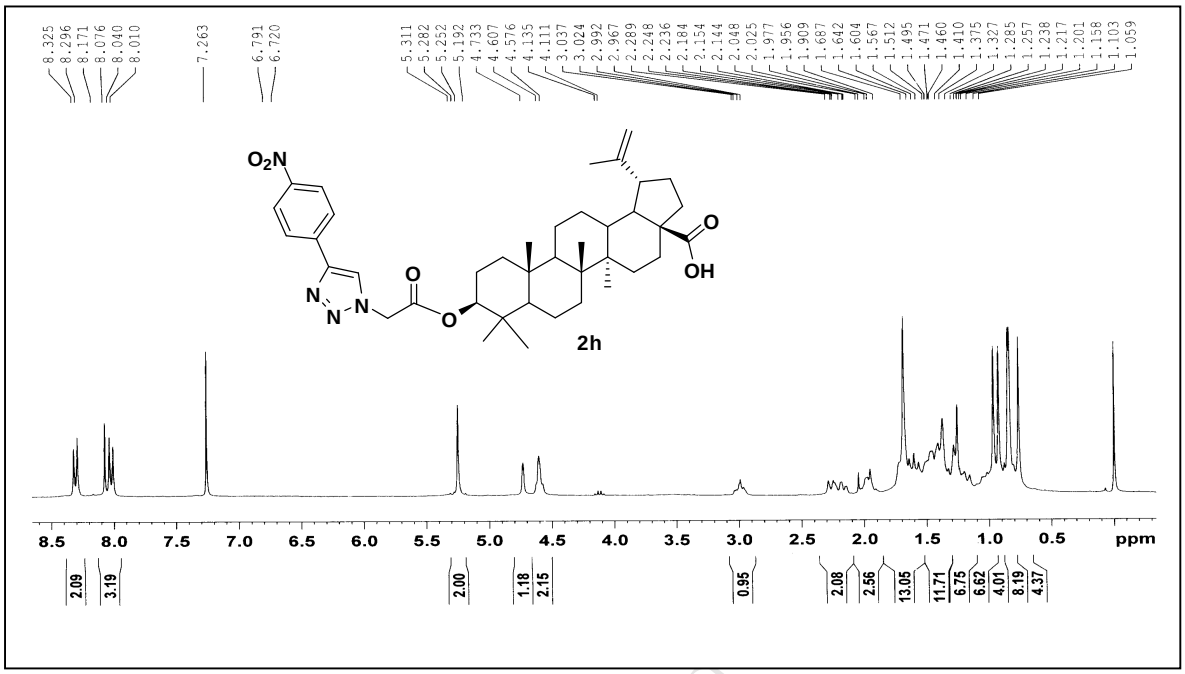

^{13}C NMR Spectrum of compound 2h

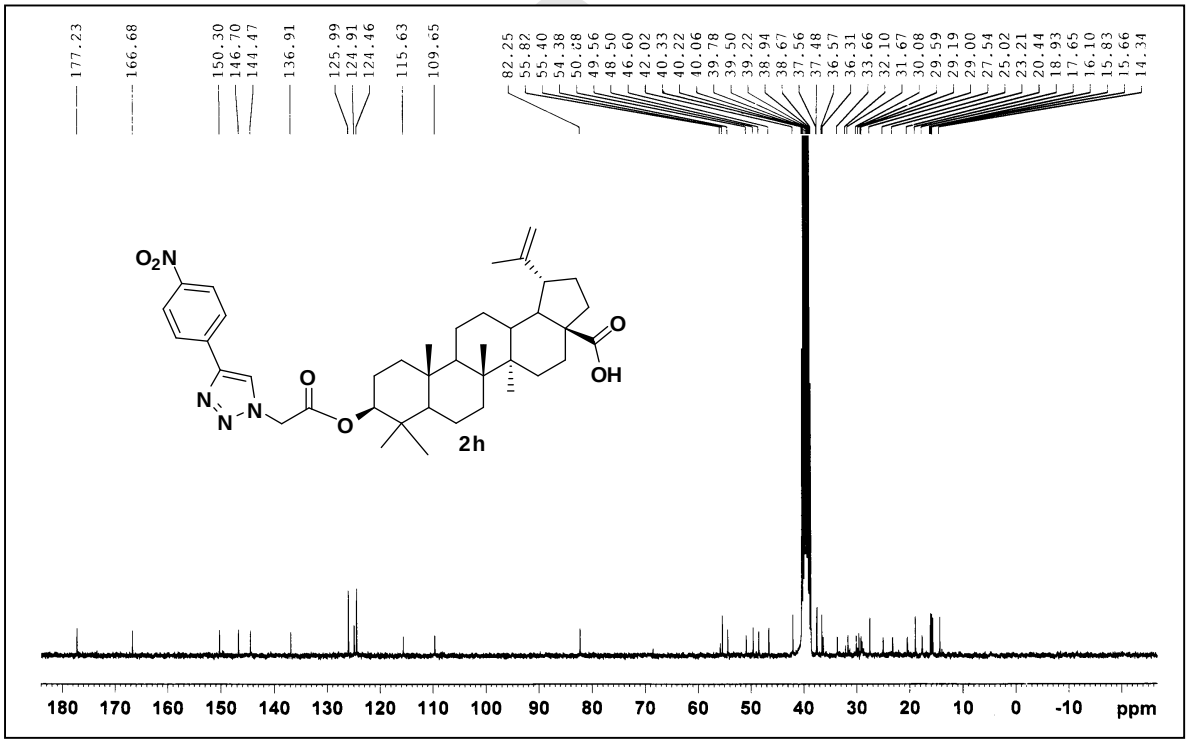

^{1}H NMR Spectrum of compound 2i

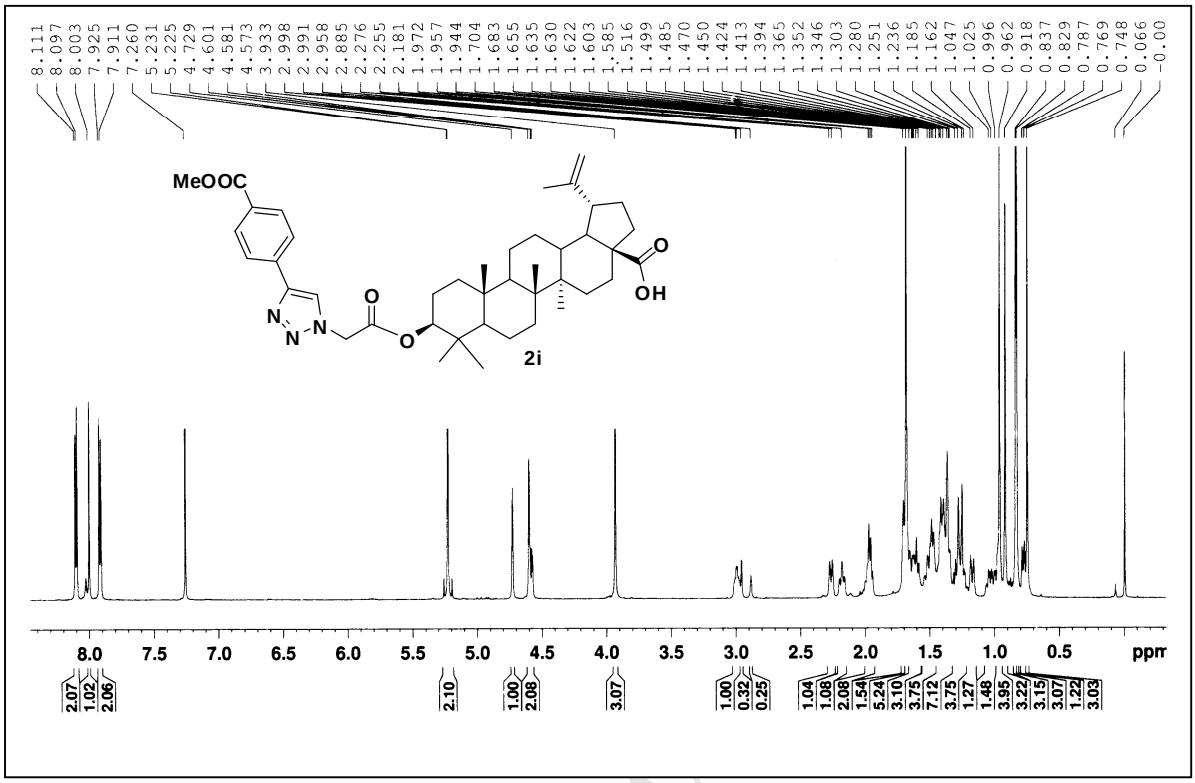

^{13}C NMR Spectrum of compound 2i

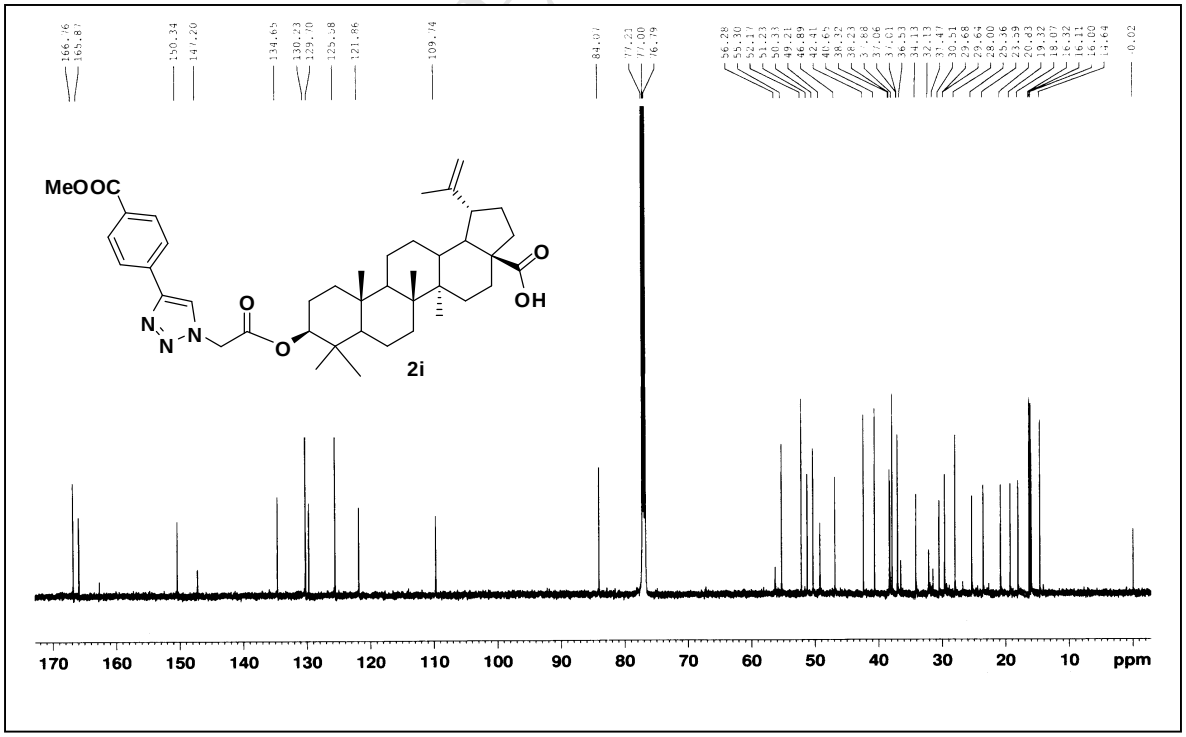

^{1}H NMR Spectrum of compound 2j

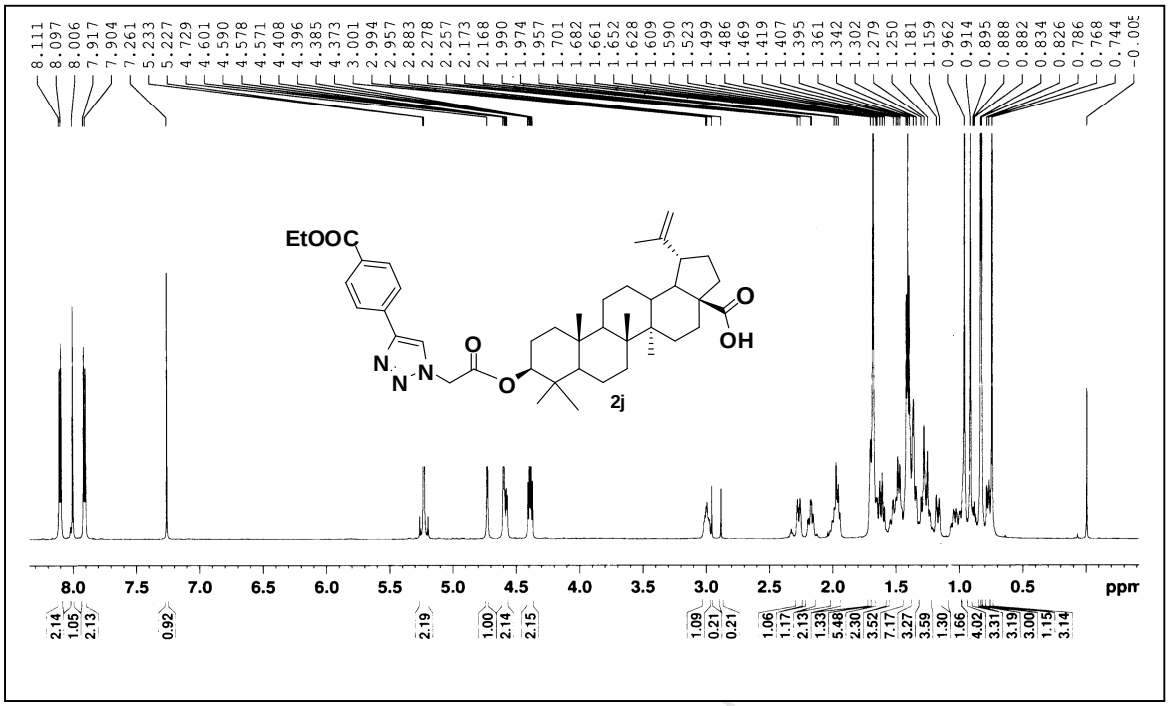

^{13}C NMR Spectrum of compound 2j

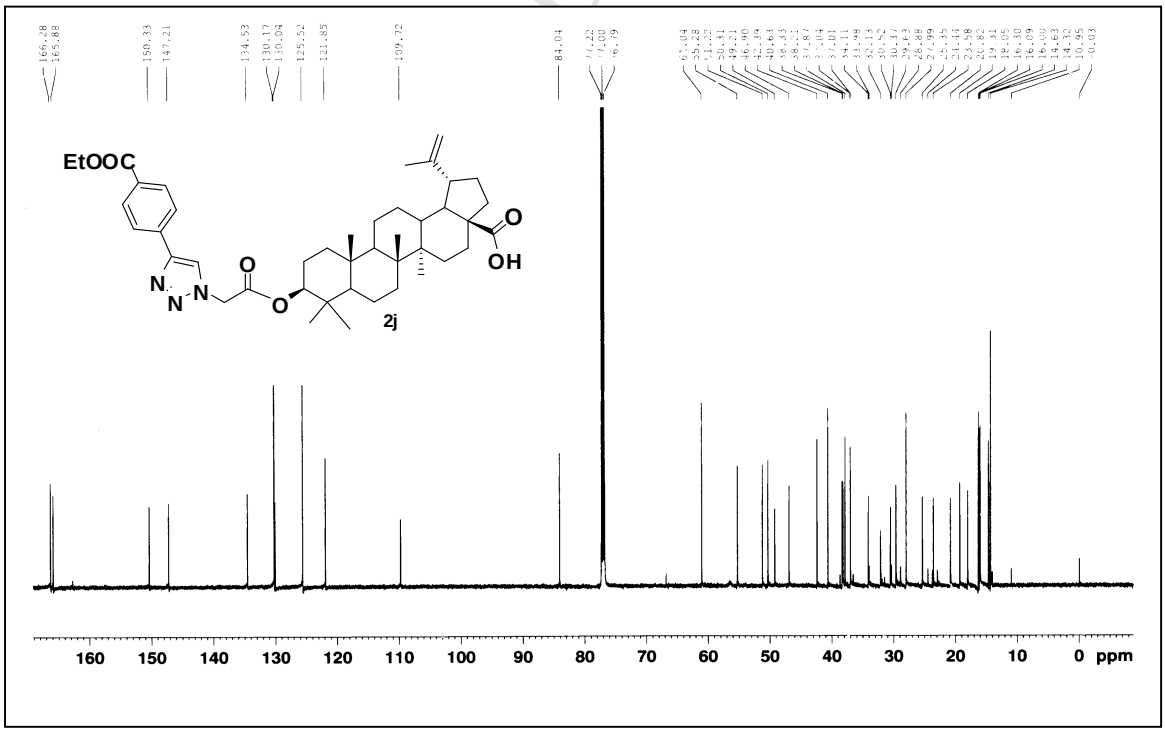

^{1}H NMR Spectrum of compound 2k

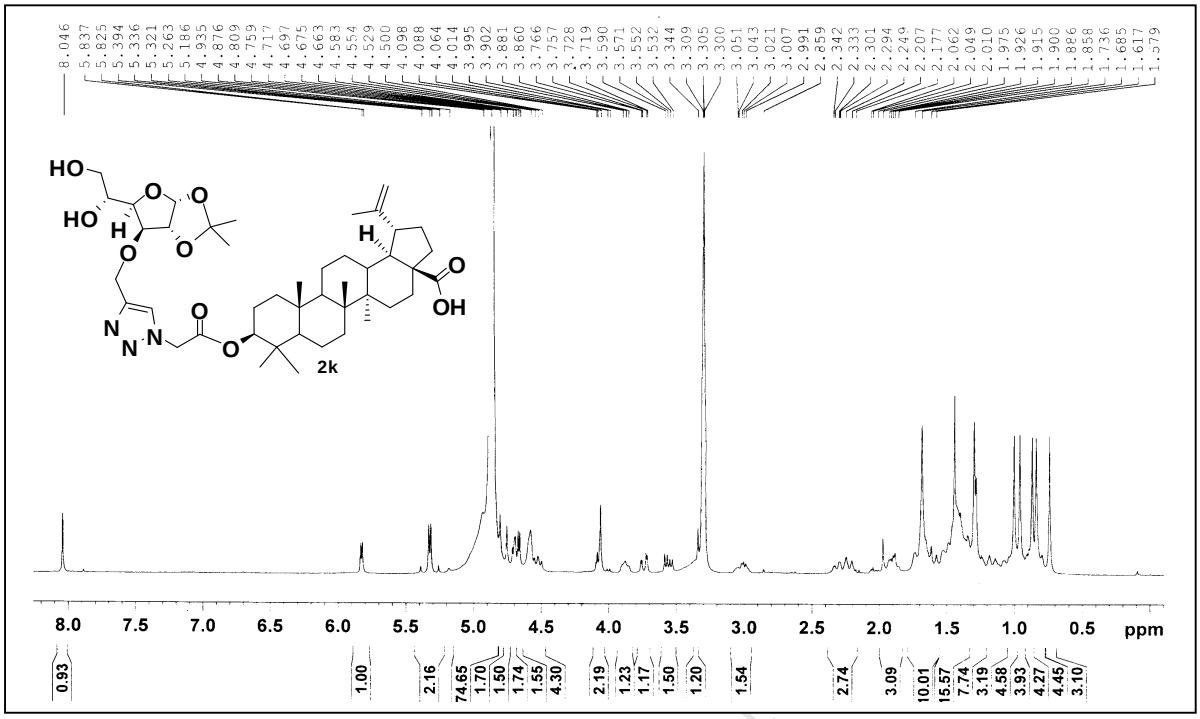

^{13}C NMR Spectrum of compound 2k

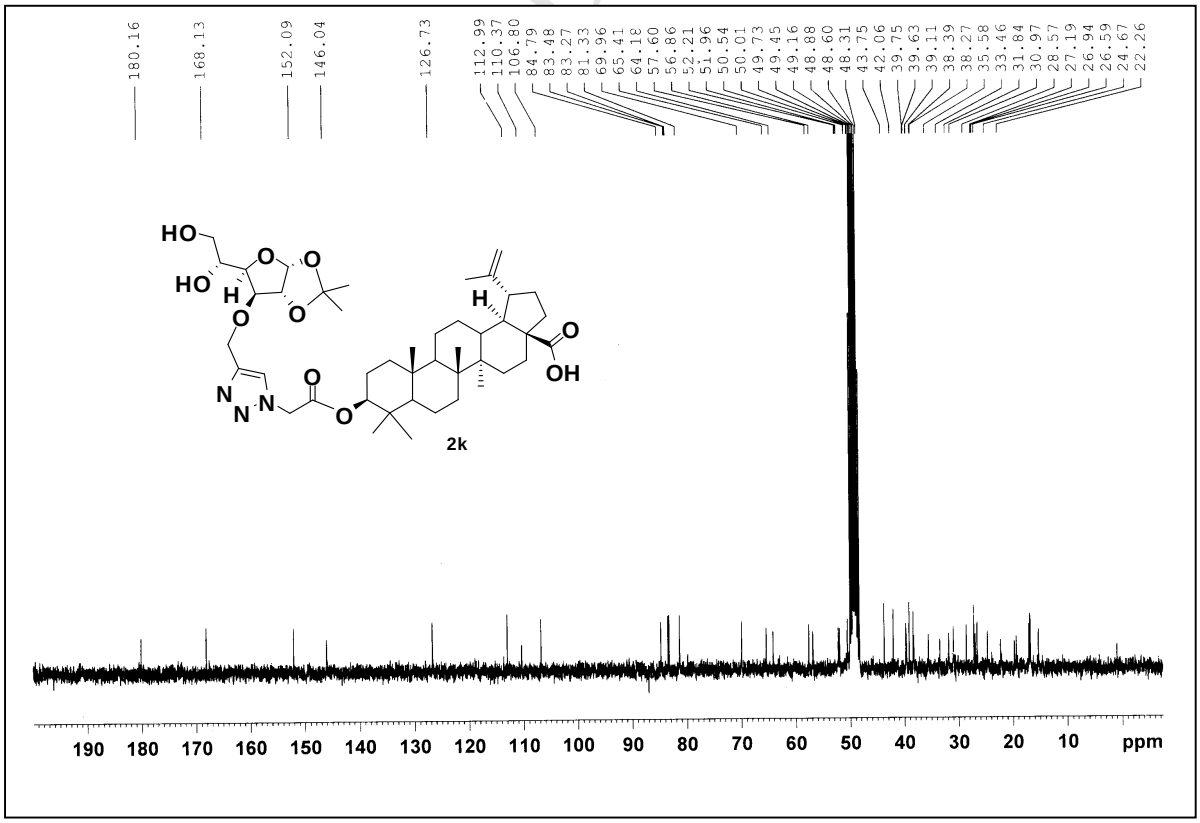

^{1}H NMR Spectrum of compound 2l

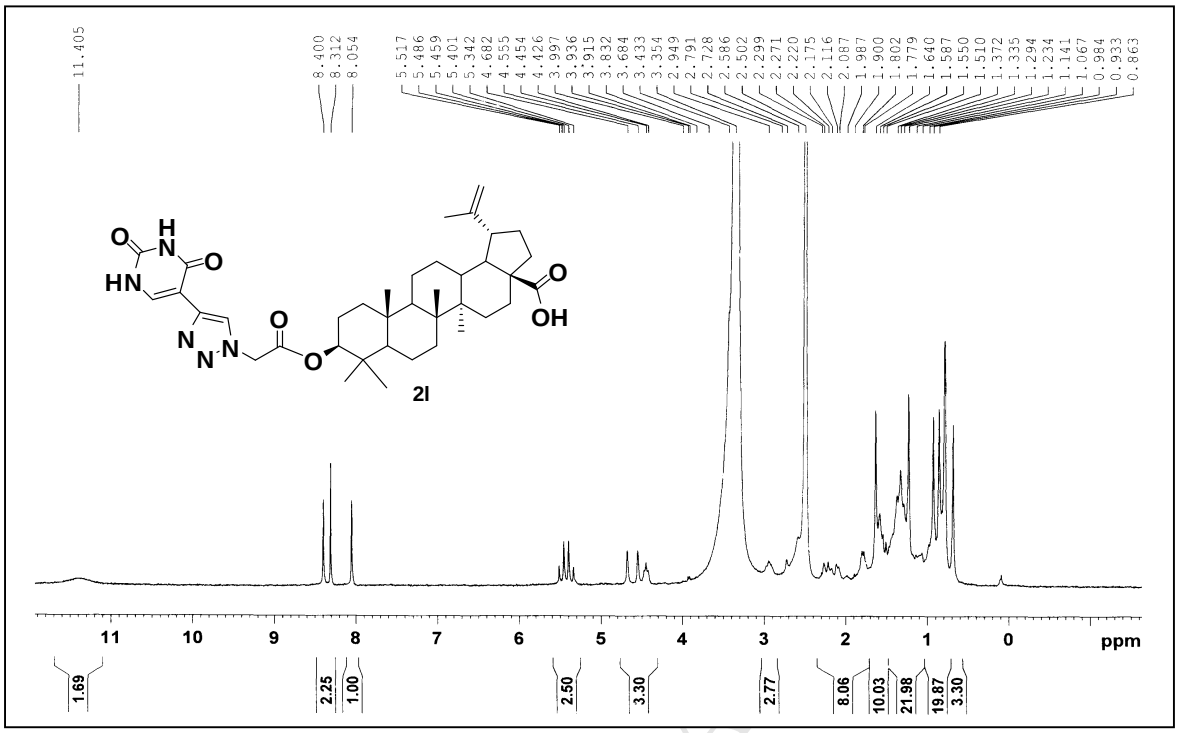

^{13}C NMR Spectrum of compound 2l

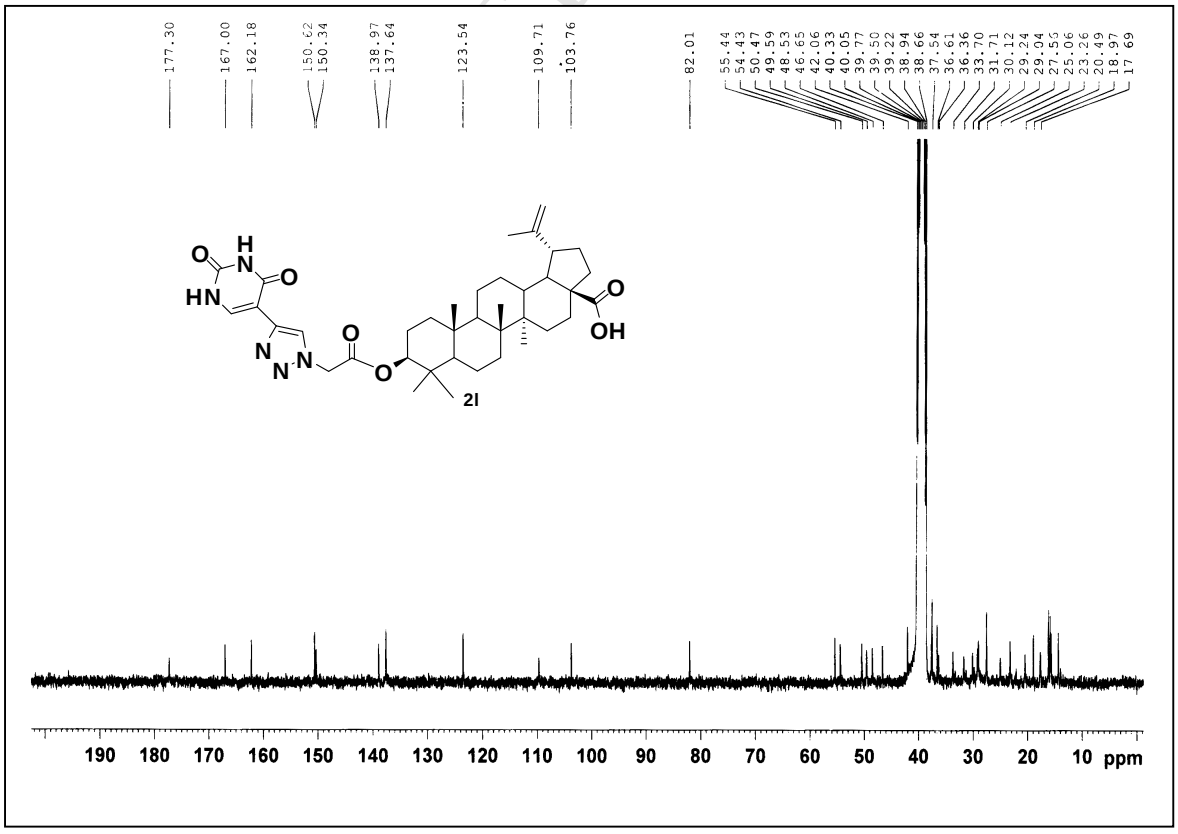

^{1}H-NMR Spectrum of 3-*O*-Chloroacetyl betulinic acid (3)

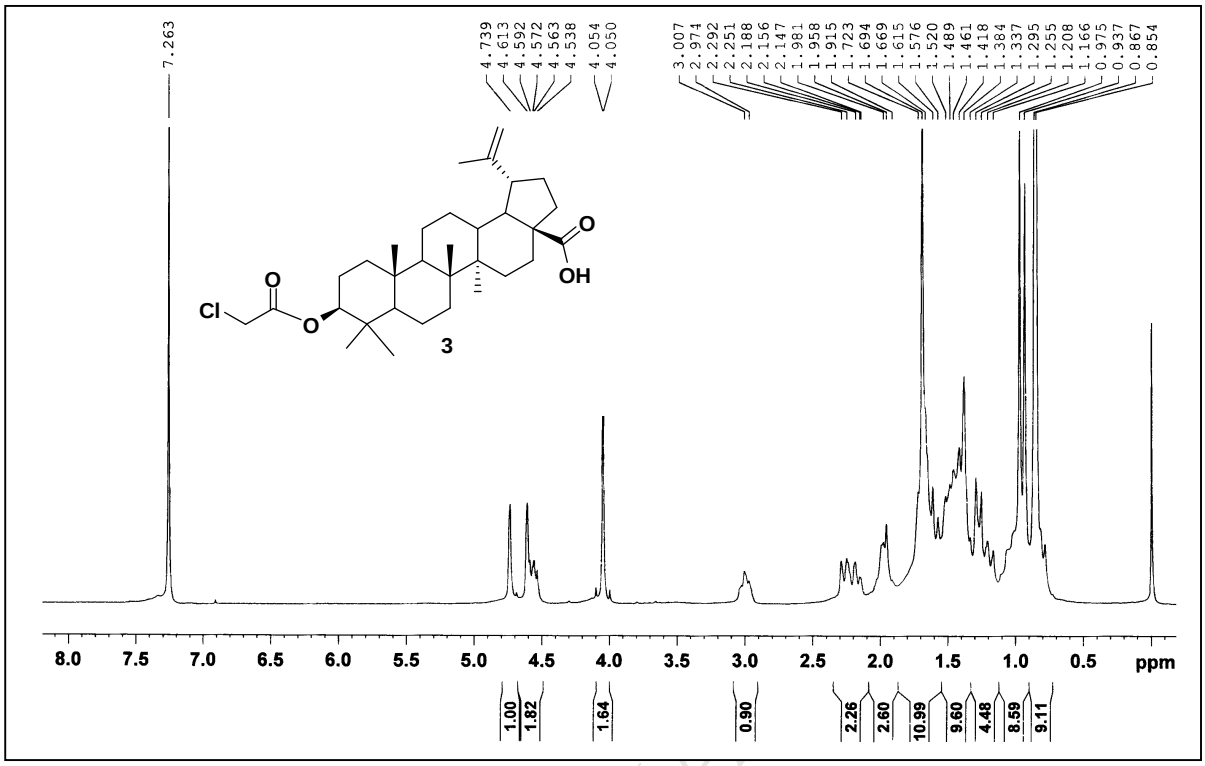

^{13}C-NMR Spectrum of 3-*O*-Chloroacetylbetulinic acid (3)

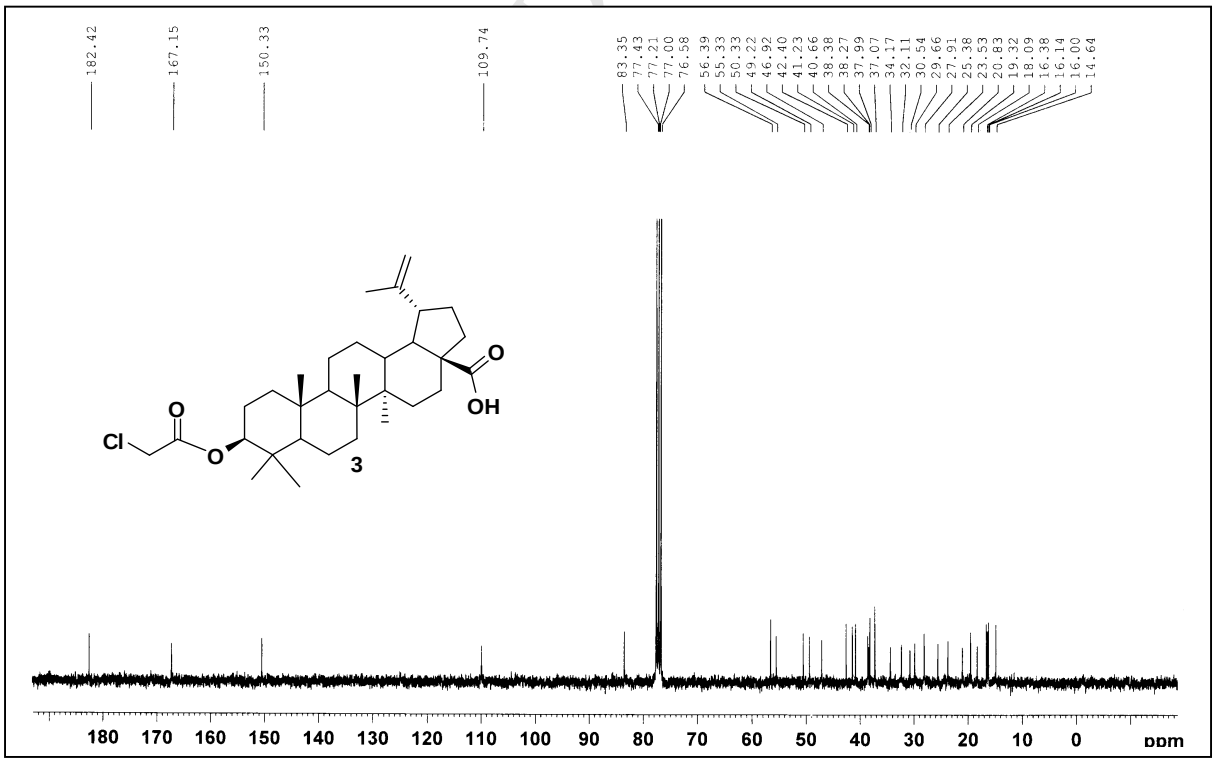

^{1}H NMR Spectrum of Betulinic acid azido acetate (4)

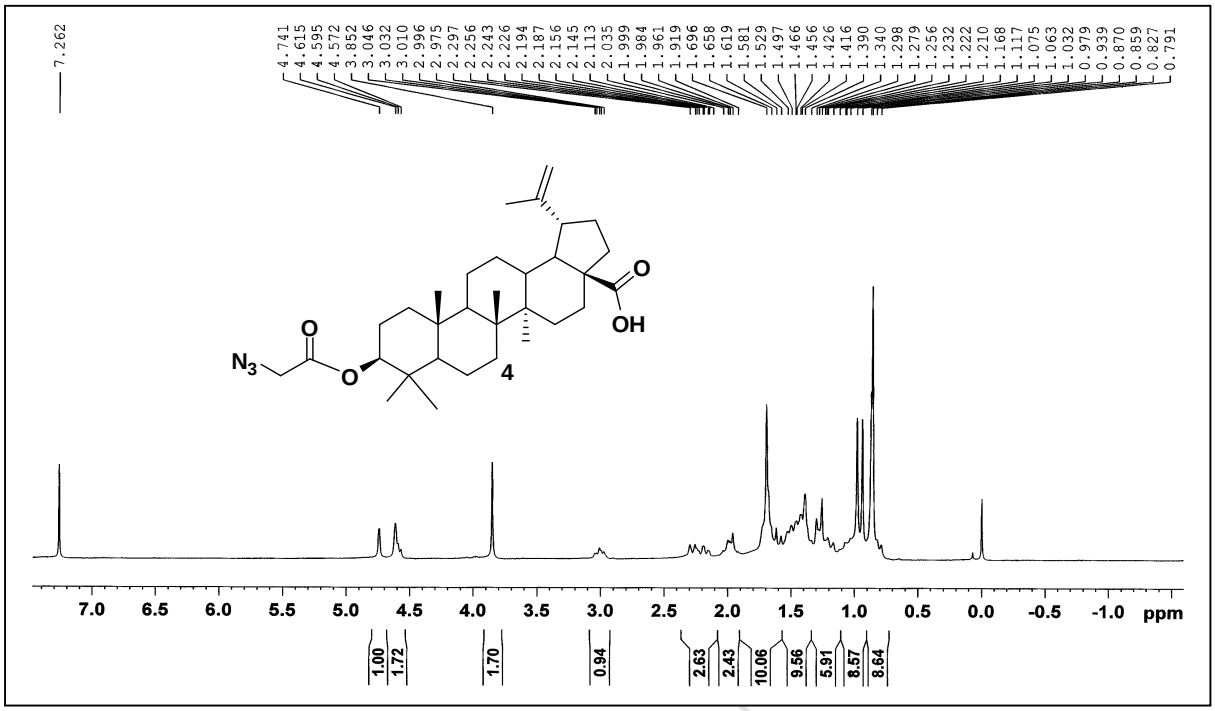

^{13}C NMR Spectrum of Betulinic acid azido acetate (4)